Functional and ultrastructural studies of apical-basal polarity in *Drosophila* nephrocytes

DISSERTATION ZUR ERLANGUNG DES
DOKTORGRADES DER NATURWISSENSCHAFTEN (DR. RER. NAT.)
DER FAKULTÄT FÜR BIOLOGIE UND VORKLINISCHE MEDIZIN DER
UNIVERSITÄT REGENSBURG

vorgelegt von
Gudrun Mendl

aus
Pocking

im Jahr
2018

Functional and ultrastructural studies of apical-basal polarity in *Drosophila* nephrocytes

DISSERTATION ZUR ERLANGUNG DES
DOKTORGRADES DER NATURWISSENSCHAFTEN (DR. RER. NAT.)
DER FAKULTÄT FÜR BIOLOGIE UND VORKLINISCHE MEDIZIN DER
UNIVERSITÄT REGENSBURG

vorgelegt von
Gudrun Mendl

aus
Pocking

im Jahr
2018

Das Promotionsgesuch wurde eingereicht am:

15.06.2018

Die Arbeit wurde angeleitet von:

Prof. Dr. Dr. Michael Krahn

Unterschrift:

_____

Gudrun Mendl

0 TABLE OF CONTENTS

1 SUMMARY

Intact apical-basal cell polarity is one of the mandatory requirements of proper cell and tissue development. Especially for more complex cell types, accurate cell function depends significantly on correct establishment of cell polarity. In the last two decades, *Drosophila* nephrocytes have been well established as model system for mammalian podocytes, one of the key components of kidney function. The main focus of podocyte research has been laid on the slit diaphragm, the core element of the podocyte filtration barrier, but the complexity of this cell type leaves many more questions unanswered.

It has been shown that there is a direct connection of slit diaphragm proteins Nephrin and NEPH1 with apical polarity proteins aPKC and Par3/ Bazooka (Baz). This work is a step towards a better understanding of the role of polarity proteins in *Drosophila* nephrocyte development and function.

The effects of single knockdown of the apical Par complex proteins aPKC, Par6, or Baz, as well as the basal polarity proteins Par1, Dlg, and Lgl was investigated regarding the localization of interacting proteins, GFP filtration/ accumulation functionality of the mutant nephrocyte cells and ultrastructural modifications of the cell architecture.

Single knockdown of the apical Par-complex proteins aPKC, Par6, or Baz revealed alterations in the localization of the remaining complex proteins. Additionally, the nephrocyte diaphragm proteins Sns (Nephrin homolog) and Kirre (NEPH1 homolog) were also mostly mislocalized in these experiments. Nephrocyte functionality in these specific knockdown cells was impaired in varying stages of severity. Functionality was decreased from 40% to over 90% in apical and basal polarity knockdown cells, with one exception for lgl-RNAi, showing a gain-of-function effect in functionality.

On the ultrastructural level, the knockdown of either one apical (aPKC, Par6, Baz) or one basal (Dlg, Par1) polarity protein resulted in modification or reduction of the typical cellular nephrocyte structures such as the number of nephrocyte filtrations slits or the manifestation of the peripheral lacuna area. In general, at least one typical nephrocyte feature was undeveloped in RNAi-knockdown mutant cells. Moreover, nephrocytes

expressing Baz_{5xA}, which cannot be phosphorylated by aPKC, displayed defects in function and ultrastructure.

Apical-basal polarity proteins play an important, still scarcely described role in nephrocyte development. The interaction of polarity proteins among each other and with components of other pathways are crucial for correct establishment of the cellular architecture and specific functional features of the nephrocyte cell.

ZUSAMMENFASSUNG

Die korrekte Entwicklung von Zellen und Geweben setzt eine intakte apikal-basale Zellpolarität voraus. Gerade komplexere Zelltypen sind ihrer Funktionalität von der korrekten Ausrichtung der Zellpolarität abhängig. In den letzten beiden Jahrzehnten wurde der *Drosophila* Nephrozyt als Modellsystem für den Säugetier-Podozyten, einen besonderen Zelltyp der Niere mit bedeutender Schlüsselfunktion, erfolgreich etabliert. Die Podozytenforschung konzentrierte sich bisher hauptsächlich auf die Schlitzmembran, das Kernelement der Podozyten-Filtrationsbarriere in der Niere.

So wurde bereits gezeigt, dass eine direkte Verbindung der Schlitzmembran-Proteine Nephrin und NEPH1 mit den apikalen Polaritätsproteinen aPKC und Par3/ Bazooka (Baz) besteht. Diese Arbeit leistet einen Beitrag dazu, die Rolle der Polaritätsproteine in der Entwicklung und Funktionsweise von *Drosophila* Nephrozyten besser zu verstehen.

Hierzu wurden die Effekte von einzelnen Knockdowns der apikalen Par-Komplex-Proteine aPKC, Par6 oder Baz, sowie der basalen Polaritätsproteine Par1, Dlg und Lgl hinsichtlich der Lokalisierung interagierender Proteine, der Filtrations-/Akkumulations-Funktionalität der mutanten Nephrozytenzellen und der ultrastrukturellen Modifizierungen der Zellarchitektur untersucht.

Das separate Herabregulieren der apikalen Par-Komplex-Proteine aPKC, Par6 und Baz führte zu Veränderungen in der Lokalisation der verbleibenden Proteine des Komplexes. Zudem waren in diesen Experimenten die Nephrozyten-Filtrationsmembranproteine Sns (Nephrin-Homolog) und Kirre (NEPH1-Homolog) ebenfalls fehllokalisiert. Darüber hinaus war die Funktionalität in diesen Knockdown-Zellen auf unterschiedlich starke Weise eingeschränkt. In den meisten Fällen wurde die Funktionalität um 40% bis über 90% eingeschränkt, mit der Ausnahme von lgl-RNAi, bei deren Knockdown ein funktionaler gain-of-function Effekt gezeigt wurde.

Auf ultrastruktureller Ebene resultierte der Knockdown einzelner apikaler (aPKC, Par6, Baz) oder basaler (Dlg, Par1) Polaritätsproteine in der Modifizierung oder Reduzierung von zellulären Strukturen wie die Anzahl der Nephrozyten-Filtrationsschlitzmembrane oder die Ausprägung des peripheren Lakunenareals. In der Regel war in diesen

Knockdown-Zellen mindestens eines der typischen Nephrozytenmerkmale unterentwickelt. Außerdem zeigten Nephrozyten, die ein durch aPKC nicht phosphorylierbares Baz_{5xA} exprimierten, Defizite in Funktionalität und Ultrastruktur.

Apikal-basale Polarität spielt eine wichtige, jedoch bislang kaum beschriebene Rolle in der Entwicklung von Nephrozyten. Die Interaktionen der Polaritätsproteine untereinander und mit Komponenten anderer Signalwege sind sowohl für die korrekte Errichtung der zellulären Architektur, als auch den Aufbau der besonderen funktionalen Eigenschaften der Nephrozytenzellen entscheidend.

2 INTRODUCTION

2.1 Cell polarity

Cell polarity is one of the key preconditions in cell integrity and function in most cell types and tissues. Functional protein networks and pathways, cytoskeletal frame and cell-cell communication mechanisms often require a clear definition of cell poles. In general, cell polarity is described as an asymmetry in structural and functional properties of the disparate cell parts. This asymmetry is created by a complex interplay of protein concentration gradients, defined exclusion or accumulation of particular proteins at a certain membrane domain, interaction of proteins as well as intra- and extracellular signaling.

2.1.1 Apical-basal polarity in epithelia

Epithelial tissue belongs to the basic types if animal tissue, together with muscle tissue, nervous tissue, and connective tissue. It is termed as a cell layer that lines inner cavities and outer body surfaces and includes functions as protection, excretion, secretion, absorption, transcellular transportation, and many more. This distinction in shape and function of the cell layer requires the polarization of the cells themselves: the apical pole is directed to the outer or luminal surface, the lateral domain is keeping the contact to neighboring cells and the basal cell pole is resting on the basement membrane, contacting the extracellular matrix and underlying connective tissue (Chen & Zhang, 2013).

There are various cues involved in the establishment of apical-basal polarity, including extracellular signals, cytoskeletal filaments, and plasma membrane components. Most importantly, the temporal and spatial organization of polarity proteins declares the distinctive regions of the cell. The exact mechanisms of cell polarity establishment can variegate between cell types and model organisms. In simple mammalian epithelia, the formation of cell polarity compartments, adherens junctions (AJ), and tight junctions (TJ) are mutual dependent on each other and thereby participate together in organizing the apical and basolateral domains (Assémat et al., 2008). Similar to these interactions, the

formation of zonula adherens and sepatate junctions (SJ) is closely intertwined with the establishment of polarity domains in the *Drosophila* embryo (Caplan et al., 2008; Tepass, 2012).

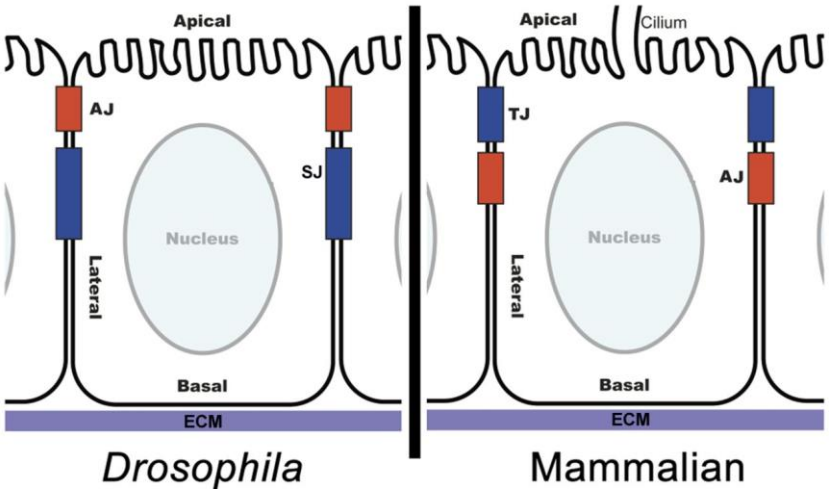

Figure 1: Apical-basal polarity in *Drosophila* and mammalian epithelial cells. Apical region (top, with microvilli), lateral region (with junctions) and basal region (adjacent to basement membrane). AJ: Adherens junction, SJ: Septate junction in invertebrates, TJ: Tight junction in mammalian cells. ECM: Extracellular matrix, including the basement membrane. Cell polarity is fundamentally defined by these cell-cell juntions. (Bergstralh & St Johnston, 2012).

In the last years, there has been great progress in cell polarity research and numerous proteins could be identified to play a role in cell polarity regulation. These proteins often function in a finely coordinated interplay of multiprotein polarity complexes in apical-basal polarity, cell migration, and (asymmetric) cell division.

There are three major protein complexes known to be essential for apical-basal polarity: the Par complex, the Crb complex, and the Scrib complex. These three complexes are partly interacting with each other, either in a supporting and activating way or via mutual exclusion, leading to the desired definition of membrane domains in the cell (Assémat et al., 2008; Tepass et al., 2001). The emphasis of this work was on the Par complex.

2.1.2 Par proteins in cell polarity

The PAR proteins were first discovered and described by Ken Kemphues and Jim Priess in *Caenorhabditis elegans* zygotes. Their screening method uncovered six genes involved in cell division and early embryogenesis, which were named *par1-6* after their partitioning defective mutant phenotype (Goldstein & Macara, 2007). The PAR proteins are highly conserved and present in all species (except *par2*), partially represented with multiple alleles (Kemphues, 2000; Watts et al., 1996). They are not members of one protein family, though some of them share common features – PAR1 and PAR4 are serine threonine kinases and PAR3 and PAR6 possess PDZ domains suggesting scaffolding purposes. PAR2 has a RING finger domain and PAR5 is a member of the 14-3-3 protein family (Goldstein & Macara 2007; Moore & Boyd 2004).

Most PAR proteins localize asymmetrically in the cell and at (or near) the cell cortex. PAR1 localizes at the basal or posterior cell pole (in *C. elegans* associated with PAR-2 (Boyd et al., 1996)) and its correct localization depends on all other PAR proteins. Its main function includes the surveillance of proper centrosome positioning upon the initiation of mitosis (Cheng et al., 2008) and the exclusion of the apical polarity protein PAR3 via phosphorylation. PAR4, also known as LKB1 (Liver-kinase B1), is a master kinase regulating cell polarity and functioning as a tumor suppressor. Single expression of PAR4 demonstrates a nuclear localization, the expression of PAR4 together with its co-factors STRAD and MO25 leads to their symmetrically cytoplasmic localization (Nakano & Takashima, 2012). PAR4/LKB1 is an upstream activator of PAR1 and many more kinases of the AMPK subfamily (Lizcano et al., 2004; Spicer et al., 2003). PAR5, or 14-3-3ε/ζ in *Drosophila*, acts as a mediator in cell polarity establishment and is, like PAR4/LKB1, symmetrically cortical and cytoplasmic localized (Goldstein & Macara, 2007). It interacts with the phosphorylated forms of *Drosophila* Par3 (Bazooka) or the mammalian PAR1b, assisting in the reciprocal antagonism of the apical aPKC/PAR-complex and basal determinant PAR1. Therefore, PAR5 is eventually enhancing the definition of apical and basal regions in the cell (Cuenca et al., 2003; Morton et al., 2002; Suzuki & Ohno, 2006).

Both PAR3 (Bazooka/Baz in *Drosophila*) and PAR6 have (several) PDZ domains, thus acting as multi-modular scaffold proteins with the ability to bind to each other and other

cell polarity regulating proteins (Macara, 2004a). Together with the atypical protein kinase C (aPKC), they interact closely as the PAR complex in the establishment of the apical region of the cell.

Upon formation of the Par complex, aPKC is presented as a heterodimeric complex with Par6, in which the N-terminal region of Par6 is binding to the regulatory domain of aPKC (Joberty et al., 2000; Suzuki et al., 2001). In this dimer, Par6 is acting as a regulatory subunit of aPKC and is involved in aPKC positioning and activity control (Atwood et al., 2007). Via binding of Cdc42:GTP to its semi-CRIB/PDZ-motif, Par6 possesses the intrinsic potential to enhance aPKC kinase activity and is therefore playing an important role in regulating aPKC activity at epithelial junctional structures (Garrard et al., 2003; Yamanaka et al., 2001).

During early cellularization of the *Drosophila* embryo, Baz is positioned at the apical pole near the newly forming adherens junctions. This initial positioning is arranged by preexisting cytoskeletal cues, involving actin filaments and transportation along microtubules, and Baz is at that point anchored by an apical scaffold (Harris & Peifer, 2005). Baz then binds to the heterodimeric complex of aPKC/Par6 to form the ternary Par complex (Goldstein & Macara, 2007; Suzuki & Ohno, 2006). This interaction leads to the initial recruitment of aPKC/Par6 to the apical membrane (Harris & Peifer, 2005; Horikoshi et al., 2009).

Within the newly formed Par complex, phosphorylation of Baz by aPKC results in a weakened interaction between these two proteins. Simultaneously, the PDZ domain of Par6 interacts with the apical located polarity protein Crumbs (Crb), enhancing the apical recruitment of the aPKC/Par6 dimer. Subsequently, these events lead to a specific spatial localization of the Par complex, with Par6 and aPKC residing at the apical membrane and Baz localizing slightly more basically at the adherens junctions (Doerflinger et al., 2010; Morais-de-Sá et al., 2010). Likewise in mammalian epithelia, Par6 and aPKC are found at the more apical apex and Par3 at the tight junctions (TJ) (Bryant & Mostov, 2008).

Par6 and aPKC interact with the apical located Crumbs (Crb) – Stardust (Sdt) - Patj complex. Crb and Sdt can both bind directly to the PDZ domain of Par6 (Hurd et al., 2003; Wang et al., 2004), and Crb phosphorylation by aPKC is essential for Crb activity

(Sotillos et al., 2004). These mutual interactions and dependencies (see Fig. 2) underline the importance of correct localization and function of polarity proteins.

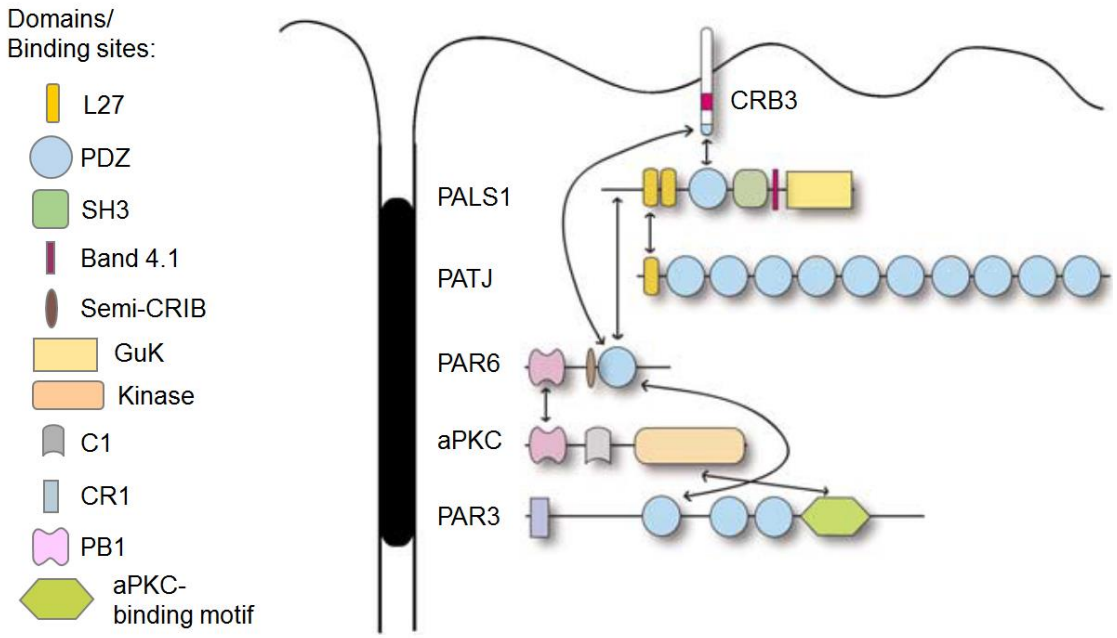

Figure 2: Domain structures of PAR (and CRB) complex components. Filled shapes represent the protein domains/ binding sites. CRB3 has a FERM-binding motif (red) and a PDZ-binding motif (blue). aPKC and Par6 interact via their PB1 domains. Par6 interacts with Par3/Baz via PDZ-PDZ domain binding, and with small GTPase Cdc42 via its semi-CRIB motif. Associated and activated aPKC is able to bind and phosphorylate Par3/Baz in its aPKC binding domain and PDZ2-3 region. Protein – protein interactions are indicated by double headed arrows (Chen & Zhang, 2013; Wang & Margolis, 2007, modified).

Apart from defining the apical region of the cell by their presence and local activity, the apical polarity complexes also interact with basal/ basolateral polarity proteins in an antagonistic manner (Fig. 3). Direct interaction and subsequent mutual exclusion of these proteins from the respective cell poles is one of the key features in the establishment of apical-basal polarity.

For example, the interaction between PAR3 and the aPKC/PAR-6 complex is subject to regulation by Lethal giant larvae (Lgl; L(2)gl), which localizes to the basolateral membrane and restricts PAR3/aPKC/PAR-6 complex activity to the apical membrane (Hutterer et al, 2004) This activity of Lgl is achieved by competing with PAR3 for binding to the aPKC/PAR-6 complex (Yamanaka et al., 2003, 2006).

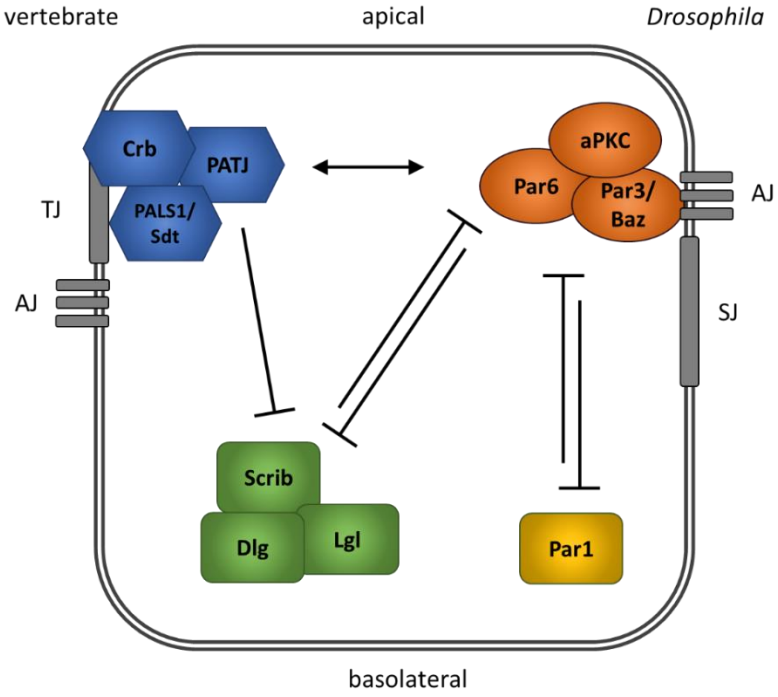

Figure 3: Interaction of apical and basal polarity protein (complexes). The Crumbs complex and Par complex work together in defining the apical cortex, depending on cell type and developmental stage. Their antagonists, the Scribble complex and the protein Par1, determine the basolateral cell region. They act in opposition to the apical polarity regulators, partly by direct interaction and phosphorylation. (Adapted from Coradini, Casarsa, & Oriana, 2011).

2.1.3 Basolateral polarity determinants

One of the three major basal polarity protein complexes is the Lethal giant larvae (Lgl)/ Discs large (Dlg)/ Scribble (Scrib) complex, defining the basolateral domain of the cell. The Scribble complex components are classified as tumor suppressors and their functions include regulation of cell polarity, cell proliferation, as well as AJ and TJ assembly and maintenance. This complex is also involved in cell adhesion (Su et al., 2012)

Lgl is a Myosin II binding protein containing WD40 repeats (Mechler et al., 1985; Strand et al., 1994) and is therefore involved in protein-protein interactions and scaffolding. The mammalian Lgl is able to bind aPKC/Par6 in absence of Par3 (Yamanaka et al., 2003), and Lgl phosphorylation by aPKC leads to its exclusion from the apical membrane domain (Plant et al., 2003). Studies indicate that Lgl might function redundantly in cell

polarity establishment to Par2 in *C. elegans*, a basal determinant missing in mammalian and insect cells (Beatty et al., 2013, 2010).

Dlg and Scrib are both multi-PDZ domain proteins. Dlg is the founding member of the MAGUK family (membrane associated guanylate kinase) (Woods & Bryant, 1991), proteins with a basic core of three particular protein interaction modules: the PDZ (PSD95/DLG/ZO-1) domain, an SH3 (Src homology 3) interaction component, and a region highly similar to the guanylate kinase (GK). These protein interaction domains predestine MAGUKs as scaffolding proteins in larger protein networks at the plasma membrane (Roberts et al., 2012). Dlg resides at the basolateral domain in epithelial cells. With maturation of the epithelium and the merging of cell-cell junctions, Dlg becomes concentrated at the apex of the basolateral domain. In larval *Drosophila* epithelial cells, loss of Dlg leads to overgrowth due to an impaired cell polarity (Bilder, 2004).

Scribble is part of the LAP (LRR (leucine-rich repeats) and PDZ domain) subfamily of PDZ domain proteins, containing a set of leucin-rich repeats at the N-terminus and four PDZ domains distributed throughout the protein (Bilder et al., 2000; Bilder & Perrimon, 2000). Loss of Scribble leads to a misdistribution of apical proteins and adherens junctions to the basolateral domain of the embryonic epithelial cell (Bilder & Perrimon, 2000). Scribble was found to be associated with the intracellular domain of E-cadherin at the lateral membrane of polarized renal epithelial cells, and necessary for correct cell-cell adhesion since its knockdown leads to adherens junction instability (Qin et al., 2005).

The kinase Par1 plays a vital role in defining the boundary between apical and basolateral domains. Par 1 and its substrates MEX-5 and MEX-6 regulate the growth of the posterior domain of the cell (Cuenca et al., 2003; Motegi & Seydoux, 2013). By Par3 phosphorylation and subsequent binding of 14-3-3 to Par3, Par1 enhances the restriction of Par3 from the lateral membrane (Benton & St Johnston, 2003). In turn, Par1 is regulated by aPKC, resulting in the translocation of phosphorylated Par1 from the membrane to an intracellular compartment (Hurov et al., 2004). Par1 is also phosphorylated and activated by Par4/LKB1 (Lizcano et al., 2004).

2.2 The mammalian kidney

The kidney (and its ortholog organs or structures in other species) is an essential part of the excretion and osmoregulatory system, responsible for removing waste and maintaining blood pressure, electrolyte and acid base homeostasis, amongst other functions.

2.2.1 The mammalian kidney and its function

The mammalian kidney filters blood to remove toxic or unwanted molecules, to release or detain water and therefore balancing the pressure and ion concentration in the blood. The filtrate leaves the body as urine via the ureter and bladder.

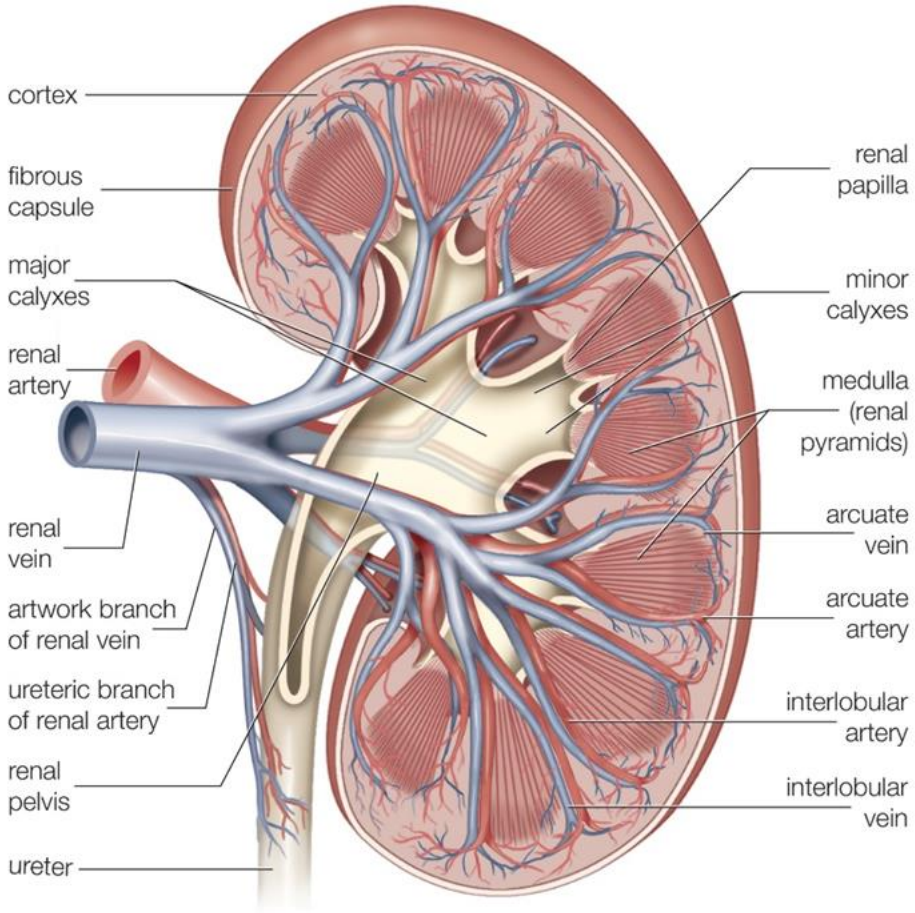

Figure 4: The anatomy of the mammalian kidney. The organ is surrounded by a fibrous capsule, the inner substance can be distinguished into the outer renal cortex and the inner renal medulla. Nephrons in cortex and medulla filter blood to urine. The renal pyramids, divided by Bertin columns, drain the urine in minor calyxes. The urine leaves the kidney via the major calyxes, the renal pelvis, and the ureter. (cartoon from Encyclopedia Britannica, Inc. 2010).

In vertebrates, the structure of the kidney is highly organized (see Fig. 4). They come in pairs and are bean-shaped, with the renal artery, the renal vein and the ureter entering and exiting at the hilum on the concave side of the organ. The mammalian kidney is either a unipapillary or a compound multipapillary organ covered by a fibrous capsule, and the parenchyma (inner substance) can be divided into two distinct regions, the cortex (*cortex renalis*) and the medulla (*medulla renalis*). So-called renal columns of cortical tissue (columns of Bertin) separate the single renal pyramids in the medulla. The pyramids open into minor calyxes, which join to major calyxes and the renal pelvis. The processed urine leaves the kidney via the the calyxes and the ureter, and is collected in the bladder. Blood supply is maintained via the renal arteries, branched in interlobar and arcuate arteries, and afferent arterioles.

The basic structural and functional entity of the kidney is the nephron, which is composed of the renal corpuscle (the glomerulus inside the Bowman's capsule) and a following tubular system (Fig. 5). Nephrons span over the cortex and the medulla of the kidney and vary in the length of the affiliated loop of Henle. The filtration of the blood takes place in the renal corpuscle, whereby the blood is transported by the afferent glomerular arteriole through the juxtamedullary apparatus into the glomerulus. The glomerulus is a capillary tuft enclosed in a tubular protrusion, the Bowman's (or glomerular) capsule, and is stabilized by the glomerular basement membrane.

A

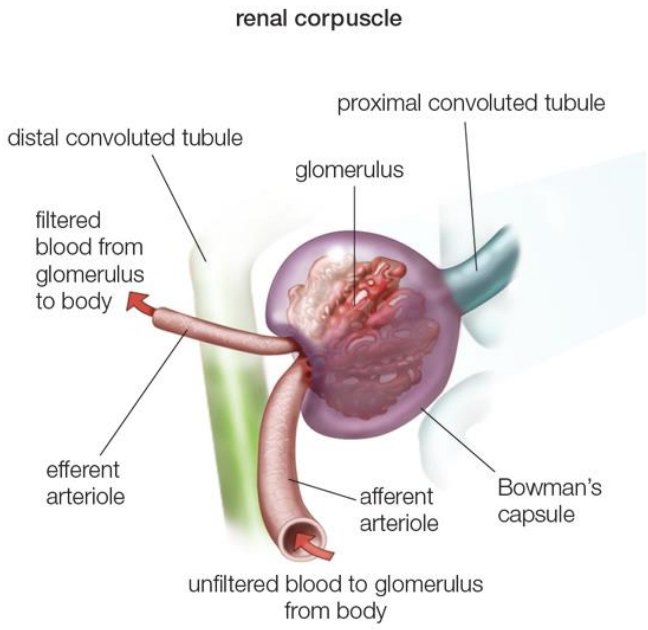

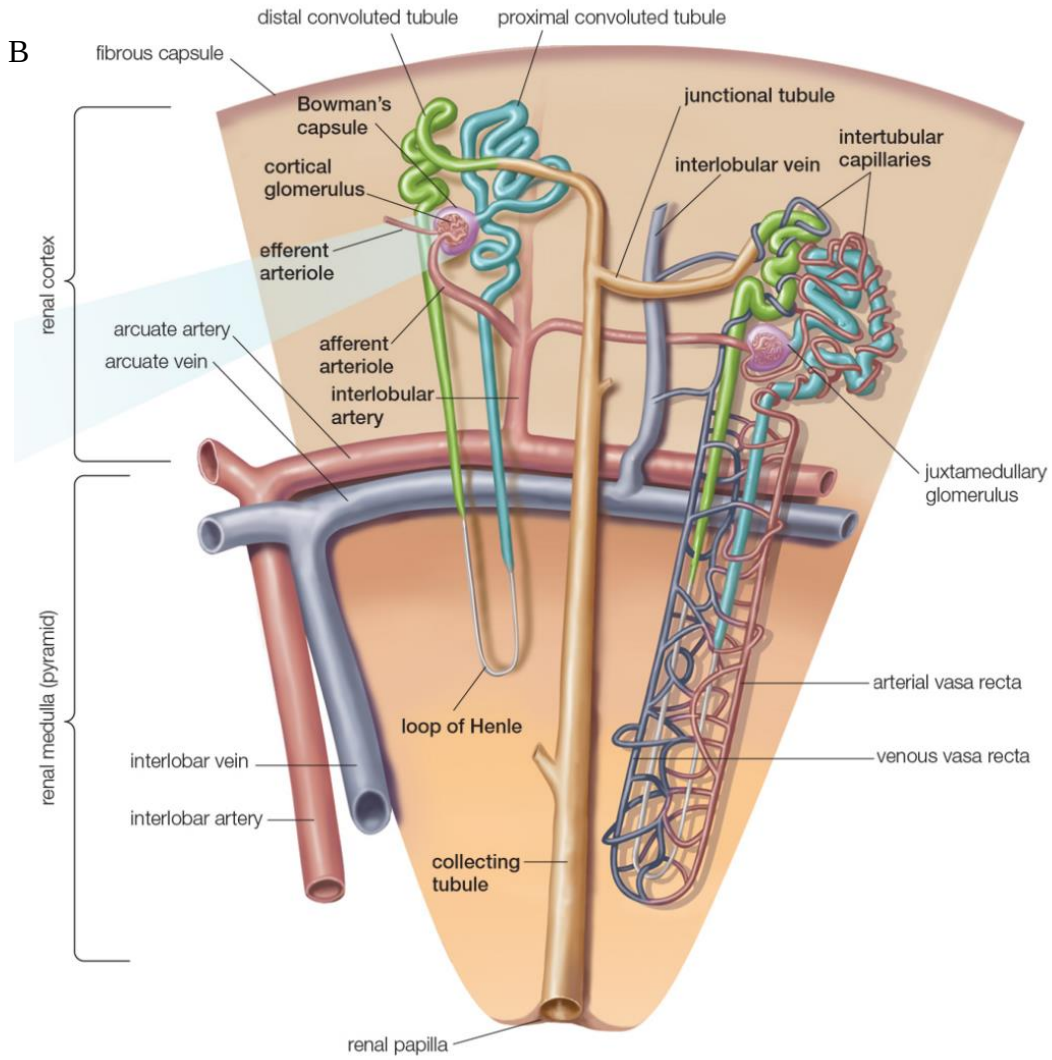

Figure 5: Renal corpuscle (A) and nephron (B). The nephron as structural unit of the kidney is located in the cortex and medulla. The renal corpuscle with Bowman's capsule and glomerulus and the proximal convoluted tubule lie in the cortex. The tubule descends into the renal pyramid (medulla), turns and transitions in the cortex from the distal convoluted tubule to the junctional tubule, eventually joining the collecting duct. An afferent arteriole enters the Bowman's capsule, forming the capillary tuft covered by podocytes. The efferent arteriole transitions into the corresponding venule after branching into a network of intertubular capillaries involved in reabsorption and homeostasis (cartoon from Encyclopedia Britannica, Inc. 2010).

The inner visceral layer of the Bowman's capsule is depicted of podocytes, which are highly specialized epithelial cells with expansive foot processes enclosing the capillary tightly. In between the interdigitating foot processes, there are small filtration slits spanned with a membranous, zipper-like structure, so-called slit diaphragms of about 25-40nm width (Reiser et al., 2000).

The podocytes account for the ultrafiltration barrier between blood and urine, where blood from the glomerular capillary is filtrated through this visceral layer resulting in glomerular filtrate in the Bowman's space. This filtrate flows to the renal tubule system, passing through the proximal convoluted tubule, the loop of Henle and the distal convoluted tubule. The tubular fluid is processed and changed in its composition by the reabsorption of small molecules, electrolytes and water through the tubular epithelial cells and by the countercurrent principle where osmotic gradients in the medulla lead to the concentration of the tubular fluid to urine.

2.2.2 The podocytes

Podocytes are of epithelial origin and mature from simple undifferentiated cells into highly specialized mesenchyme-like cells throughout glomerular development. During transition from the S-shaped body stage to the capillary loop stage of the nephron-to-be they change expression patterns of certain marker proteins, lose their ability for mitosis and start to establish their unique cell structure with a voluminous cell body and branching, interdigitating foot processes (Mundel & Kriz, 1995). Long primary processes are extending from the cell body in the urinary space, which ramify in numerous foot processes. These foot processes wrap around the glomerular capillaries and interlock with the processes from adjacent podocytes, forming a tight net with narrow slits winding in between the cell extensions (see Fig. 6; Pavenstädt et al. 2003). While the cell body is mainly filled with organelles, the foot processes are stabilized by various filaments – microtubules and intermediate filaments in the cell body, and microfilaments and a thin cortex of actin filaments in the foot processes (Drenckhahn & Franke, 1988).

The filtration slits between the processes are bridged by a membranous structure, namely the slit diaphragm, which is made of a set of particular proteins. Moreover, the foot processes are covered with a negatively charged glycocalyx which acts not only as a supporting electrostatic spacer bar between the cell protrusions, but also contributes to the defined surface charges of the filtration barrier (Gelberg et al., 1996; Kerjaschki, 1994). The glomerular filtration barrier (GFB) is completed with the opposing fenestrated endothelium lining the vascular space and the glomerular basement membrane in between (Reiser & Altintas, 2016). This barrier is a molecular sieve based on size- and charge-

selection whereby the strictest size filter is probably displayed by the fenestrated endothelium (Haraldsson et al., 2008).

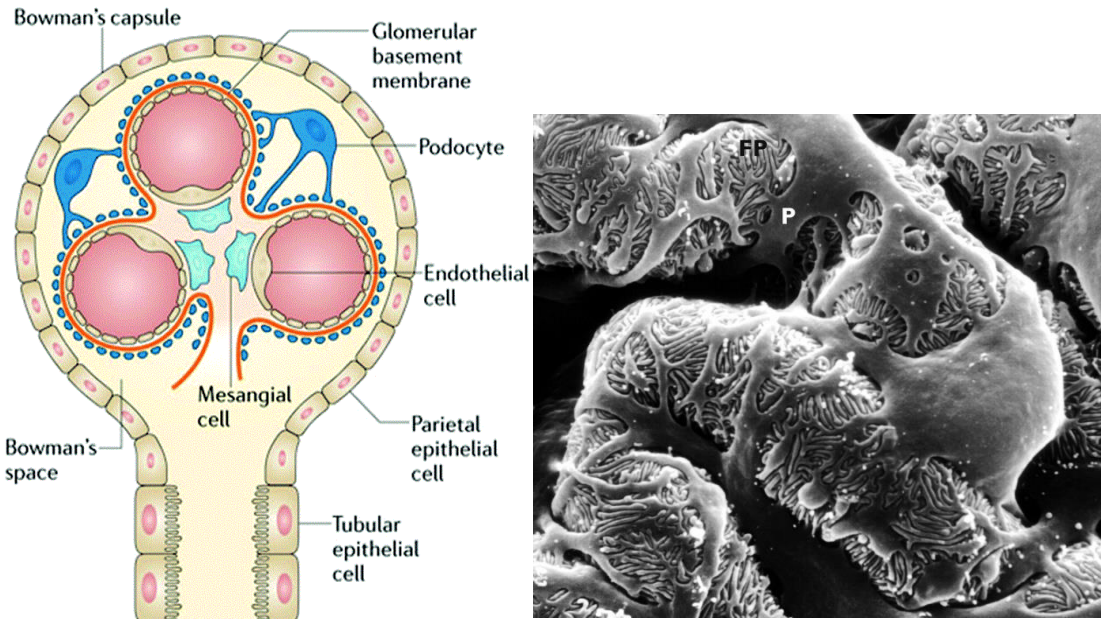

Figure 6: Left: Scheme of a renal corpuscle section with podocytes (blue) enclosing the capillaries (adapted from Kurts et al., 2013). Right: Scanning electron micrograph of wildtype rat podocytes covering the urinary side of the glomerular capillaries. Rat kidney, 6.000x magnification (Pavenstadt et al., 2003)

Podocytes have a distinct polarization in apical and basal cell membrane regions perpendicular to the glomerular basement membrane, and these regions are separated by the intercellular junctions of the foot processes (Holzman & Garg, 2009). The categorization of polarity domains of the podocyte cell membrane is proven to be essential for the cell's ultrastructure and function. It has been shown that loss of the apical polarity protein Crumbs2b leads to disorganization of foot process architecture and absence of slit diaphragms (Ebarasi et al., 2009). Moreover, the podocyte-specific deletion of aPKCι in mice causes foot process effacement and nephrotic syndrome, resulting in early death of the mice (Hirose et al., 2009; Huber et al., 2009). Hartleben and colleagues reported in 2012 that the basolateral polarity protein Scribble is expressed in podocytes and translocates to the developing foot processes during podocyte maturation (see Fig. 7, Hartleben et al., 2012). In contrast to the effect of apical protein complex depletion, they could not detect any anomalies in structure or function of podocyte cells in podocyte-

specific *Scribble* knockout mice, a result that highlights the importance of apical polarity determinants in podocyte differentiation.

The exact (signaling) mechanisms of how podocytes obtain their polarization and orientation, and establish and maintain their dense braiding of foot protrusions are widely unknown.

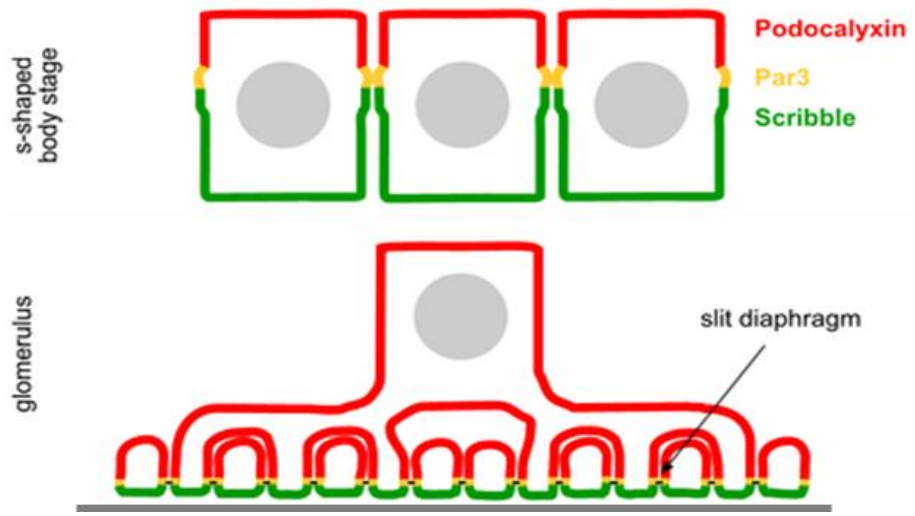

Figure 7: Polarity in podocytes in s-shaped body stage and mature glomerulus. In earlier stages (s-shaped body stage), PAR3 localizes to the apical sited cell junctions, while Scribble appears to be concentrated below PAR3. During podocyte maturation, the apical membrane (in red, marker: Podocalyxin) expands, while the basolateral membrane (in green, marker: Scribble) shrinks in relation to the apical domain. Intercellular junctions (in yellow, marker: PAR3), in glomerular stage with slit diaphragms (black), mark the separation of apical and basolateral membrane domains. Glomerular basement membrane as grey line (Modified from Hartleben et al., 2012).

2.2.3 The slit diaphragm of mammalian podocytes

The filtration slit diaphragm bridges the slit between neighboring podocyte foot processes and can be described as a modified cell junction. The molecular structure of the slit diaphragm shows typical morphological features and protein markers for adherens junctions like P-cadherin, FAT and β-catenin (Inoue et al., 2001; Reiser et al., 2000) as well as scaffold proteins associated with tight junctions like ZO-1, MAGI-1 and MAGI-2 (Hirabayashi et al., 2005; Lehtonen et al., 2005; Schnabel, Anderson, &

Farquhar, 1990). Reiser and colleagues (2000) compared the appearance of slit diaphragms of cultured podocytes in TEM micrographs and found a strong similarity to the zipper-like structure of cadherin-based adherens junctions. They based their model on P-cadherin as a core protein for the slit diaphragm, however this particular hypothesis could not be confirmed in subsequent research. Following studies could show that, apart from numerous typical cell junction proteins, the slit diaphragm is composed of a set of unique proteins that are - in this combination - not found in other junction types, mainly nephrin (NPHS1), NEPH1 and podocin (NPHS2) (Boute et al., 2000; Donoviel et al., 2001; Kestilä et al., 1998). The interaction of these proteins account for the membranous structure of the slit diaphragm as well as for a hetero-oligomeric receptor complex involved in signaling pathways (Barletta et al., 2003; Gerke et al., 2003; Khoshnoodi et al., 2003).

Nephrin (NPHS1) was the first of the slit diaphragm specific protein to be discovered and described by Kestilä et al. (1998). It is a member of the Ig superfamily with a transmembrane domain and eight extracellular IgG-like domains that facilitate protein-protein interactions in the filtration slit. Mutations in the *NPHS1 g*ene cause CNF (congenital nephrotic syndrome of the Finnish type), a hereditary disease characterized by massive proteinuria shortly after birth (Beltcheva et al., 2001). Loss or inactivation of nephrin results in podocyte foot processes effacement and the absence of slit diaphragms (Putaala et al., 2001). In the glomerular podocytes, nephrin is localized at the transition of basal and apical membrane domains. Its extracellular domains are able to interact with the extracellular domains of other nephrin or NEPH1 molecules from neighboring foot processes to form the slit diaphragm (see Fig. 8) (Gerke et al., 2003).

In 2008, Hartleben et al. described a plausible interaction between the junctional complex Nephrin-NEPH1 and the aPKC/Par cell polarity complex. They could show binding of Nephrin-NEPH1 to the aPKC/Par3/Par6 complex, mediated through conserved C-terminal residues in Nephrin/NEPH1 and the PDZ domain of Par3. This study emphasizes the link of cell recognition with cell polarity regulation as being vital for the accurate establishment of intricate cell architecture.

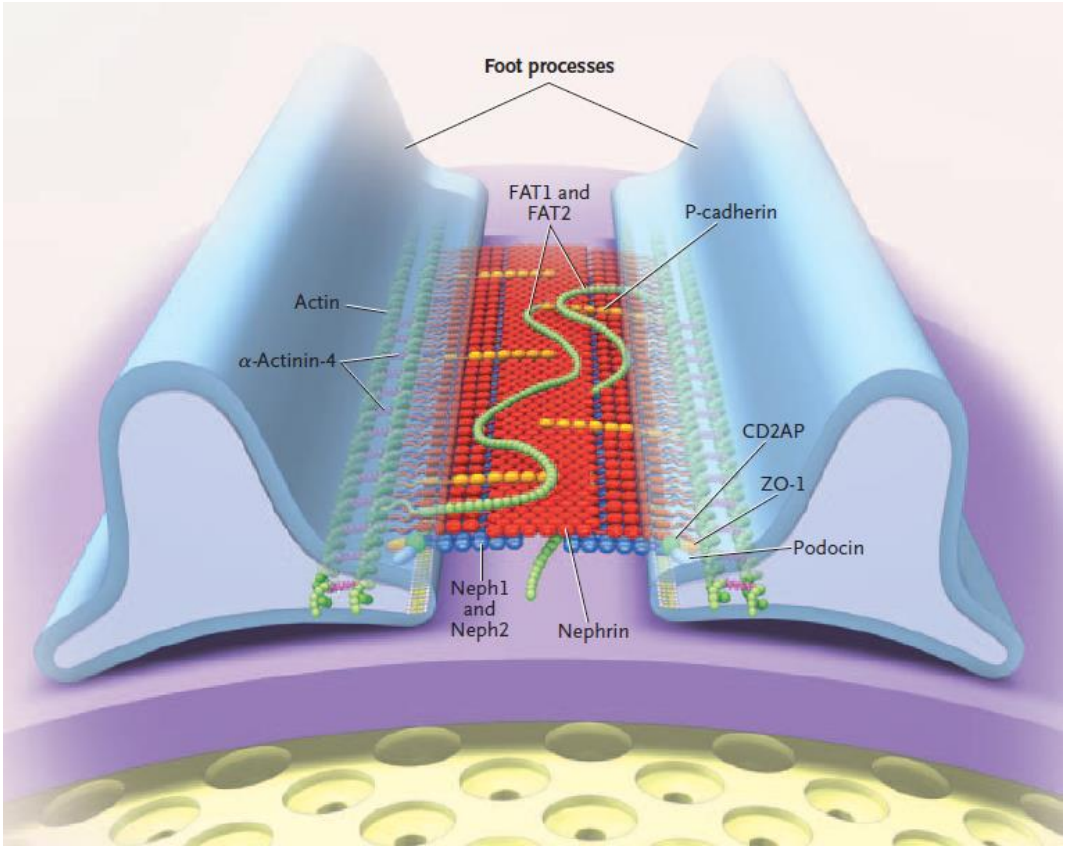

Figure 8: Schematic outline of the glomerular slit diaphragm. Nephrin undergoes homophilic interaction in the small gap between neighboring podocyte foot processes, forming a central dense sheet with pores on both sides. This intercellular junction also contains NEPH-1 and NEPH-2, interacting with each other as well as with nephrin molecules. NEPH and Nephrin molecules interact with the intracellular proteins podocin and CD2-associated protein (CD2AP) which connect the SD protein complex to ZO-1 and actin strands. The slit diaphragm is anchored to the underlying actin cytoskeleton and is involved in several cellular processes like cell polarity, cellular architecture or signaling pathways. Typical adherens junction proteins P-cadherin and FAT proteins are also located at the slit diaphragm. (Simons & Huber, 2008; Tryggvason, Patrakka, & Wartiovaara, 2006).

NEPH1 is a transmembrane domain and contains five extracellular immunoglobulin-like domains (Donoviel et al., 2001). It is part of a family of closely related proteins (NEPH1-3) which bind to the C-terminal domain of podocin (NPHS2) via a conserved podocin-binding motif (Sellin et al., 2002). Loss of NEPH1 leads to podocyte foot processes effacement and proteinuria in newborn mice (Donoviel et al., 2001). NEPH1 molecules interact via their extracellular domains with other NEPH1 or nephrin molecules to form *cis*- or *trans*- homodimerizations and heterodimerizations (Barletta et

al., 2003; Gerke et al., 2003). As per the current model, these particular homo- and heterophilic interactions of nephrin and NEPH1 in the extracellular space between the foot processes generate a porous, but still relatively stable slit diaphragm. However, a new study proposes that the Nephrin and NEPH1 molecules do not form dimers but rather form the podocyte cell junctions as single molecules in a flexible, multilayered manner (Grahammer et al., 2016).

Like the loss of nephrin and NEPH1, the loss of podocin (NPHS2) also results in foot processes effacement and loss of slit diaphragms (Boute et al., 2000; Roselli et al., 2004). Podocin belongs to the stomatin family and is a membrane-associated protein, recruiting its complex partners to cholesterol-rich membrane domains. It interacts with both nephrin and NEPH1 (Huber et al. 2001; Sellin et al., 2002), forming an outside-in signal transducing receptor complex at the intercellular junction that is mediating between extracellular cues and the actin cytoskeleton (George & Holzman, 2012).

2.2.4 Podocyte pathologies

The integrity of the podocytes within the glomerulus is essential for correct glomerular filtration and kidney function. A malfunctioning glomerular filtration barrier (GFB) is a common feature of nephrotic syndrome and although integrity of the GFB depends on each of its three layers, podocytes are considered to be most essential for barrier stability and maintenance (Bierzynska et al., 2015; Menon et al., 2012).

Nephrotic syndrome is a widespread kidney disorder and describes a diverse group of conditions with different manifestations, and underlying causes can be genetic as well as idiopathic. Primary nephrotic syndrome can be triggered by for instance, minimal change disease (MCD), focal segmental glomerulosclerosis (FSGS) or membranous glomerulonephritis (MGN), whereas diabetic nephropathy and lupus nephritis (by systemic lupus erythematosus) are two of the main causes for secondary nephrotic syndrome (Kerjaschki, 2001; Somlo & Mundel, 2000). Typical features of nephrotic syndrome are podocyte foot processes effacement, podocyte detachment from the glomerular basement membrane (GBM), podocyte apoptosis, and GBM thickening (Jefferson et al., 2008; Schena & Gesualdo, 2005; Wolf & Ziyadeh, 2007). In accordance

with the pathobiology, diagnostic criteria for nephrotic syndrome are proteinuria, hypoalbuminemia, hyperlipidemia and edema (Hull & Goldsmith, 2008).

Despite the importance of studying and understanding kidney pathologies, podocyte research was overlooked for many years. However, since the late 1990s and the identification of Nephrin, the value of podocytes and their contribution to kidney function and health practically skyrocketed.

2.3 The insect nephrocyte: a model for the vertebrate podocyte

The invertebrate system has - despite its alterity – many parallels to the mammalian system on molecular and physiological levels. Highly conserved genes and homologous proteins paired with the advantages of insect research (e.g. short generation span, high reproduction rate, simple genetic manipulation, etc.) have made *Drosophila melanogaster* a valuable asset in understanding the basic of human diseases.

2.3.1 The insect excretory system

Opposed to mammals, insects have an open circulation system with the hemolymph fluid filling the body cavity and bathing the organs. Circulation is ensured by muscular movements of the animal and by the dorsal vessel (the insect "heart"). This vessel is a muscular, flexible tube in the thorax and abdomen and maintains the circulation of the hemolymph by pumping the fluid from posterior to anterior through an aorta-like structure into the body. The hemolymph supplies the organs with nutrients and oxygen and receives at the same time their metabolic waste products.

The main excretory and osmoregulatory organs of insects are the Malpighian tubules and nephrocytes. Other than the closed system of a nephron in mammals, the insect excretory organs are spatially and functionally separated into different systems. The Malpighian tubules are two pairs of long, distally closed tubes that open directly into the mid- or hindgut, floating freely in the hemolymph in the anterior (right pair) and posterior (left pair) part of the abdomen (see Fig. 9; Sözen et al. 1997). They regulate the salt and water balance by taking up water, ions, and other molecules from the hemolymph. This filtered

hemolymph is then transported as primary urine via the tubules to the hindgut. While passing through hindgut and rectum, the primary urine is processed to secondary urine and eventually released from the body (Klowden, 2007). Compared to the mammal kidney, the Malpighian tubules represent the proximal and distal convoluted tubules of the nephron.

The nephrocytes are highly specialized, podocyte-like cells responsible for endocytosis, metabolism and/or storage of (toxic) waste. The two main populations of nephrocytes are the pericardial nephrocytes, which are beaded in two strings alongside the dorsal vessel, and the garland nephrocytes, that are surrounding the oesophagus in a ring-like structure.

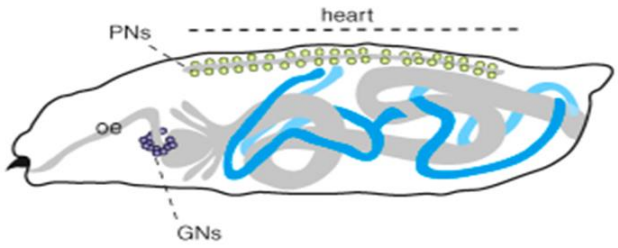

Figure 9: Cartoon of the Drosophila larva with Malpighian tubules (blue), pericardial nephrocytes (PN, green), and garland nephrocytes (GN, violet). The gut system (oesophagus (oe), proventriculus, mid- and hindgut) is depicted in grey, the heart vessel as a thin line at the dorsal side (cartoon from Denholm & Skaer, 2009).

2.3.2 The *Drosophila* garland nephrocyte

The *Drosophila* nephrocyte bears some striking similarities to the mammalian podocyte both in ultrastructure and function.

The garland nephrocytes are binucleate cells of mesodermal origin and reach the average size of 20-30 µm in diameter (Demerec, 1950). In late embryonic stages (between stage 13 and 17), mononucleate garland nephrocyte cells fuse to generate binucleate cells, an event that is at least partly directed by the proteins Sticks-and-stones (Sns) and Kin-of-Irre (Kirre), the *Drosophila* orthologs of Nephrin and Neph1 (Zhuang et al., 2009). Garland nephrocytes are clustered in a population of about 30 cells and surround the oesophagus in a ring-like ("garland") structure, connected by a thin strand, but are otherwise floating freely in the hemolymph.

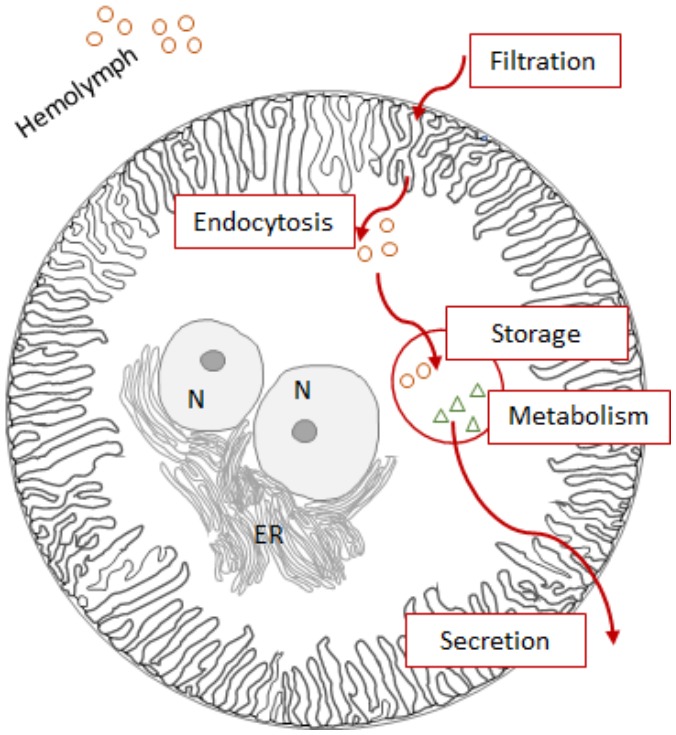

Figure 10: Cartoon of the *Drosophila* nephrocyte and its main functions. The invagination of the plasma membrane leaves a lacuna-like morphology in the cell periphery. In between the lacuna entrances, the nephrocyte diaphragms (thin black line) span the filtration pores. The cell is covered by a basement membrane (outer grey line). Molecules are taken up into the labyrinthine channels and are endocytosed by the cell. N= Nucleus, ER= endoplasmic reticulum. (Graphic adapted from Denholm & Skaer, 2009)

The plasma membrane of the cells is strongly invaginated, leaving a highly complex labyrinthine system of lacunae enclosed by nephrocyte foot processes at the outer cell cortex. The lacuna entrances in between the foot processes are marked by 30 nm wide slit pores that are bridged by so-called nephrocyte diaphragms (ND) (Weavers et al., 2009; Zhang et al., 2013). Each nephrocyte is encompassed by a basement membrane that acts together with the nephrocyte diaphragms as a size- and charge-selective barrier. Molecules are taken up from the hemolymph into the labyrinthine channels and are endocytosed from the sides of the nephrocyte foot processes. Contrary to podocyte filtration where the filtrate is passing the filtration barrier, it is endocytosed and processed or stored by the nephrocytes (see Fig. 10, Denholm & Skaer, 2009).

The major slit diaphragm components of the mammalian podocyte have their *Drosophila* orthologs: nephrin, neph1, podocin, CD2AP and ZO-1 are expressed in the nephrocyte and interact in keeping to the complexes at the podocyte slit diaphragm.

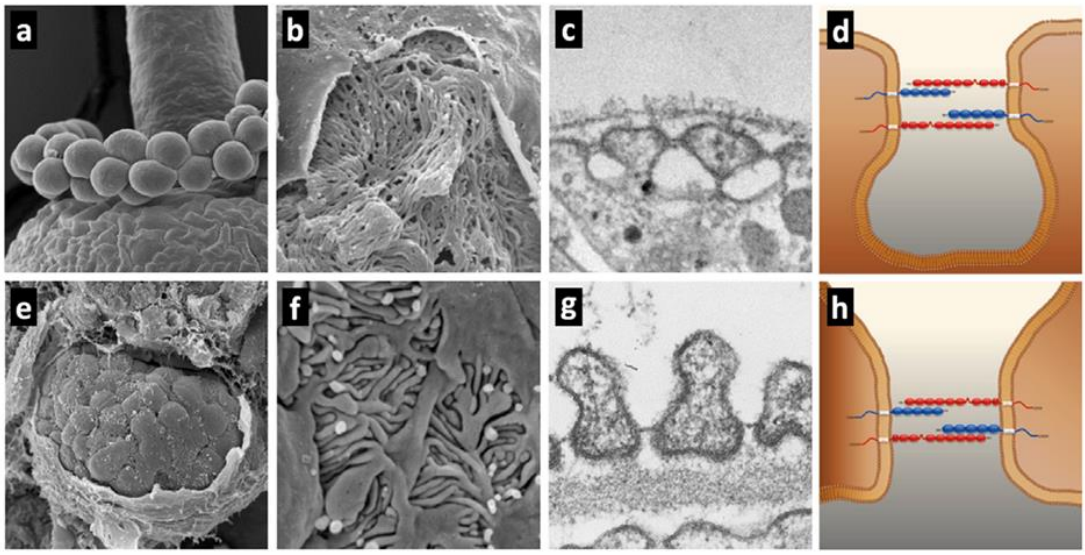

Figure 11: Comparison of Drosophila nephrocyte (upper panels) and murine podocytes (lower panels). The nephrocytes are formed in a garland-like structure near the esophagus (a). The nephrocyte diaphragm underneath the basement membrane (b, c) shows strong resemblance to the vertebrate podocyte foot processes network (f) and slit diaphragm (g). Diaphragms are formed within one nephrocyte (d) or in between adjacent podocyte FPs (h). A single mouse glomerulus covered by the Bowman's capsule (e) (Helmstädter et al., 2012).

2.3.3 The Irre Cell Recognition module

Some proteins of the immunoglobulin superfamily (IgSF) are part of an evolutionary conserved group engaged in cell recognition. In *Drosophila*, these proteins are Irregular Chiasm C/Roughest (IrreC/Rst), Kin of irre (Kirre), Sticks and stones (Sns) and Hibris (Hbs). Fischbach and colleagues (2009) named this group the Irre Cell Recognition module (IRM). The shorter proteins Kirre and Rst create and maintain heterophilic interaction with their partners, the longer proteins SNS and Hbs, to form a functional unit (Fischbach et al., 2009).

In *Drosophila* myogenesis, Kirre (also called Dumbfounded (Duf)) and Rst are expressed in founder myoblasts (Ruiz-Gómez et al., 2000; Strünkelnberg et al., 2001), whereas Sns

and its paralog Hibris (Hbs) are expressed in fusion competent myoblasts (Artero et al., 2001; Bour et al., 2000; Shelton et al., 2009). On the respective cell surfaces, they act as ligand-receptor pairs and mediate myoblast fusion, myotube and muscle development. But the function of these proteins as mediators in cell recognition, cell adhesion and fusion is not restricted to muscle tissue.

Bao and Cagan described in 2005 the interaction and importance of Hibris and Roughest in regulating *Drosophila* eye morphogenesis and patterning. Hibris and Roughest are expressed in complementary cell types, and by mediating the preferential adhesion between them they generate the accurate pattern of interommatidial precursor cells during pupal eye development.

Moreover, all four proteins of the IRM are involved in long range signaling and therefore organizing the structured arrangement of sensory sensilla in the *Drosophila* wing disc. They ensure the regular spaced array of sensory organs by cell recognition and cell sorting processes in early development. All these systems taken together, the Irre Cell Recognition module is vital for organizing repetitive and strictly arranged structures (Linneweber, Winking, & Fischbach, 2015).

2.3.4 The nephrocyte diaphragm in *Drosophila*

The major components of the podocyte slit diaphragm, Nephrin and NEPH1, are co-expressed at the site of the cell junction and form the diaphragm by homo- and heterodimerization via their respective extracellular domains (Kestilä et al., 1998; Liu et al., 2003). Mutations in either of those proteins result in foot processes effacement, loss of slit diaphragms and proteinuria (Donoviel et al., 2001; Kestilä et al., 1998).

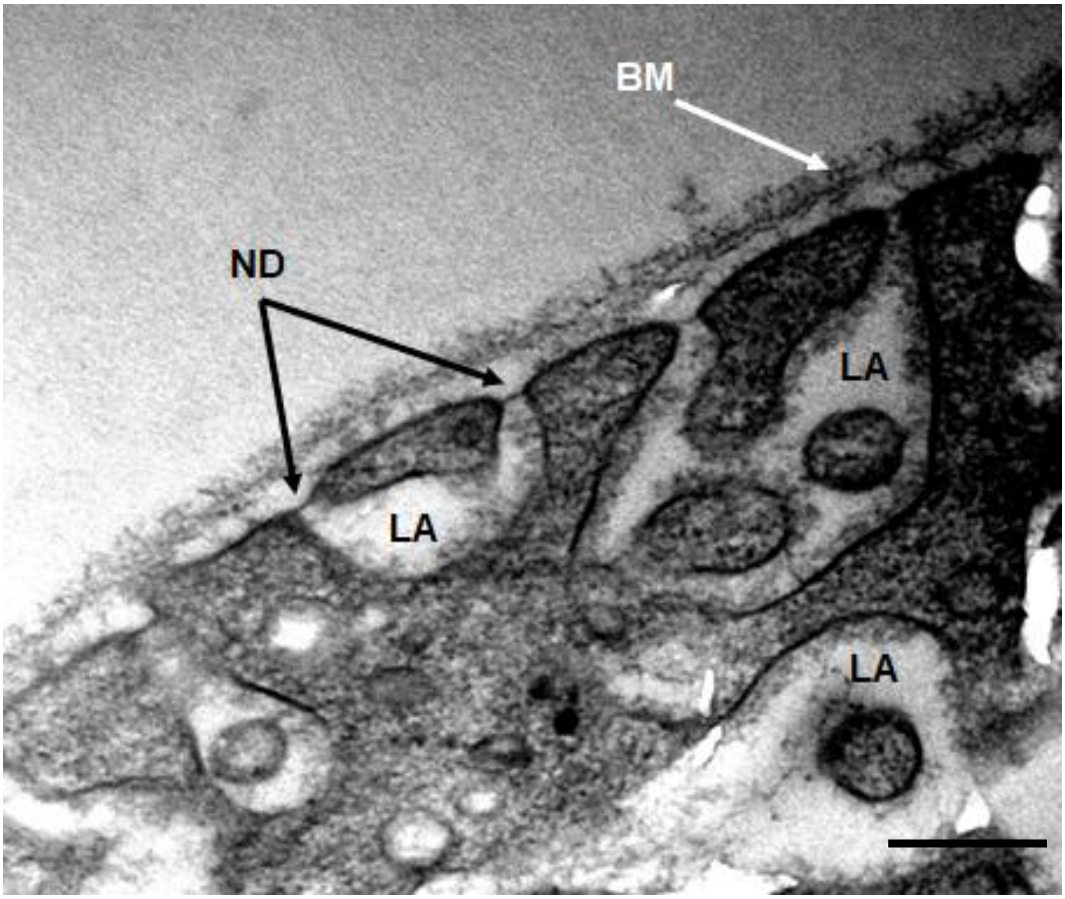

Figure 12: Nephrocyte diaphragm and part of lacuna area. Nephrocyte diaphragms (ND) span membrane-like over small slit pores on the nephrocyte cell surface. Affiliating membrane invaginations open into the lacuna area (LA)/ labyrinthine system. Nephrocytes are enveloped by a basement membrane (BM). TEM micrograph, 30.000x magnification, scale bar= 250nm. Imaged by K. Schadendorf.

The *Drosophila* Nephrin orthologs are Sns and Hbs, the NEPH1 orthologs Kirre and Rst. Sns and Kirre are expressed in the garland nephrocytes from mid embryogenesis on to adulthood and co-localize at the plasma membrane. These two proteins are probably stabilizing each other at the plasma membrane since loss or knockdown of either protein results in loss or mislocalization of the other. Additionally, *Sns* or *Kirre* mutant garland nephrocytes lack nephrocyte diaphragms and form hardly and labyrinthine channels at any stage in their development (Weavers et al., 2009). In consistence, the cell surface of mutants for either *sns* or *hbs* or *kirre* and *rst* is smoothened by the reduction or absence of filtration pores and the normally spherical cell shape is compromised (Weavers et al., 2009; Zhuang et al., 2009). These phenotypical changes, especially of slit diaphragms

and lacunae formation/ foot processes effacement, are described in an analogous way in *nephrin* or *neph1* mutant podocytes.

In context of the IRM, Sns and Kirre are interaction partners in a complementary system and are expressed individually in different cell types. In nephrocytes on the other hand, Sns and Kirre are co-expressed in the same cell and co-localize at cell junctions (Weavers et al., 2009). In the mammalian podocyte, Nephrin and NEPH1 are also co-expressed in the same cell (Barletta et al., 2003), demonstrating the similarity between nephrocyte and podocyte slit diaphragm structure.

In 2008, Hartleben and colleagues found a connection between cell recognition guided by the Nephrin-NEPH1-complex and polarity signaling dependent on the PAR-complex. In vertebrate epithelial cells, the PAR-complex localizes to tight junctions. In podocytes, however, the cell junction is based on a Nephrin-NEPH1-protein complex and typical tight junctions are missing. PAR3 is able to interact with NEPH1 and Nephrin via its first PDZ domain as well as with Nephrin and consequently, inhibition of the PAR-complex (by knockdown of aPKC) leads to a phenotype similar to NEPH1 or Nephrin deletion. Their study emphasizes the link of cell recognition with cell polarity regulation as being vital for the accurate establishment of intricate 3D cell architecture.

The proteins Kirre and Rst are the *Drosophila* orthologs to Neph1 and paralog to each other, functioning redundantly in myoblast fusion (Strünkelnberg et al., 2001). They are expressed in and located at the surface of myoblast founder cells. Both are single-pass transmembrane proteins with five extracellular Ig domains, the intracellular domain has three conserved motifs.

The homology between the podocyte slit diaphragm and nephrocyte diaphragm provides the welcome opportunity for basic research on a notably developed and intricate structure in a simpler, but still highly manipulative setting.

2.4 Aim of study

The establishment of apical-basal polarity is a crucial developmental process, laying the groundwork for developing the cell to a functional entity. Previous studies on apical-basal polarization cover a wide range of different cell types, but the situation in *Drosophila* nephrocytes has not been described yet. This highly specialized cell is utilizied as model system for the mammalian podocyte which is involved in a variety of kidney disorders. Both nephrocyte and podocyte share a fine-tuned and complex cell architecture depending greatly on correct polarity establishment of the cell.

It is unknown to what extent polarity proteins play a role in the particular constructed nephrocyte cell. In this study, the influence of apical and basal polarity proteins on nephrocyte structure and function was analyzed, following previous research by Hartleben et al. who described a direkt interaction between Nephrin/ NEPH1 and aPKC. We investigated the effect of single knockdowns of apical and basal polarity proteins on localization, filtration/ accumulation ability and ultrastructural development in *Drosophila* nephrocyte cells. Moreover, the impact of a phosphorylation-mutant Baz on nephrocyte development was evaluated.

3 MATERIALS AND METHODS

3.1 Material

3.1.1 Solutions and media

Solutions were prepared with distilled water and either autoclaved or sterile-filtered.

Table 1: Solutions and media

Name	Composition	Usage
2x SDS Loading Buffer	126 mM Tris (pH 6,8), 4% SDS; 0.2% bromophenol blue, 20% glycerol, 200 mM DTT	SDS-PAGE
6x DNA loading dye	3 ml 30% glycerol, 35 mg bromophenol blue, 10 ml H_2O	DNA preparation
Apple juice agar	10g Agar, 340ml apple juice, 17g sugar, 30ml 10% Nipagin; adj. 1 L ddH2O	Collecting eggs and larvae
Buffer P1/S1	50 mM Tris-HCl, 10 mM EDTA, 100 µg/ml RNase A	Protein purification
Buffer P2/S2	20 mM NaOH, 3.5 mM SDS	Protein purification
Buffer P3/S3	3 M Potassium acetate	Protein purification
Coomassie Brilliant Blue (CBB) solution	15,6 M methanol, 4 mM conc. Coomassie Brilliant Blue, 1,6 M Acetic Acid	Protein purification
DAPI	0.5 µg/µl (working conc.)	DNA staining

Table 1 continued

Name	Composition	Usage
Embryo glue	Glue from adhesive tape (Tesa®), dissolved in Hexan	Microinjection of *Drosophila* embryos
Epoxy resin	23 g glycerol ether, 15.4 g DDSA (Dodecenylsuccinic anhydride), 10.2 g MNA (Methyl nadic anhydride), 0.77 g DMP (2,4,6-Trisdimethylamino-methylphenol)	Embedding medium TEM
Ethanol	70% or 99.9% p.a.	DNA isolation
Fly food	712 g cornmeal, 95 g soy flour, 168 g dry yeast, 450 g malt extract, 150 ml 10% nipagin (700 ml 99% ethanol, 300 ml H2O, 100 g Nipagin), 45 ml propionic acid, 50 g agar, 400 g sugar beet syrup, in 9.75 l H2O.	Standard fly food (kindly provided by Schneuwly Lab, University of Regensburg)
Glutathione elution buffer	30 mM glutathione, 50 mM TRIS-HCl pH 7.5, 150 mM NaCl	Protein purification
Heat fixation saline	0.4% NaCl, 0.03% Triton X-100	Fixation saline
HL3.1 saline	4.10 g NaCl, 0.37 g KCl, 0.22 g CaCl2 dihydrate, 0.81 g MgCl2 hexahydrate, 0.84 g NaHCO3, 1.7 g Trehalose, 39.36 g Sucrose, 1.19 g HEPES; adj. 1 L, pH 7.1	Dissection saline for Drosophila larval tissue
Injection Buffer	5 mM KCl, 0.1 mM sodium phosphate, pH 6.8	Microinjection of *D.* embryos

Table 1 continued

Name	Composition	Usage
Injection buffer (10x)	5 mM KLc, 0.1 mM $NaPO_4$, pH 6.8	Injection
LB_0 medium	10 g tryptone, 5 g yeast extract, 10 g NaCl; adj. 1L	*E. coli* liquid culture medium
LB_0 Plates	10 g tryptone, 5 g yeast extract, 5 g NaCl, 15 g Agar-Agar, pH 7.0	*E. coli* culture plates
LEW buffer (2M)	1x PBS, 2M NaCl	Protein purification
LEW buffer (300 mM)	1x PBS, 300 mM NaCl	Protein purification
Lysis buffer	TNT buffer, Pepstatin A, Leupeptin, Aprotinin, PMSF (1:500 each)	Protein purification
Methylene blue solution	A pinch of methylene blue powder in 0.1% TAE	DNA preparation
Mowiol	4.8 g Mowiol 4-88, 12 g glycerol, 36 ml PBS	Mounting medium LSM
PBS (10x)	58.44 g/mol NaCl, 74.55 g/mol KCl, 141.96 g/mol Na_2HPO_4, 136 g/mol KH_2PO_4	Washing Buffer, 10x stock
PBTw	1x PBS, 0.1% Tween-20	Washing buffer
PBTx	1x PBS, 0.1% Triton X-100	Washing buffer
PFA	4 g para-formaldehyde in 100 ml 1x PBS	Fixation

Table 1 continued

Name	Composition	Usage
Richardson's Staining solution	Sol. A.: 100 ml tristilled water, 1 g azure II; Sol. B.: 100 ml tristilled water, 1 g borax anhydrous, 1 g methylene blue	Histological staining
SDS Running Buffer (10x)	1.92 M glycine, 250 mM Tris, 1% SDS	SDS- PAGE
T4 ligase buffer	400 mM Tris-HCl, 100 mM $MgCl_2$, 100 mM DTT, 5 mM ATP	Ligation
TAE (1x)	2 mM Tris, 1 mM EDTA, 4 mM AcOH	Agarose gel electrophoresis
TNT buffer	150 mM NaCl, 50 mM Tris, 8 mM Triton X-100	Protein purification
YTA medium	16 g tryptone, 10 g yeast extract, 5 g NaCl; adj. 1L	Protein purification

3.1.2 Reagents, (bio)chemicals and kits

Following reagents, chemicals and commercial kits were used in this study. Kit reactions were performed according to manufacturer's instructions.

Table 2: Reagents, (bio)chemicals and kits

Name	Usage	Company
Agar	Bacterial growth	Roth, Karlsruhe
Ampicillin	Selection of *E. coli*	Roth, Karlsruhe
Aprotinin (2 µg/ml)	Protease inhibition	Roth, Karlsruhe
APS, Ammonium peroxidisulfate	SDS-Page	Thermo Fisher Scientific, Waltham
Bradford Roti®-Quant	Protein concentration measurement	Roth, Karlsruhe
Bromophenol blue	Loading dye	Bio-Rad, Munich
BSA, Fraction V	Immunhistology	Roth, Karlsruhe
CaCl2 dihydrate	HL3.1 saline	Merck, Darmstadt
Chloramphenicol	Selection of *E. coli*	Roth, Karlsruhe
Coomassie Brilliant Blue	Protein purification	Thermo Fisher Scientific, Waltham
dNTPs (dATP, dCTP, dGTP, dTTP)	PCR	Thermo Fisher Scientific, Waltham
dodecyl sulfate (SDS) ultrapure	SDS-PAGE	AppliChem, Darmstadt
DTT, 1,4-Dithiothreitol	Protein purification	Roth, Karlsruhe

Table 2 continued

Name	Usage	Company
Ethidium bromide	Agarose gel electrophoresis	Sigma-Aldrich, St. Louis
Ethylendiamintetraacetate (EDTA)	Buffer P1/S1	Sigma-Aldrich, St. Louis
Glutardialdehyde	Fixation	Fluka Chemie AG, Buchs
Glycerol	Various applications	Roth, Karlsruhe
HEPES	HL 3.1 saline	Roth, Karlsruhe
Isopropyl-β-D-thiogalactopyranosid (IPTG)	protein purification	Roth, Karlsruhe
Kanamycin	Selection of *E. coli*	Roth, Karlsruhe
KCl	Injection	Merck, Darmstadt
Leupeptin (2 µg/ml)	Protease inhibition	Roth, Karlsruhe
Lysozyme	Protein purification	Sigma-Aldrich, St. Louis
Mercaptoethanol, 2-	Protein purification	Merck, Darmstadt
$MgCl_2$ hexahydrate	HL3.1 saline	Merck, Darmstadt
N,N,N',N'-tetramethylethylenediamine (TEMED)	SDS-Page	Roth, Karlsruhe
NaCl	Various applications	Merck, Darmstadt
NaHCO3	HL3.1 saline	Merck, Darmstadt

Table 2 continued

Name	Usage	Company
NHS	Immunhistology	Pan - Biotech GmbH
Nipagin (methylparaben)	Fly food	Sigma-Aldrich, St. Louis
NucleoBond® PC100	DNA isolation	Macherey-Nagel, Düren
NucleoSpin® Gel and PCR cleanup	DNA preparation	Macherey-Nagel, Düren
Oil 10 S VOLTALEF®	injection for transgenic fly generation	VWR, Radnor
para-Formaldehyde	Fixation	Merck, Darmstadt
pENTR/D-TOPP Cloning Kit	Gateway cloning	Thermo Fisher Scientific, Waltham
Pepstatin A (2 µg/ml)	Protease inhibition	Roth, Karlsruhe
PMSF (0.5 M)	Protease inhibition	Roth, Karlsruhe
Protino glutathione Agarose 4B	Protein purification	Macherey-Nagel, Düren
RNAse A	Buffer P1/S1	Roth, Karlsruhe
Sodium Cacodylate	EM	Roth, Karlsruhe
Sucrose	HL 3.1 saline	Roth, Karlsruhe
Trehalose	HL 3.1 saline	Roth, Karlsruhe
Tris Base	buffering	Sigma-Aldrich, St. Louis

Table 2 continued

Name	Usage	Company
TritonX-100	Immunhistology	Roth, Karlsruhe
Tween-20	Immunhistology	Roth, Karlsruhe
Uranyl acetate	EM	Fluka Chemie AG, Buchs
GeneRuler 1 kb DNA ladder	Agarose gel electrophoresis	Thermo Fisher Scientific, Waltham
GeneRuler 100 bp DNA ladder	Agarose gel electrophoresis	Thermo Fisher Scientific, Waltham

3.1.3 Plasmids

Plasmids were obtained from GE Healthcare Life Sciences (Amersham, UK), Invitrogen (Carslbad, USA), and Murphy lab (Carnegie Institution for Science, Baltimore, USA).

Table 3: Plasmids

Plasmid	Description	Source
pENTR™	Gateway cloning	Thermo Fisher Scientific
pGEX6P1	Gateway cloning	GE Health Care Life Sciences
pTWH	Gateway cloning	Murphy lab

3.1.4 Oligonucleotides

Following oligonucleotides were used for cloning and sequencing of the desired gene constructs. They were designed with DNADynamo (BlueTractorSoftware, UK) and synthesized by Metabion international AG (Planegg, Germany) or Microsynth AG (Balgach, Switzerland). The oligonucleotides were resolved in sterile de-ionized H_2O to the final concentration of 50 pmol/µl (stock solution).

Table 4: List of oligonucleotides for cloning and sequencing

Name	Sequence 5'-3'
Baz-shRNA-2-F	CTAGCAGTGCTCTAAGTCCAAGTCAAACGTAGTTATA TTCAAGCATACGTTTGACTTGGACTTAGAGCGCG
Baz-shRNA-2-R	AATTCGCGCTCTAAGTCCAAGTCAAACGTATGCTTGA ATATAACTACGTTTGACTTGGACTTAGAGCACTG
sns-intra-AscI-F	AAAGGCGCGCCTTCATCAGCGCCGCAAG
sns-AscI-R	AAAGGCGCGCCTATACGAGGTGTCCGTCC
GST-Seq-F	TGCGTTCCCAAAATTAGTTTG
GST-Seq-R	GACGGGCTTGTCTGCTCCCG
Valium20-seq-F:	ACCAGCAACCAAGTAAATCAAC
Valium20-seq-R	GCGGCTCTAGTTCTTTGC

3.1.5 Enzymes

Following enzymes were used for restriction digests, ligations, and other enzymatic reactions.

Table 5: List of enzymes

Name	Utilization	Company
AscI	Restriction digest	Thermo Fisher Scientific
BstBIS	Restriction digest	Thermo Fisher Scientific
SacII	Restriction digest	Thermo Fisher Scientific
SmaI	Restriction digest	Thermo Fisher Scientific
Gateway® LR Clonase™	Gateway cloning	Thermo Fisher Scientific
T4 Ligase	Ligation	Thermo Fisher Scientific
FastAP Alkaline Phosphatase	Dephosphorylation	Thermo Fisher Scientific
Pfu.s. Polymerase	PCR	Lab internal (kindly provided by Schneuwly lab, University of Regensburg)

3.1.6 Antibodies

Antibodies were diluted in PBT_w and BSA/ NHS shortly before use (see chapter 3.6). The antibody-mixes were used at 4°C/ on ice unless stated otherwise.

Table 6: List of primary antibodies

Target	Species	Use	Dilution	Origin/Reference
αaPKC	Rabbit	IF	1:500	Santa Cruz, #sc-216
αBazooka PDZ1-3	Guinea Pig	IF	1:400	Homemade (Krahn lab)
αDE-Cadherin	Rat	IF	1:5	DSHB Cat#DN-Ex #8, RRID:AB_528121
αDlg	Mouse	IF	1:25	DSHB Cat# 4F3 anti-discs large, RRID:AB_528203
αGFP	Chicken	IF	1:2000	Aves Lab #1020
αGFP	Mouse	IF	1:500	Santa Cruz, #sc-9996
αKirre	Rabbit	IF	1:200	Fischbach Lab, Freiburg
αPar1	Rabbit	IF	1:200	St. Johnston Lab
αPar6	Rat	IF	1:400	Homemade (Krahn lab)
αSns	Chicken	IF	1:1000	Homemade (Krahn lab)

Table 7: List of secondary antibodies

Antibody	Use	Dilution	Origin/Reference
Alexa Fluor 488 anti-Chicken	IF	1:200	Thermo Fisher, #A-11039
Alexa Fluor 488 anti-Guinea Pig	IF	1:200	Thermo Fisher, #A-11073
Alexa Fluor 488 anti-Mouse	IF	1:200	Thermo Fisher, #A-32723
Alexa Fluor 488 anti-Rabbit	IF	1:200	Thermo Fisher, #A-11034
Alexa Fluor 568 anti-Chicken	IF	1:200	Thermo Fisher, #A-11041
Alexa Fluor 568 anti-Guinea pig	IF	1:200	Thermo Fisher, #A-11075
Alexa Fluor 568 anti-Mouse	IF	1:200	Thermo Fisher, #A-11004
Alexa Fluor 568 anti-Rabbit	IF	1:200	Thermo Fisher, #A-11011
Alexa Fluor 568 anti-Rat	IF	1:200	Thermo Fisher, #A-11077
Alexa Fluor 647 anti-Chicken	IF	1:200	Thermo Fisher, #A-21449
Alexa Fluor 647 anti-Guinea pig	IF	1:200	Thermo Fisher, #A-21450
Alexa Fluor 647 anti-Mouse	IF	1:200	Thermo Fisher, #A-32728
Alexa Fluor 647 anti-Rabbit	IF	1:200	Thermo Fisher, # A3-2733
Alexa Fluor 647 anti-Rat	IF	1:200	Thermo Fisher, #A-21247

3.1.7 Instruments and software

Table 8: List of instruments

Instrument	Utilization	Company
Eco-Mini System E	SDS-PAGE	Analytik Jena , Jena
Evolution™ 201/220 UV-Vis-Spectrophotometer	Spectrophotometer	Thermo Fisher Scientific
InjectMan NI2	Microinjection	Eppendorf, Hamburg
Light table	DNA visualization	Dörr/ Danubia, Neu-Ulm
LSM 710 Meta	Confocal microscopy	Carl Zeiss, Jena
Master Cycler Nexus Gradient	PCR	Eppendorf, Hamburg
NanoDrop® 1000	DNA concentration	Eppendorf, Hamburg
Stereo microscope/ binocluar	Dissecting, Preparations, Lethality tests	Motic, China
Thermomixer®	Heating	Eppendorf, Hamburg
UV transilluminator	DNA visualization	Intas, Göttingen
Zeiss CEM 902	TEM	Carl Zeiss, Jena

Table 9: List of software and data bases

Software/ data base	Application	Company
Adobe Photoshop CS5	Image processing	Adobe Systems Inc.
DNADynamo	Design and sequence check of DNA constructs	BlueTractorSoftware, UK
Flybase	database for *Drosophila* genetics	
ImageJ	Calculating GFP intensity, nephrocyte diaphragm ratio	NIH, USA, version1.49p
NCBI	database for biomedical and genomic information	
Zen 2 black edition	Image processing	Carl Zeiss, version 10.0.0.910
Zen 2.1 lite blue edition	Image processing	Carl Zeiss, version 6.1.7601
ZEN 2010 software	Confocal microscopy	Carl Zeiss, Jena

3.2 Molecular methods

3.2.1 PCR (Polymerase chain reaction)

DNA fragments of the desired genes were amplified by the PCR method (Mullis & Faloona, 1987) according to standard protocols. Reactions were done in 25 µl or 50 µl total reaction volume. Typically, 20-100 ng/µl of plasmid DNA were mixed with 200 nM of forward and reverse primer, 250 µM of each dNTP (Bioline), 0.7 µl polymerase (for 50 µl total volume), 5-10 µl of the corresponding reaction buffer, and adjusted with sterile distilled H_2O to 50 µl total volume. For most applications Pfu S polymerase (lab internal) was used.

For running PCR, the thermocycler Master Cycler Nexus Gradient (Eppendorf, Germany) was used. If needed, PCR programs were adjusted from standard conditions (see tab. 10) to fit specific primer requirements.

Table 10: Standard PCR program

Step	Temperature	Time
1. Initial denaturation	95 °C	5 min
2. Denaturation	95 °C	30 sec
3. Annealing	Depending on primer sequence 50-65 °C	20 - 30 sec
4. Elongation	72 °C	Depending on product length (1 min/kb)
Repeat steps 2.-4.: 30x		
5. Final elongation	72 °C	5 -10 min
6. Pause	10 - 12 °C	-

3.2.2 Agarose gel electrophoresis

DNA fragments were analyzed via agarose gel electrophoresis. First, The samples were mixed with the adjusted amount of 6x loading dye (Thermo Fisher Scientific) and run in parallel with 10 µl GeneRuler 1 kb or 100bp (Thermo Fisher Scientific). DNA fragments from enzymatic digestion were run in 1% (> 500bp) or 2% (<500 bp) agarose gels containing TAE buffer and 0.5 µg/ml ethidium bromide. PCR products and digested vectors were run in analogous gels without ethidium bromide and post-stainined with methylene blue solution. Gels were run approx. 20 minutes at 120-140 V. Resulting DNA bands treated with ethidium bromide were visualized and documented with a UV transilluminator (Intas), methylene blue stained gels were processed on a light table (Danubia).

For purification of PCR products, the kit Nucleo Spin®Gel (Macherey-Nagel) was used according to the manufacturer protocol. The samples were eluted in 30 µl autoclaved distilled H_2O.

3.2.3 Measurement of DNA concentration

The concentration and qualitiy of purified DNA was measured with a NanoDrop 1000 spectrophotometer (Thermo Fisher Scientific). The absorption maximum for double-stranded DNA lies at 260 nm, for protein contaminations at 280 nm. The ratio of these values denotes the purity of DNA solution. If possible, DNA concentration of Midi-preparations was adjusted to 1 µg/µl.

3.2.4 Enzymatic reactions

Applying the methods of molecular cloning, DNA fragments were prepared to be used in generation of transgenix flies or antibody production.

The desired DNA sequence was obtained from PCR and purified (see chapter 3.2.1 et seq.). Next, entry vector and PCR products were digested with the same enzyme to fabricate matching DNA strand ends. 26 µl of PCR elution sample was mixed with 1 µl

of enzyme and 3 µl corresponding buffer, and incubated at 37°C for 2 hours. If needed, enzymes were inactivated at 82°C for 20 minutes.

For vector preparation, 1 µg of vector DNA (pENTR) was mixed with 2 µl enzyme, 4 µl correspoding buffer and 33 µl sterile distilled H_2O, and incubated at 37°C overnight. The vector-enzyme solution was purified via methylene-blue agarose gels (see chapter 3.2.2) and eluted in 26 µl H_2O. For the dephosphorylation of the vector, 1 µl of FastAP Thermosensitive Alkaline Phosphatase (Thermo Fisher Scientific) was added and incubated at 37°C for 30 minutes. The dephosphorylation reaction was inactivated by incubating the solution at 75°C for 20 minutes.

Finally, digested DNA fragments and vector were ligated with the T4 ligase (Thermo Fisher Scientific). For each sample, three ligation reactions were prepared (see tab. 11) to achieve optimal ligation results and verify vector quality. The reactions were incubated at room temperature (21°C) overnight and subsequently transformed into DH5α cells (see chapter 3.6.5).

Table 11: Ligation reaction

Components	Setup 1, ratio 1:1	Setup 2, ratio 1:4	control
H_2O	16.8 µl	15.3 µl	17.3 µl
T4 ligase buffer	2 µl	2 µl	2 µl
Vector	0.5 µl	0.5 µl	0.5 µl
Insert	0.5 µl	2.0 µl	-
T4 ligase	0.2 µl	0.2 µl	0.2 µl

For analytical digestions of plasmid DNA, 10 µl of DNA amplified in Mini-preparation (see 3.6.6) was added to a pre-mixed solution of restriction enzymes, the corresponding buffer and water. The total volume of the digest reaction was 20 µl, set up in compliance with manufacturer's instructions (Thermo Fisher Scientific) and the samples were run on

agarose gels (see 3.2.2). To obtain specific patterns of DNA fragments, enzymes were chosen according to their restriction sequence predicted in DNADynamo. The correct constructs were confirmed by the unique band patterns visible in the agarose gel and negative samples could be revealed.

3.2.5 Transformation of chemically competent *E. coli* cells

Different chemical competent *E. coli* cells were transformed with previous prepared plasmid DNA for DNA amplification or protein expression (see chapter 3.3). Per sample, 100µl of frozen *E. coli* cells were thawn on ice, inoculated with 100 ng of purified plasmid DNA and incubated on ice for 30 minutes. Then, the cells were heatshocked at 42°C for 1 minute in a thermoblock (Eppendorf) and immediatley cooled on ice for 5 minutes. After adding 400 µl of LB medium, the cells were shaken at 37°C for 45-60 minutes and at last plated on pre-warmed LB plates containing the corresponding antibiotic for selection purposes.

Table 12: Bacterial strains for transformation

Strain	Genotype	Application	Source
DH5α	φ80dlacZΔM15, Δ(lacZYAargF) U169, deoR, recA1, endA1, hsdR17 (rK-, mK+), phoA, supE44, λ-, thi-1, gyrA96, relA1	Amplification of plasmid DNA	Invitrogen
BL21 Star™(DE3)	F-*omp*T *hsd*SB (rB-, mB-) *gal dcm rne*131	Expression of recombinant proteins	Invitrogen

3.2.6 Isolation of plasmid DNA – Mini preparation

DNA plasmids were amplified in transformed *E. coli* cells and isolated via alkaline lysis with SDS. Per sample, 2 ml of LB medium including antibiotic were inoculated with a single colony of transformed *E. coli* and incubated shaking at 37°C for 6-8 hours or overnight. Cell pellets were obtained by centrifugating the samples at 6000 rpm for 1 minute. Pellets were resuspended in 100 µl buffer P1 (including 100 µg/ml RNAse A) and vortexed. 200 µl of buffer P2 were added and the solution was vortexed, followed by adding 150 µl buffer P3 and mixing by inversion 3-4 times. The samples were centrifuged at 14.000 rpm for 6 minutes at 4°C and the supernatant was transferred to fresh Eppendorf cups filled with 900 µl 99 % EtOH. After thorough mixing, the solution was centrifuged at 14.500 rpm for 12 minutes at 4°C, and the supernatant was discarded. The resulting pellets were washed by adding 1 ml of 70 % EtOH, spun down at 14.000 rpm for 3 minutes, and subsequently dried in a 65°C drying incubator until all residual Ethanol evaporated. The dried DNA pellets were resuspended in 25 µl sterile, distilled H_2O. 10 µl of Mini-preparation DNA was used in test restriction digest (20 µl total volume) to confirm the correct construct via agarose gel electrophoresis (see 3.2.4).

3.2.7 Isolation of plasmid DNA – Midi preparation

The preparation of high-quality plasmid DNA in sufficient amounts requires adjustments in the isolation method, therefore the kit NucleoBond® PC 100 (Macherey-Nagel) was used and performed according to the enclosed protocol. The basic principle of alkaline lysis with SDS remained.

55-65 ml LB medium was inoculated with 20 µl of Mini-culture (see 3.6.6) and incubated overnight (max. 12 hours) shaking at 37°C. The culture was then centrifuged at 5000 rpm for 5 minutes. The bacterial pellet was completely resuspended in 4 ml buffer S1, mixed with 4 ml buffer S2 and incubated for 3 minutes. After adding 4 ml buffer S3, the solution was thoroughly vortexed, incubated for 5 minutes on ice, and mixed again. The supernatant obtained from centrifugation at 10.000 rpm for 8 minutes was then filtered through a primed column. The column was washed twice with washing buffer N3. Eventually, the DNA was eluted from the column with 5 ml elution buffer N5, mixed

well with 3.5 ml isopropanol and centrifuged at 12.000 rpm for 30 minutes at 4°C. The DNA pellet was washed with 4-6 ml 70 % EtOH p.a. at 12.000 rpm for 10 minutes. After discarding the supernatant, the pellet was dried thoroughly in the 65°C drying incubator and dissolved in 100 µl sterile, distilled water. Concentration and quality were measured (see 3.2.3) before proceeding.

3.2.8 Sequencing

Prior to further usage, the plasmid DNA generated in Midi-preparation was analyzed externally at Seqlab/ Microsynth (Göttingen, Germany). For this purpose, 1.2 µg plasmid DNA and 30 pmol sequencing primer were filled up with sterile, distilled H_2O to 15 µl and sent immediately to Seqlab/ Microsynth.

3.2.9 Gateway cloning

The innovative Gateway™ cloning technology has been used for efficient and accurate cloning of the desired construct into specific destination vectors. In this study, this method was used for the generation of transgenic flies.

The transfer from the pENTR vector to the destination vector is achieved via a LR recombination reaction mediated by the enzyme λ integrase (Gateway® LR Clonase™). The ORF/gene of interest in the pENTR vector is flanked by *attL1* and a*ttL2* recombination sites, while the gene *ccd*B gene in the destination vector is flanked by *attR1* and *attR2* recombination sites. λ integrase catalyses a direction-specific recombination reaction where the ORF and *ccd*B are exchanged, and flanked by new recombination sites *attB1/B2* and *attP1/P2*, respectively. The resulting expression clone can be selected by ampicillin resistance, while the by-product clone carries Kanamycin-resistance and the lethal *ccd*B gene sequence (Hartley, Temple, & Brasch, 2000).

The gene of interest was first cloned into the pENTR vector and screened for accuracy by sequencing. Then, 100 ng of pENTR vector and 90 ng of destination vector were mixed with 0.4 µl of clonase mix. The solution was incubated at 25°C for 1 hour and subsequently transformed into DH5α cells. Positive clones were selected by ampicillin resistance and toxic effects of *ccd*B gene product on standard *E. coli* strains.

3.3 Biochemical methods

3.3.1 Protein purification

For the expression of the tagged protein fragment 200 ml YTA medium were inoculated with 2ml overnight culture of BL21* bacteria carrying the desired plasmid. Cultures were shaken at 240 rpm at 37°C until they reached OD_{600} of 0.6 and then shortly chilled on ice. During cooling down, 2% (of the final volume) of ethanol p.a., 3% of KH_2PO_4 and IPTG to a final concentration of 0.5 mM were added to induce protein expression. The cultures were subsequently incubated at 18°C overnight. To harvest the bacteria, the cultures were centrifuged at 6000 rpm for 5 minutes and the pellet was frozen at -80°C for at least 30 minutes. Afterwards, the pellet was resuspended in 10ml of Lysis buffer containing 1% TritonX-100, protease inhibitors and 10mM β-mercaptoethanol, and then carefully shaken at 4°C for 30 minutes. To break up all the cells, the solution was sonicated for 15 seconds in six cycles, shaken again for 10 minutes on ice, and mixed with lysozyme (final concentration 1 mg/ml). The lysate was vortexed for 2 seconds immediately after adding the enzyme, after 2 minutes and 4 minutes, and finally centrifuged at 11.500 rpm for 15 minutes at 4°C.

The fusion proteins were purified with 10 µl of Protino glutathione Agarose 4B beads (GST) per milliliter of supernatant and incubated for two hours shaking at 4°C. Following incubation, the beads were washed once with LEW 300 mM NaCl, once with LEW 2 mM NaCl, and again with LEW 300 mM NaCl. In each washing step, the beads were incubated shortly in the washing buffer and then centrifuged for 30 seconds at 3500 rpm. GST fusion protein was eluted in glutathione elution buffer. For a higher yield, several batches were separately inoculated, purified and finally pooled.

3.3.2 Measuring protein concentrations

Protein concentrations in solutions were estimated via Bradford Assay. Per sample, 200µl Roti-Quant (Roth) were mixed with 800µl H_20 and 10µl of the protein solution. The absorption was measured at 595 nm with a spectrophotometer (Thermo Scientific). A BSA standard curve was used for calibration.

3.3.3 SDS-polyacrylamide gel electrophoresis

Proteins were analyzed and checked for accuracy and quality by electrophoretic separation via SDS-polyacrylamide gel electrophoresis (SDS-PAGE). 10% resolving gels with a 5% stacking gel were used (see tab. 13). The protein samples were mixed with 2x SDS loading buffer at a ration of 1:1 and boiled at 95°C for five minutes, shortly spun down and loaded into the gel pockets. As a (size) marker of molecular weight, 3-5 µl of PageRuler Prestained Protein Ladder (Thermo Scientific) were loaded. Gels were run in 1x SDS running buffer at 120V for 1 hour.

Table 13: SDS-PAGE gel recipe

Resolving gel 10%		Stacking gel 5%	
Water	3.65 ml	Water	3.5 ml
Acrylamide	5 ml	Acrylamide	830 µl
1 M Tris-HCl pH 8.8	5.75 ml	1 M Tris-HCl pH 6.8	630 µl
10% SDS	150 µl	10% SDS	50 µl
10% APS	150 µl	10% APS	50 µl
TEMED	6 µl	TEMED	5 µl

3.3.4 Antibody production

A sufficient amount of recombinant Sns for polyclonal antibody production was prepared in the lab and subsequently sent to Davids Biotechnologie GmbH (Regensburg) for further preparation and animal injection. The Sns antibody was raised in chicken egg. The specificity of this antibody was tested and verified via immunostainings.

3.4 Fly genetics and methods

3.4.1 Fly breeding

Fly stocks were kept in glass vials with standard food (Ashburner, 1989) with some dry yeast added on top. The standard medium was made of 712 g cornmeal, 95 g soya flour, 168 g dry yeast, 450 g malt extract, 150 ml 10% nipagin (700 ml 99% ethanol, 300 ml H2O, 100 g Nipagin), 45 ml propionic acid, 50 g agar, 400 g sugar beet syrup, solved in 9.75 l H_2O.

Vials were renewed every four to five weeks. Fly stock vials were kept at 18°C for storage or at 25°C for amplifying stocks and running experiments. Prior to dissecting the garland nephrocytes, vials containing 1st instar larvae were transferred to 29°C until the larvae reached 3rd larval instar.

3.4.2 Generation of transgenic flies

Flies were either bought from stock centers (see 3.4.3) or generated by using the ϕC31 integrase system. This system is derived from the *Streptomyces* bacteriophage ϕC31 and describes a site-specific recombinase encoded within the bacteriophage genome. The ϕC31 integrase mediates recombination between two 34 bp attachement sites (*att*), with one site in the donor plasmid (*att*B) and the other in the landing site of the host genome (*att*P). The recombination results in two new sites (*att*R and *att*L) unsuitable for the ϕC31 integrase, thus ensuring an irreversible recombination and creating a unidirectional integration of a certain sequence into a target genome. Originally working in phage and bacteria, this system also functions efficiently in other cells types including mammalian and insect cells. To generate a steady hereditary transgenic (fly) line, it is essential to reach stable integration of exogenous DNA into the germline of the host. Therefore, to enhance germline transformation in Drosophila embryos, the used fly lines expressed the ϕC31 integrase under control of the regulatory element of the *nanos* gene. Moreover, they have a precisely mapped *att*P landing site to direct transgene insertion into a predetermined intergenic location, providing stable and comparable gene expression (Bischof et al., 2007).

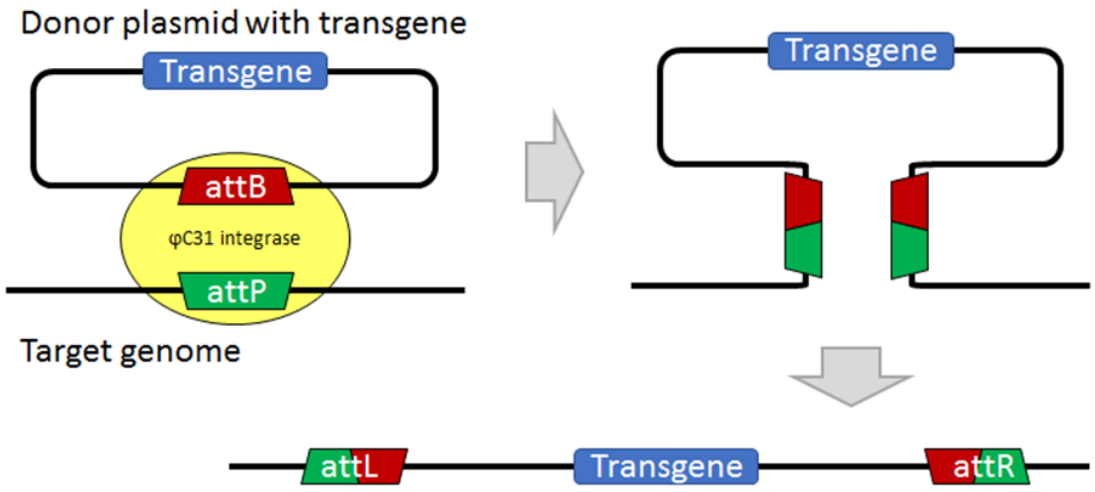

Figure 13: The ϕC31 integrase system. The enzyme facilitates unidirectional recombination between the attB site of the donor plasmid and the attP site in the target genome. After recombination, an attL site and an attR site are flanking the integrated transgene. (Figure modified from https://www.systembio.com/genome-engineering-phiC31-integrase.)

The donor plasmid carrying the transgene was introduced into the posterior part of the *Drosophila* embryo by microinjection.

20 µg plasmid DNA (column purified) were mixed with 5 µl 10x Injection Buffer, and the final volume was adjusted with water to 50 µl. Prior to injection, this mix was centrifuged for 30 minutes at top speed to precipitate any coarse particles. 1 µl of the supernatant was carefully pipetted into a glass injection needle (made from glass capillaries by a micropipet puller (Sutter Instruments Co.) without air bubbles at the needle tip. The injection needle was then installed in the micropipette holder. The inject workstation consisted of an inverse microscope, a micropipette holder and the micromanipulatior InjectMan NI2 (Eppendorf, Hamburg, Germany).

Embryos for injection were prepared following the protocol by Bachmann & Knust, 2008. Flies carrying the required landing site were kept in plastic cages covered by an apple juice agar plate and yeast paste for at least 2-3 days at 21°C before starting injections. Prior to injection, females were emptied from older embryos and egg-laying was

synchronized by frequently changing the covering agar plates. For injection, the egg-laying period was set for 30 minutes. Embryos from these plates were collected in a small basket with a gauze sieve and dechorionated in fresh house hold bleach for a maximum of 2 minutes. The dechorionated embryos were then thoroughly washed with water, carefully dried by touching the basket with a paper towel and transferred onto a small piece of apple juice agar (15 x 15 mm^2) with a fine paintbrush. Subsequently, the embryos on the agar block were uniformly oriented in several straight rows and in appropriate spacing (for the injection needle), with their posterior poles facing to the same direction. These line-ups were carefully transferred to a glue-coated cover slip (see 3.1) by softly pressing the sticky side onto the embryos. The cover slips were then dried in a desiccator for a certain amount of time depending on the surrounding temperature and humidity in the desiccator/ working environment. The properly dried embryos were covered with a drop of 10S Voltalef oil which prevents further dehydration, but ensures oxygen supply.

The properly prepared cover slip was placed into the microscope and the DNA solution (for preparation see chapter 3.2) was injected into the posterior part of the embryos with the help of the injection micromanipulator. Subsequently, the cover slip was placed onto an apple juice plate and stored at 18°C for 48 hours. Between 24 and 48 hours, the hatched larvae were collected and transferred into *Drosophila* vials. Adult flies were crossed to w^-*; gla/CyO* flies, and the offspring was selected for successful transgenic manipulation (marker: red eyes).

3.4.3 Fly stocks

Unless specially generated in the lab, fly stocks were obtained from following stock centers: Bloomington Drosophila Stock Center (BDSC, Indiana University, Bloomington, USA), Vienna Drosophila Resource Center (VDRC, Vienna Biocenter Core Facilities GmbH (VBCF), Vienna, Austria), Kyoto Stock Center (Kyoto Institute of Technology, Kyoto, Japan), NIG-FLY (Fly Stocks of National Institute of genetics, Shizuoka, Japan).

Table 14: List of fly stocks

Fly stock	Description	Reference
da::GAL4	Gal4 driver line, ubiquitous expression under daughterless promoter control	Krahn lab stock collection
sns::GAL4	Gal4 driver line, expression of Gal4 in pericardial and garland nephroctyes, also in muscle cells	(Kocherlakota et al., 2008)
sns::GAL4, ANF-GFP-GFP	Gal4 driver line, expression of Gal4 in nephroctyes; ubiquitous expression of ANF-GFP-GFP for accumulation assay	Krahn lab stock collection
sns::GAL4, ANF-GFP-GFP; baz-RNAi sh2	see above, combined with baz-RNAi sh2	Krahn lab stock collection
UAS::aPKC-RNAi	RNAi	BDSC #34332
UAS::baz-RNAi	RNAi	BDSC #39072
UAS::baz-RNAi sh2	RNAi	Krahn lab stock collection
UAS::dlg-RNAi	RNAi	BDSC #25780
UAS::kirre-RNAi	RNAi	VDRC #V109585
UAS::lgl-RNAi	RNAi	BDSC #35773
UAS::mCherry-RNAi	RNAi	BDSC #35778

Table 14 continued

Fly stock	Description	Reference
UAS::par1-RNAi (-1)	RNAi	BDSC #32410
UAS::par1-RNAi (-2)	RNAi	NIG-FLY #8201R-1
UAS::par6-RNAi	RNAi	VDRC #V19730
UAS::Baz WT	Overexpression of Bazooka	Krahn lab stock collection
UAS::Baz 5xA	Overexpression of Bazooka 5xA phosphorylation mutant Baz5xA = BazT522A, S628A, S700A, T712A, S741A	Krahn lab stock collection
UAS::Baz 5xD	Overexpression of Bazooka 5xD phosphorylation mutant Baz5xD = BazT522D, S628D, S700D, T712D, S741D	Krahn lab stock collection
UAS::aPKC-CAAX	Overexpression of aPKC-CAAX farnesylation mutant	Sol Sotillos
UAS::aPKC-CAAX DN	Overexpression of aPKC-CAAX farnesylation mutant with dominant negative kinase-dead mutation	Sol Sotillos
Ubi::Lgl-GFP	GFP-Tag	Krahn lab stock collection
GFP-Par-1	GFP-Trap	St. Johnston

Table 14 continued

Fly stock	Description	Reference
GFP-Dlg	GFP-Trap	BDSC #50859
attP 25C	Wildtype control line	Krahn lab stock collection
attP 86F	Wildtype control line	Krahn lab stock collection

3.4.4 UAS-Gal4-System

Most fly experiments were performed using the UAS-GAL4-System. This system derives from the yeast *Saccharomyces cerevisiae* and was implemented in *Drosophila melanogaster*. The driver line contains the yeast transcriptional activator GAL4 under the control of a nearby genomic enhancer which results in a cell-type and tissue-specific expression of GAL4. The flies of the reporter line carry a transgene consisting of an upstream activating sequence (UAS) next to a gene of interest (e.g. a RNAi sequence, St Johnston, 2002). After mating of the desired driver and reporter line, GAL4 binds to the UAS, leading to a specified expression of the gene of interest in the offspring. This expression can additionally be modulated and increased by temperature settings, starting from 25°C to induce GAL4 expression up to 29°C for maximum gene expression.

3.4.5 Lethality assay

Lethality assays were used to assess the efficiency of the utilized RNAi-lines. After crossing the RNAi-fly line with the ubiquitous driver line daughterless (Ubi::da), 100 eggs resulting from this cross were collected and placed on a fresh apple juice agar plate. The development and survival of the eggs and larvae had to be observed and documented daily. To keep the agar plates fresh, some drops of tap water were added regularly and

surviving larvae were fed with yeast paste. Flies that reached adulthood were counted as survivors. These assays were repeated three times for each tested fly line.

3.5 GFP Accumulation assay

For measuring the filtration ability of larval *Drosophila* nephrocytes, a GFP accumulation assay was established. This method was adapted from (Zhang et al., 2013) and modified to fit the demands of the experiments of this thesis.

The UAS-Gal4 system was used to manipulate the gene of interest specifically in nephrocyte cells. The driver line is a homemade fly strain that contains the sequence for the GAL4 protein coupled to the sns promoter as well as the Ubi::ANF-GFP-GFP construct. The ANF-GFP-GFP construct leads to the ubiquitous production of GFP-GFP and its secretion into the hemolymph. The sns promoter is active in both garland and pericardial nephrocytes as well as in muscle tissue. In combination with the responder line containing the UAS::*gene-of-interest* construct, an expression of the gene of interest is achieved specifically in both garland and pericardial nephrocyte cells.

3.5.1 Fly crosses

Parental fly crosses were kept on 25°C and flipped three times per week into a new glass vial provided with standard fly food. Vials with 1st and 2nd instar larvae were transferred to 29°C to enhance both ANF-GFP-GFP and RNAi-expression. As soon as the 3rd instar larvae entered the wandering stage they were picked up carefully with a blunt sorting needle, collected on a small apple juice plate and quickly rinsed with a few drops of tap water to remove remains of yeast and fly food. Afterwards they were sorted for positive GFP-expression (green fluorescing pericardial nephrocytes and hemolymph) with a Leica MZ10F fluorescent binocular using the UV-filter. This step had to be carried out as quickly as possible to minimize the bleaching effect of the fluorescing light beam.

3.5.2 Sample preparation and DAPI staining

GFP-positive larvae were then dissected in cold HL3.1 saline (see 3.6.1). The sample tissues including the garland nephrocytes were pooled in 1.5 ml Eppendorf cup in freshly prepared 4% PFA (in 1x PBS, pH 7.4) and fixed for 1 hour. Afterwards, the samples were stained with DAPI (1:1000) in 1x PBT_w for 20 minutes, washed once in 1x PBT_w and twice in 1x PBS for 15 minutes each. All fixation and washing steps were carried out on a rocker at room temperature. The samples were transferred on a clean microscopic slide and mounted in Mowiol after removing excess PBS with a piece of filter paper. Slides were kept in the dark to avoid bleaching of the GFP, dried over night at room temperature and imaged with the LSM 710 the following day.

3.5.3 Confocal microscopy

Images were taken on a laser scanning confocal microscope (LSM 710 Meta) using the C Apo 63x/1.2 water objective and ZEN 2010 software (Carl Zeiss). Z-stack images of the nephrocyte clusters were taken to ensure the even distribution of GFP within the nephrocyte cells and to assure a center plane image of each nephrocyte displaying the nuclei. Additionally, with every nephrocyte cluster a part of the proventriculus was imaged for background correction determination. Laser parameter were set for minimal bleaching (GFP: 2,5% laser and DAPI: 4,5% laser) and all images throughout the study were taken with the identical parameters to ensure comparability.

3.5.4 Data processing

Images were analyzed using the software ImageJ (version1.49p, NIH, USA). The GFP accumulation inside the nephrocyte cells and thus their function and integrity upon RNAi-knockdown of a certain gene was defined by the “corrected total cell fluorescence (ctcf) of nephrocyte per area”.

The GFP accumulation assay is based on following formulas:

1. $ctcf_{Neph}$ = Integrated $density_{Neph}$ - $area_{Neph}$ x mean gray $value_{Background}$
2. GFP $accumulation_{Neph}$ = $ctcf_{Neph}$ / $area_{Neph}$

Measurement parameters in ImageJ were mandatorily pre-set on “area” and “integrated density”. GFP intensity was measured as grey (pixel) value. The overall GFP intensity of a cell is presented by the integrated density, which is the product of grey (pixel) value of the cell area and the cell area itself. As background correction, the mean grey (pixel) value of the (auto-fluorescent) proventriculus present in the same image multiplied with the nephrocyte cell area was implemented.

3.6 Immunohistochemistry

3.6.1 Dissection of nephrocytes

The 3rd larval instar larvae were transferred to a glass dissection plate and dissected in ice-cold HL3.1 saline (Feng et al., 2004) using the stereo microscope (Motic, Hongkong). With two pairs of fine tweezers, one larva was carefully fixed on the ground and decapitated. The protruding gut was brought out completely and entangled until the anterior part with the proventiculus could be identified. The garland nephrocytes are attached to the proventriculus in a chain-like structure surrounding the esophagus, connected by a thin tissue chord. To preserve the integrity of the garland nephrocytes and for easier handling, the complete proventriculus together with parts of the esophagus and gut was obtained and treated as one tissue sample.

3.6.2 Chemical fixation

For chemical fixation, the tissue samples of one genotype were pooled. After dissection, they were immediately transferred to a 1.5 ml Eppendorf cup containing fresh

formaldehyde solution (4% *para*-formaldehyde in 1x PBS) and fixed on a rocker for 15 min at room temperature. Afterwards, the samples were washed three times with 1x PBS for 15 min each.

3.6.3 Heat fixation

For heat fixation, two to three larvae were dissected at once and the tissue samples were carefully pipetted into boiling heat fixation saline with a saturated pipet. After incubation for 10 seconds the tissue samples were quickly transferred into a glass vial with ice-cold HL3.1 saline. The samples were pooled (10-15 per genotype) and stored shortly (<1h) in ice-cold saline until further processing.

3.6.4 Immunostaining of nephrocytes

After fixation (chemical or heat fixation) the samples were blocked in PBT_w (1x PBS + 0.1% Tween-20) with 1% BSA for 30 to 60 min at room temperature, followed by the incubation with the primary antibodies in PBT_w + 1% BSA at 4°C overnight. Next, the samples were washed four times with PBT_w at room temperature for 15 minutes each.

For some primary antibodies, it was necessary to introduce an incubation step in methanol for 1 hour at room temperature to improve antibody-binding to the respective epitopes. This step had to be carried out before blocking and two short washing steps with PBT_w were added before continuing with the blocking in PBT_w + 1% BSA.

The secondary antibodies were prepared in PBT_w + 5% NHS and incubated with the samples for two hours at room temperature. Afterwards, the samples were washed in PBT_w four times for 15 minutes each, whereby DAPI (0.5 µg/µl, 1x PBT_w) was added to the first washing step. The samples were pipetted onto a microscope slide (R. Langenbrinck GmbH, Emmendingen, Germany) and excess liquid was carefully removed with a piece of filter paper. Finally, the samples were mounted in 40-50 µl Mowiol and dried overnight at room temperature.

3.6.5 Confocal microscopy

Images were taken on a laser scanning confocal microscope (LSM 710 Meta using either LD LCI Planar Apo 25x/0.8 or C Apo 63x/1.2 water objective lenses and ZEN 2010 software (Carl Zeiss). Images were processed using ZEN 2011 software (blue and black edition), ImageJ (version1.49p, NIH, USA) and Photoshop CS5 (Adobe).

3.7 Transmission electron microscopy

All micrographs were taken at a Zeiss CEM 902 operated at 80 kV equipped with a wide-angle Dual Speed 2K CCD camera (TRS, Moorenweis, Germany).

3.7.1 Preparation of slot grids

For all transmission electron microscopy experiments, copper slot grids (G2500C, 2 mM x 1 mM) coated with 1.5% (w/v) pioloform were used as carrier for ultra-thin sections.

The grids were manually prepared beforehand. A thoroughly cleaned microscopic slide was immersed into 1.5 % pioloform (1.5 g pioloform in 100 ml chloroform) for 30 seconds to produce a thin pioloform film on the slide. After scraping along the edges of the microscopic slide with a razor blade, this pioloform film was carefully released on a water (Millipore) bath surface. The copper grids were placed on the pioloform film with the glossy side facing down. The grid-packed film could be taken up by a piece of parafilm and be stored in a petri dish until use. Before use, the grids were pricked out of the pioloform film layer with a hollow needle on the outside of the grid.

3.7.2 Sample preparation – High Pressure Freezing

The advantage of high-pressure freezing (HPF) is an improved preservation of the sample tissue compared to other conventional methods. Herefore, the nephrocyte cells were

dissected as described in the beginning of 3.6.1. The tissue package of proventriculus and nephrocytes was then placed on a gold plated flat specimen carrier (200 µm depth, 1.2 mM diameter, Leica, Wetzlar) containing a drop of HL3.1 saline. The carriers were fastened in the corresponding holder (Bionet Pads) and high-pressure frozen in liquid nitrogen in a EM PACT2/RTS (Leica, Wezlar). Samples were stored in a liquid nitrogen depot until further processing.

3.7.3 Automatic freeze substitution (AFS) and epon embedding

The frozen samples were embedded in fresh epoxy resin using the protocol in tab. 15 in a Leica EM AFS2 (Leica, Wezlar). The samples were transferred into the pre-cooled substitution solution in the AFS, substituted in acetone, 2% osmium tetroxide, 5% H_2O and 0.25% uranyl acetate, and finally embedded in fresh Epon resin. The last polymerization step at 60°C was carried out in an external incubator.

Table 15: Protocol for freeze substitution and epon embedding

Incubation temperature	Solution/ Resin	Incubation time
-140 °C	acetone / 2% OsO_4 / 5% H_2O / 0.25% UAc	19 h
-140 to -90 °C	acetone / 2% OsO_4 / 5% H_2O / 0.25% UAc	3 h
-90 °C	acetone / 2% OsO_4 / 5% H_2O / 0.25% UAc	3 h
-90 to -60 °C	acetone / 2% OsO_4 / 5% H_2O / 0.25% UAc	3 h
-60 °C	acetone / 2% OsO_4 / 5% H_2O / 0.25% UAc	3 h
-60 to -30 °C	acetone / 2% OsO_4 / 5% H_2O / 0.25% UAc	3 h
-30 °C	acetone / 2% OsO_4 / 5% H_2O / 0.25% UAc	3 h
-30 to 0 °C	acetone / 2% OsO_4 / 5% H_2O / 0.25% UAc	3 h
0 °C	acetone / 2% OsO_4 / 5% H_2O / 0.25% UAc	3 h
0 °C	acetone	2x 10 min
0 to 4 °C	acetone	1x 10 min
4 to 25 °C	acetone/ Epon 2+1	1x 1h
25 °C	acetone/ Epon 2+1	1x 1h
25 °C	acetone/ Epon 1+1	1x 2 h
25 °C	acetone/ Epon 1+2	1x 12 h
30 °C	Epon (fresh)	1x 2 h
60 °C	Epon	1x 2 d

3.7.4 Sample trimming

The excess epoxy resin was manually removed to make the specimen carrier accessible for further steps. By exposing the carrier to alternating cold (liquid nitrogen) and heat (simmering water on a magnetic stirrer), the carrier fell off and left the tissue sample in the epoxy resin block ready for trimming.

Trimming of the sample blocks was done either manually using a fresh razor blade or with glass knives fixed in the Pyramitome (LKB, Bromma). The sample blocks were trimmed to a desired and reasonable size with the nephrocyte cells in the middle of the resulting section.

3.7.5 Ultramicrotomy

The trimmed sample block was installed in the ultramicrotome Leica EM UC7 (Leica, Wetzlar) with the appropriate holder. The ultramicrotome was equipped with a diamond knife boat (Diatome AG, Biel, CH), either the knife type histo (45° knife angle, 0.2-5 µm section thickness) or the knife type ultra (35° knife angle, 30-200 nm section thickness).

Prior to sectioning, the knife boat was filled with sterile filtered water (Millipore). The necessary parameters (perfect angle of resin block and knife, sectioning window and sectioning speed) were set and after the cutting process, the section ribbons floating on the water surface were taken up by a copper fish grid and immediately placed on a microscope slide (semi-thin sections) or a clean slot grid coated with pioloform (ultra-thin sections).

First, semi-thin sections (1 µm) were taken from the sample to determine the desired cross-section area. These semi-thin sections were placed on a microscope slide, stained with Richardson's staining solution and, after drying, examined with a Leica DM750 microscope.

For ultrastructural analysis and immunolabeling, ultra-thin sections of 50 to 70 nm were cut. These sections were transferred on a copper slot grid coated with pioloform. The excess water was carefully removed with a piece of filter paper and after thorough drying

the grids, they were separated cautiously using a pair of fine tweezers. The slot grids carrying the sections were stored in gridboxes until further processing.

3.7.6 Uranyl acetate and lead citrate staining

The ultra-thin sections were additionally contrasted by 1% (w/v) uranyl acetate and 1% (w/v) lead citrate to enhance contrast in TEM analysis. To remove precipitates all solutions were first centrifuged for 3 min at maximum speed in a table top centrifuge. The staining solutions were prepared in a series of droplets on a piece of parafilm, followed by five drops of sterile-filtered water (Millipore). The grids were placed with the sections facing down on the first drop of uranyl acetate and incubated for 20 minutes in the dark at room temperature. Afterwards, the grids were incubated on a drop of lead acetate for 1 minute and immediately transferred to the first water droplet. The five washing steps were carried out for 30 seconds each. The excess of water on the grids was carefully removed with a piece of filter paper and the grids were left air-drying in crossed tweezers. The prepared grids were stored in grid boxes in a cool and dry place until usage.

4 RESULTS

4.1 Localization of Par complex components and basolateral polarity proteins in wild type nephrocytes

The correct establishment of apical-basal polarity is vital for functional nephrocyte cells. Even though the complicated overall 3D-structure and the close, distinct interaction of neighbouring cells of their mammal podocyte counterparts are missing, the purpose of the nephrocyte cell is highly compromised if the cell architecture is impaired.

In epithelial cells, the localization of the Par complex components follows a specific pattern where aPKC and Par6 are positioned at the apical domain of the cell, and Par3/Baz slightly below at the marginal zone (Harris & Peifer, 2005). The interaction of all three complex proteins is necessary to establish their localization correctly.

To evaluate the original situation of polarity protein localization in nephrocytes, immunostainings were first performed in wildtype control flies. Nephrocytes of attP25C L3 larvae were dissected as described in chapter 3.4. Immunostainings of the cells included the Par complex proteins Baz (Bazooka), aPKC and Par6, as well as the nephrocyte diaphragm component Sns (sticks-and-stones) as a marker for the cell cortex (Fig 14).

Firstly, Sns staining is displayed in a very well-defined and clear line at the outmost boundaries of the nephrocyte (Fig. 14 A, B in blue). In both stainings, Sns can be seen enriched at cell-cell contacts, indicating an enhanced expression of Sns and therefore nephrocyte diaphragms (ND) at the contact sites. Baz localizes predominantly at the cell cortex (Fig. 14 A, in green), with occasional spots in the cytoplasm. These spots occur mostly perinuclear and probably mark Baz protein at the site of the endoplasmic reticulum and in vesicles. aPKC is also located cortically of the cell, but appears in a more broader area and in a blurred, less defined manner (Fig. 14 A, B in red). In both stainings, aPKC expression is increased at the site of cell-cell-contact between nephrocytes. As the other Par complex components, Par6 localizes cortical as well, with a visible enrichment at cell-cell contacts (Fig. 4.1 B, in green).

In wildtype cells, Sns strongly co-localizes with both Baz (Fig. 14 A, zoom) and Par6 (Fig. 14 B, zoom). aPKC is due to its wider distribution only partly co-localizing with sns at the cell boundary. This result corresponds to the findings of Hartleben et al. (2008) where they showed the co-localization of aPKC, Par6 and Par3 in mouse podocytes.

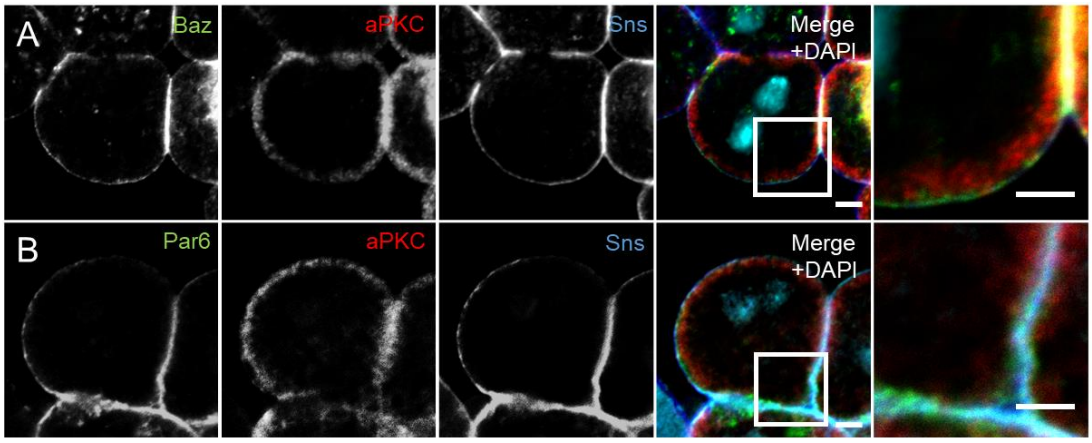

Figure 14: Localization of the Par complex proteins Bazooka, aPKC, and Par6 in the wildtype larval nephrocyte. Cortical expression of Baz (A) and Par6 (B) in a clear line, whereas aPKC appears cortical in a broader range. All proteins co-localize, with aPKC intruding from the cortex into the cytoplasm. Scale bar = 5 µm, Scale bar zoom = 5µm

As seen in this chapter, the localization of the apical polarity determinants in nephrocytes is very distinct. The Par complex proteins are also co-localizing in the nephrocyte cell, but their distribution at the apical region is to some extent different from the epithelial cell. The streaked pattern of aPKC/Par6 and Baz from epithelial cells is not as explicit, and apart from aPKC, the proteins Baz and Par6 seem to be spatially linked to the cell membrane, Sns and the nephrocyte diaphragm.

To assess the prevalence and localization of basolateral proteins Lgl, Dlg and Par1, immunostainings were performed in wildtype nephrocytes and nephrocytes obtained from GFP-Trap lines, respectively (see chapter 3.6.4 and chapter 3.4.3, table 14). The cells were prepared as in chapter 3.4.

Stainings in wildtype (attP 25C) nephrocytes revealed a cytoplasmic distribution of Dlg with a slight enhancement at the cortical lacuna area, while localization of Sns is restricted to the membrane (Fig. 15 A).

For further Dlg and Par1 localization experiments, GFP-Trap fly lines were used since these cells were planned to be supplementary examined in TEM analysis. Hence, Dlg and Par1 proteins in these lines are GFP-fusion proteins expressed under their endogenous promoter. To investigate the localization of Lgl, a ubiqutiously expressed, GFP-tagged line was used.

Stainings for GFP-tagged Dlg confirmed the distribution pattern of Dlg and Sns (see Fig. 15 B). In the Par1-GFP Trap nephrocytes, Par1 is clearly cytoplasmic localized and appears quite dispersed throughout the cell in an irregluar pattern (Fig. 15 C).

In contrast, Lgl was found to localize in a broken line at the cell membrane and seems to partially co-localize with the nephrocyte diaphragm marker Sns (see Fig. 15 D). Sns showed normal cortical localization in all stainings.

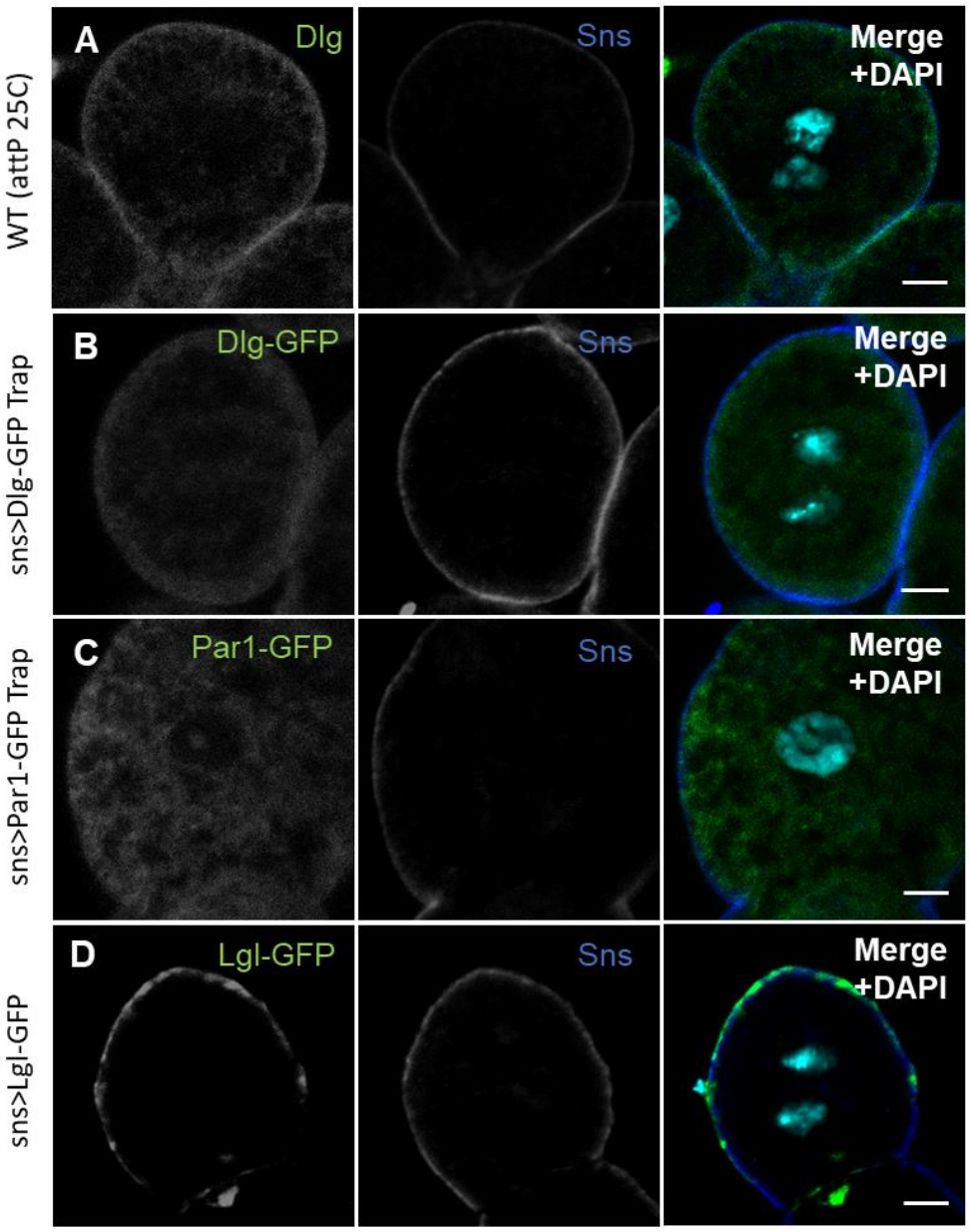

Figure 15: Localization of basolateral proteins Dlg and Par1 in nephrocytes. Staining of Dlg and Sns in wildtype nephrocytes (attP 25C, A) with cytoplasmic distribution of Dlg with enhancement at the cortex and strict cortical localization of Sns. Same distribution pattern in Dlg-GFP Trap nephrocytes (B). Cytoplasmic distribution of Par1(-GFP Trap) with cortical Sns staining in Par1-GFP Trap nephrocytes (C). Lgl is localized strictly cortical (D) and partly co-localizing with Sns. Scale bar = 5 µm

4.2 Localization of Par complex components in knockdown mutant nephrocytes

Regarding the distribution of the apical polarity proteins in the nephrocyte, it would be interesting to know how the localization of these proteins is influenced when one of the complex components is missing.

For the following RNAi experiments, the RNAi line of the g*ene of interest* was crossed with a sns::GAL4-driver line, leading to a specific knockdown of g*ene of interest* expression in nephrocyte cells. During development, the offspring was kept on 29°C to ensure optimal conditions for RNAi-expression.

To be able to compare protein expression levels and localization in control and sample larvae, a mCherry-RNAi line was crossed with the same sns::GAL4-driver line, and all samples were handled in parallel with the same solutions and mix of antibodies. Confocal images were taken at Zeiss LSM 710 Meta using at first the exact same microscope parameter settings for both control and sample stainings ("ctrl. (control) settings"), plus subsequently optimizing the parameter settings for the sample stainings ("opt. (optimized) settings").

4.2.1 Knockdown of aPKC results in mislocalization of interaction partners Par6, Baz, and Sns/ Kirre

aPKC is one of the key proteins in the regulation of cell fate decisions. In cell polarity establishment, the phosphorylation of other polarity proteins by aPKC is an essential step (reviewed in Tepass, 2012). In this experiment, the impact of reducing aPKC activity was to be determined in regard to apical-basal polarity in nephrocytes.

In the mCherry-RNAi control staining, both Par6 and Sns show normal expression and localization, and an even distribution in a clear line at the nephrocyte cortex (Fig. 16 A). Baz is localized predominantly at the cell cortex and in a cloudish manner in the cytoplasm, with a slight concentration in the perinuclear area. This cytoplasmic localization is probably indicating the region of endoplasmic reticulum (in reference to ultrastructural studies in chapter 4.4).

Upon downregulation of aPKC, the localization of Baz, Par6, and Sns shows differing severities of distortion (Fig 16 B, C). Sns is still localized preponderantly at the cell cortex, but loses its evenly defined lineage. Instead, the filtration slit marker shows a slight misdistribution along the cortex in a spotty pattern, with occasional, (almost) empty gaps in between.

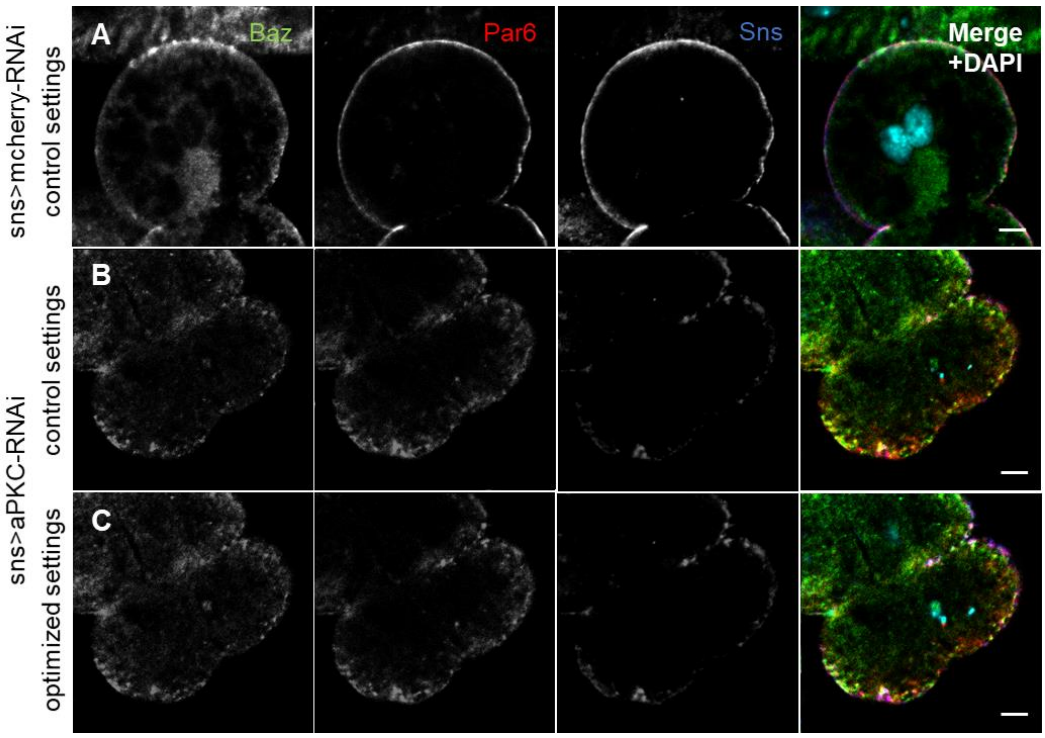

Figure 16: Localization of Baz, Par6, and Sns in aPKC knockdown nephrocytes. Normal localization in sns>mCherry-RNAi cells (control, A). Distorted localization of Baz, Par6, and Sns in the sns>aPKC-RNAi mutant (B, C). Baz is distributed mainly cytoplasmic and in cortical spots, Par6 and Sns lose their even, continuous cortical localization (B, C). Scale bar = 5 µm

Baz and Par6 localization is most affected by the downregulation of aPKC in the nephrocyte. Compared to the mCherry-RNAi control, the knockdown leads to a shifted distribution of both proteins into the cytoplasm (Fig 16 A, B). Though Baz and Par6 are still present at the cell boundary, the cortical localization is losing its defined shaping and is displayed in concentrated spots (as seen with Sns). The increased intensity of the Baz staining measured with control parameter settings indicates an overall heightened level of Baz protein in aPKC-RNAi nephrocytes (Fig. 16 B). Apart from relying on the

aPKC/Par6-dimer, the positioning of Baz at the apical domain is also ensured by its diverse interaction with cell adhesion molecules (JAM, nectins), therefore Baz is not completely losing its apical/ cortical localization.

In an analogous experiment using the same knockdown lines, the impact on Kirre, the Drosophila NEPH1 homolog, was analyzed. Like Sns, Kirre was still found at the cortex of aPKC-RNAi nephrocytes. Instead of the distinct localization, strong expression, and even distribution at the outer cell boundary as seen in the mCherry-RNAi control (Fig. 17 A), Kirre is displayed in either concentrated in spots or is even completely missing from the cell cortex (Fig. 17 B, C). The spots even occur slightly dispatched from the cell cortex

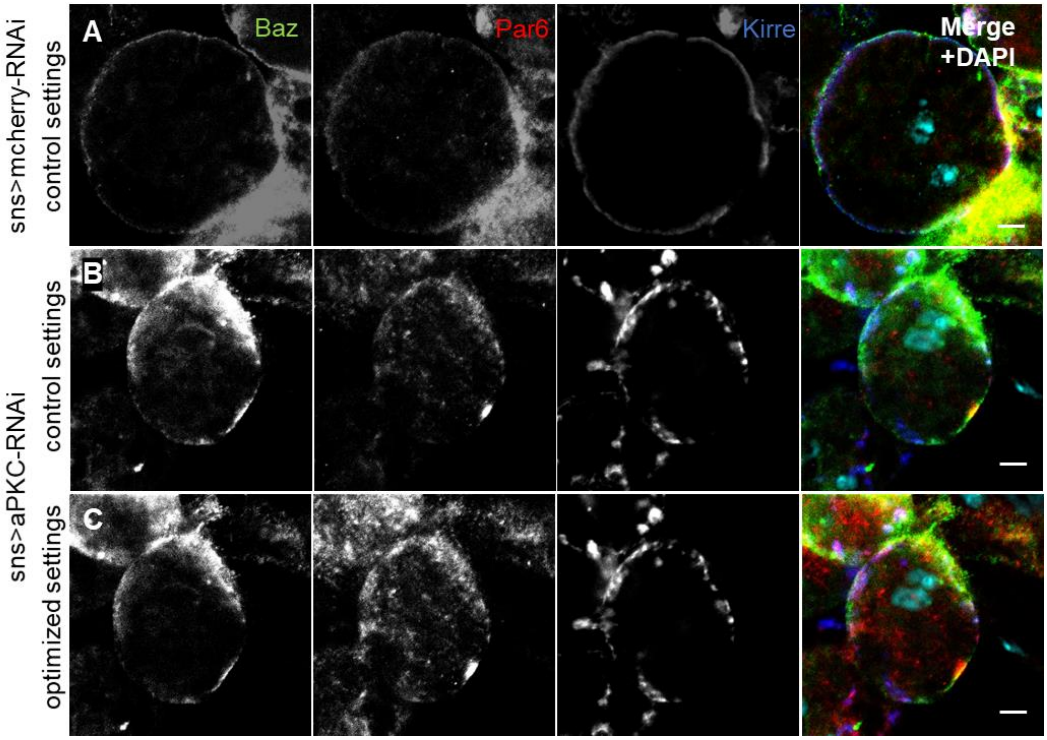

Figure 17: Localization of Baz, Par6, and Kirre in aPKC knockdown nephrocytes. Normal localization in sns>mCherry-RNAi cells (control, A). Distorted localization of Baz, Par6, and Kirre in the sns>aPKC-RNAi mutant (B, C). Baz and Par6 are distributed mainly cytoplasmic, Kirre loses its even and continuous cortical localization (B, C). Scale bar = 5 µm

Also, Baz shows again a cytoplasmic distribution as seen in the staining in Fig. 16. The cortical localization of Baz is still maintained, but the staining is stretching far out into the inner compartments of the cell as well (Fig. 17 B). The protein level of Baz is also elevated compared to the mCherry-RNAi control staining. Par6 loses also its cortical localization and is found partly cortical, partly cytoplasmic. This phenotype is comparable with the previous staining with Sns.

4.2.2 Knockdown of Par6 affects localization of Baz, aPKC, and Sns/ Kirre

Par6 functions as regulatory subunit of aPKC and, in interaction with active Cdc42, controls positioning of aPKC and regulates negatively the kinase activity (Atwood et al., 2007). In Drosophila neuroblasts and epithelial cells, loss of Par6 displays a similar phenotype as a aPKC loss of function mutant, instead of causing overactivation of aPKC. Therefore, the situation and effect of Par6 knockdown in the nephrocyte was analyzed.

The mCherry-control staining shows the normal localization of Baz, aPKC, and Sns (Fig. 18 A). All three proteins are distinctly localized at the cell cortex. aPKC displays the typical broader distribution as seen as in the beforementioned control and wildtype stainings. Though Baz is principally localized cortically, slight cytoplasmic aggregations of the protein can be identified which presumptively visualize the network of the endoplasmic reticulum. Sns staining is naturally limited to a distinct cortical line.

Upon downregulation of Par6, Baz, aPKC and Sns are still located at the cortex, the original position for all these proteins, but additionally, their localization is shifted from the cortex to the cytoplasm (Fig. 18 B, C). The overall cortical restriction of all investigated protein is lost. This effect is similar to the phenotype of the aPKC knockdown.

Apart from cortical areas with increased expression, Baz protein expression is almost evenly spread in the cell cytoplasm. Baz stainings sometimes revealed relatively defined cytoplasmic spots of Baz, mostly in the vicinity of the nuclei. However, in wildtype or control nephrocytes stainings, Baz never placed out evenly in the cytoplasm as seen in Fig. 18 B.

aPKC and Sns staining patterns showed similar manifestations. aPKC and Sns distribution is also reallocated from the cortex to the cytoplasm and protein expression can be found irregular dispensed in the cell (Fig 18 B), instead of remaining in their typical distinct localization at the cortex.

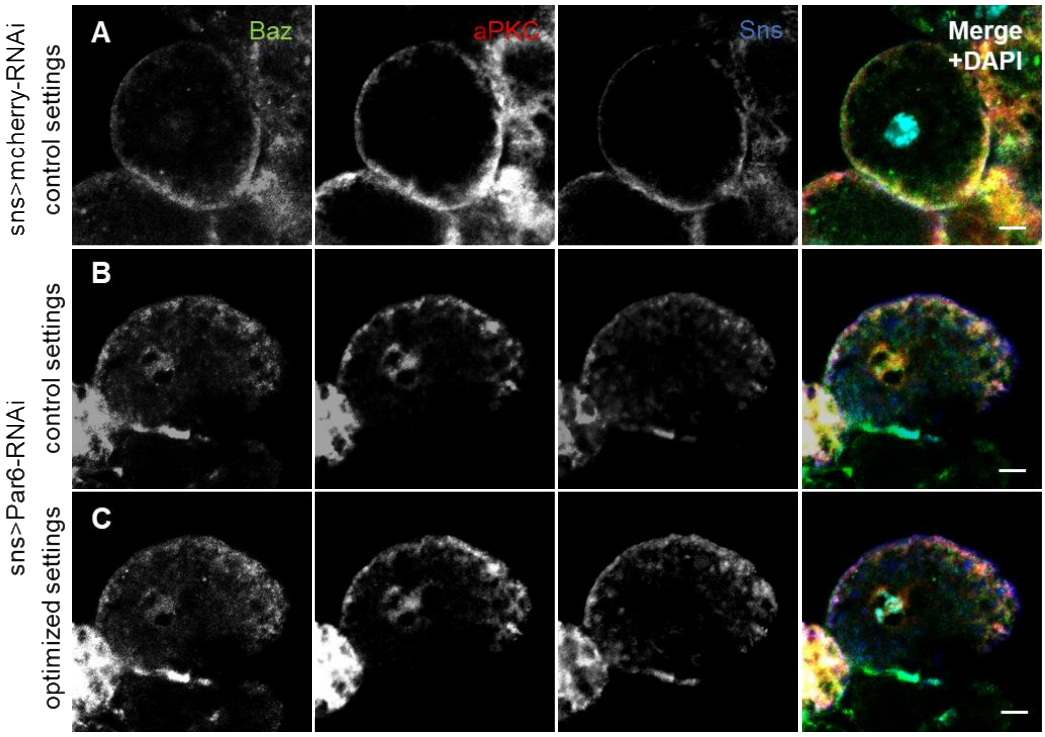

Figure 18: Localization of Baz, aPKC, and Sns in Par6 knockdown nephrocytes. Normal localization of the proteins in sns>mCherry-RNAi cells (control, A). In the sns>par6-RNAi mutant (B, C), Baz, aPKC, and Sns localization is distorted and shifted from the cortex into the cytoplasm. All three proteins show irregular distributed clouds or spots (B, C) compared to the even distribution in the control staining. Scale bar = 5 µm

In conclusion, the reduction of Par6 activity in the nephrocyte cell leads to a defective positioning of both aPKC and Bazooka. The loss of Par6 protein interrupts the aPKC/Par6-heterodimer and its binding to Baz, failing to from a functional Par complex. Subsequently, correct recruitment of aPKC to the apical region and the local phosphorylation of Baz seems is affected. From these results, it cannot be definitely stated if the mislocalization of Sns is due to deficient distribution of the polarity proteins aPKC and Baz, or if Sns positioning is influenced by additional factors.

Stainings of mCherry-RNAi nephrocytes reveal the typical localization of Baz, aPKC, and Kirre (Fig. 19 A). All proteins are restricted to the cortex, with occasional cytoplasmic spots of Baz in the endoplasmic reticulum area of the cell.

Par6 downregulation led to a severe mislocalization of Baz and aPKC (Fig. 19 B) in this staining. Baz lost its cortical definition and spread to the cytoplasm in an erratically, cloudish manner. aPKC expression seems decreased in this mutant and the protein is distributed evenly throughout the cell. (Fig. 19 C). As in the previous staining, positioning of aPKC and Baz is massively impeded. Other than Sns, Kirre staining is lost apart from few irregular spots (Fig. 19 C). Although Sns and Kirre proteins are known for close interaction and co-localization, they might be differently influenced by particular proteins, in this case Par6.

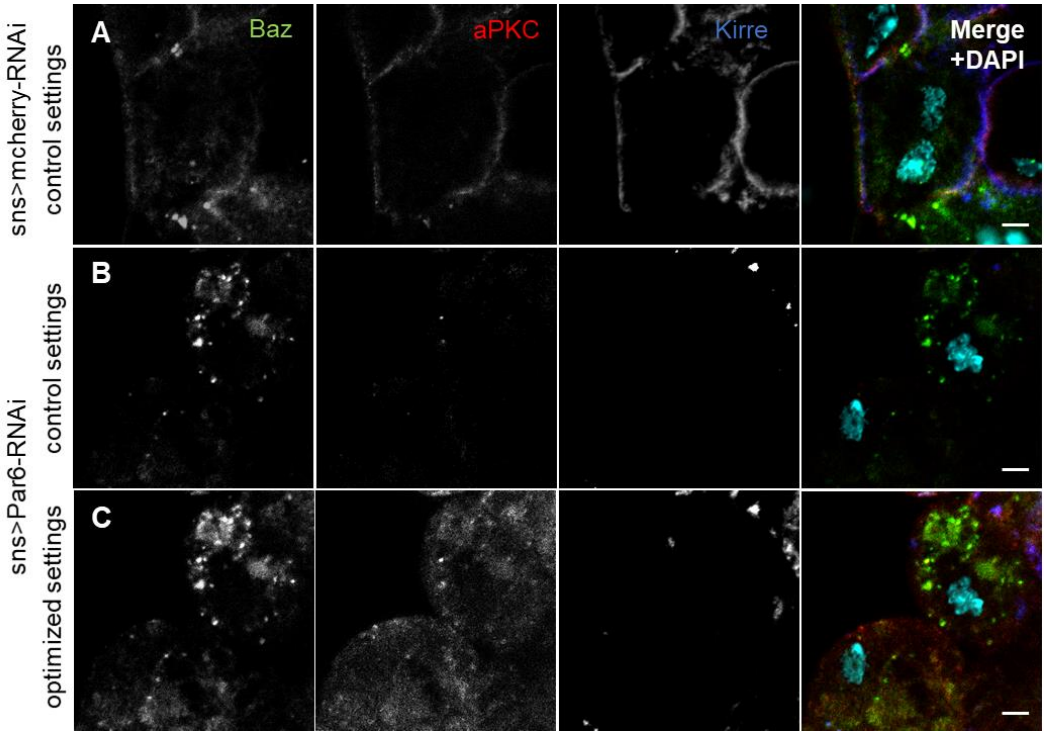

Figure 19: Localization of Baz, aPKC, and Kirre in Par6 knockdown nephrocytes. Normal localization of the proteins in sns>mCherry-RNAi cells (control, A). In the sns>par6-RNAi mutant (B, C), Baz, aPKC, and Sns localization is highly distorted. All three proteins are seemingly downregulated. Scale bar = 5 µm

4.2.3 Knockdown of Bazooka has a mild impact on the localization of Par complex partners aPKC and Par6 and filtration slit proteins Sns/ Kirre

As the last of the three Par complex components, the impact of Bazooka depletion was tested in nephrocytes. Bazooka is involved with numerous proteins critical for epithelial polarization, including adherens junction (AJ) proteins as Armadillo (Arm, β-catenin) and Echinoid (Ed) (Wei et al., 2005). While binding to Baz is not relevant for positioning the AJ proteins Arm and Ed, the intercation and phosphorylation is important for aPKC/Par6 recruitment and positioning to the accurate apical membrane domain (Harris & Peifer, 2005; Horikoshi et al., 2009), resulting in a stratified apical domain in epthelial cells. In podocytes, AJ and TJ migrate and morph to form the slit diaphragm (SD). At the site of these specially modified junctions, Par3/Baz acts as a scaffolding protein recruiting the aPKC/Par6-heterodimer (Ebnet et al., 2001). Additionally, it is able to bind NEPH-Nephrin proteins and functions as a linker between the apical complex aPKC/Par6 and slit diaphragm complex NEPH1/Nephrin (Hartleben et al., 2008). Following these findings in podocytes, the influence of a Bazooka knockdown on the localization of aPKC, Par6 and NEPH-Nephrin was analyzed via immunhistochemistry.

In the mCherry-RNAi control staining in Fig. 20 A, Par6, aPKC and Sns are normally localized and distributed in the nephrocytes. The stainings of all three proteins show a distinct cortical line, which is typically slightly broader for aPKC.

The downregulation of Bazooka via RNAi affects Par6, aPKC and Sns to a similar extent and leads to a moderate delocalization of these proteins. Their predominant localization remains at the cell cortex, but the stainings display a spotty, more irregular distribution with spurs of each protein into the cytoplasm. The overall width of the cortical distribution of these proteins in the Baz knockdown is approximately expanded to three times compared to the width of the mCherry-RNAi control staining (Fig. 20 B, C).

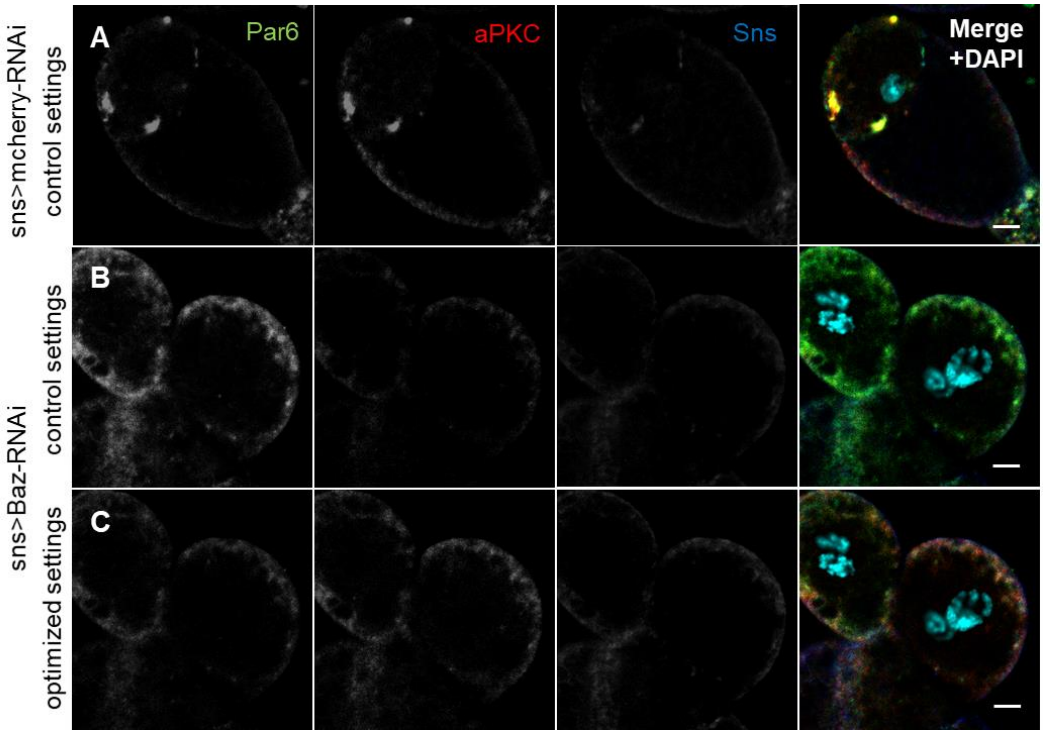

Figure 20: Localization of Par6, aPKC, and Sns in Baz knockdown nephrocytes. Normal localization in sns>mCherry-RNAi cells (control, A). Slightly distorted localization of Par6, aPKC and Sns in the sns>baz-RNAi mutant (B, C). All three proteins are distributed broader and more irregular (B, C) compared to the control staining. Scale bar = 5 µm

According to the control settings of the laser parameters, the intensity of the protein staining suggests a slight upregulation of Bazooka, while aPKC seems to be faintly downregulated compared to the control staining (Fig. 21 A, B). Sns staining intensities are equivalent in both the control and Baz-knockdown.

These findings were repeated in the Baz-knockdown stained with Kirre, the NEPH1-homolog. In Fig. 21 A, mCherry-RNAi control stainings of Par6, aPKC and Kirre display the typical cortical localization in a fine line. The distribution of all three proteins is blurred and less constricted to the cortex of the Baz-knockdown nephrocyte (Fig. 21 B, C). As stated before, the general effect of the Baz-knockdown on localization of the Par-complex components is apparent, but rather mild.

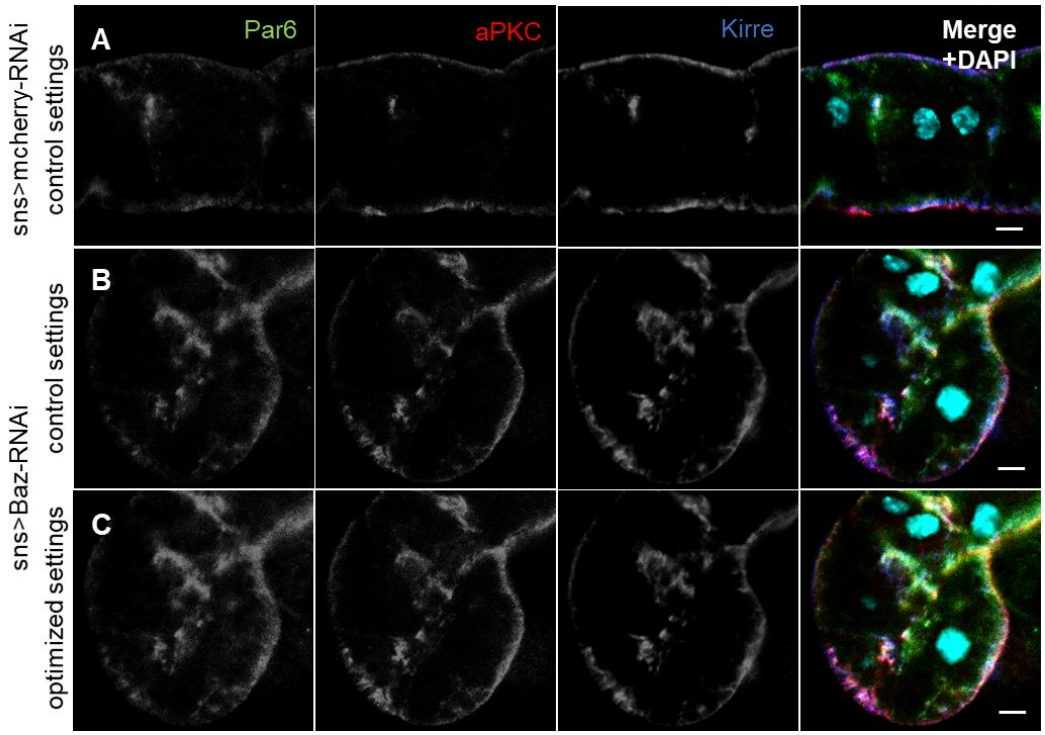

Figure 21: Localization of Par6, aPKC, and Kirre in Baz knockdown nephrocytes. Normal localization in sns>mCherry-RNAi cells (control, A). Slightly distorted localization of Par6, aPKC and Kirre in the sns>baz-RNAi mutant (B, C). All three proteins are distributed broader and more irregular (B, C) compared to the control staining. Scale bar = 5 µm

4.2.4 Non-phosphorylatable Bazooka impairs correct localization of Par-complex partners

The phosphorylation of Bazooka by aPKC is crucial for Baz/aPKC binding and correct Baz/aPKC-complex function in apical polarity establishment (Morais-de-Sá et al., 2010a). aPKC interacts with Bazook via binding in the PDZ2-3 domain and the aPKC-binding motif of Bazooka. There are several phosphorylation sites for aPKC identified in Bazooka, among them are five serines/threonines located in the PDZ2-3 domain. In epithelial cells, the phosphorylation of these sites are important for accurate development (Feicht, 2017).

These five specific phosphorylation sites were identified by Sabrina Wohlhaupter (Krahn Lab, University of Regensburg) while screening Bazooka for phosphorylation sites for aPKC kinase activity. Preceding this work, a non-phosphorylatable form of Bazooka was cloned for usage in *Drosophila* flies. In this construct, referred to as Baz_{5xA}, five potential phosphorylation sites for aPKC were replaced by alanine ($Baz_{T522A, S628A, S700A, T712A, S714A}$). In the phosphomimetic variant Baz_{5xD}, the same sites were replaced by aspartatic acid.

To investigate the role of Bazooka in establishing the distinct apical structure of nephrocytes further, the effect of its phosphorylation by aPKC was tested and the non-phosphorylatable Baz_{5xA} was introduced in nephrocytes. Hence, sns::GAL4 females were crossed to males to either carrying GFP-tagged UAS::Baz (wildtype), UAS::Baz_{5xA} or UAS::Baz_{5xD}.

As seen in Fig. 22 A and C, overexpression of both the wildtype (UAS::Baz) and phosphomimetic (UAS::Baz_{5xD}) version does not affect the localization of Bazooka and its interaction partners aPKC and Sns. In the wildtype control, Bazooka and aPKC are correctly established in the cortical area of the cell in a broader spectrum (Fig. 22 A), whereas Sns is restricted to the cell membrane as normally. The UAS::Baz_{5xD} mutant displays no influence of the mutant protein on the localization of aPKC and Sns, while the localization of Baz_{5xD} itself is not as pronounced as in the control stainings.

The strongest effect is visible in the Baz_{5xA} mutant cells. This specific Bazooka variant, which cannot be phosphorylated by aPKC, leads to mislocalization of $Baz_{5xA,}$ aPKC, and Sns in variable extent (Fig. 22 B). Baz_{5xA} and Sns are still found at the cell cortex, but are

less defined. Especially Baz_{5xA} localization is shifted to the cytoplasm and shows vesicle-like aggregations. Sns expression is spotty and smudged, and possibly overexpressed in the region of the endoplasmic reticulum. aPKC localization is most affected by expressing Baz_{5xA}. It is lost from its distinct apical region and instead evenly distributed in the cell, indicating the importance of the functional interaction between Bazooka and aPKC for correct localization of both proteins.

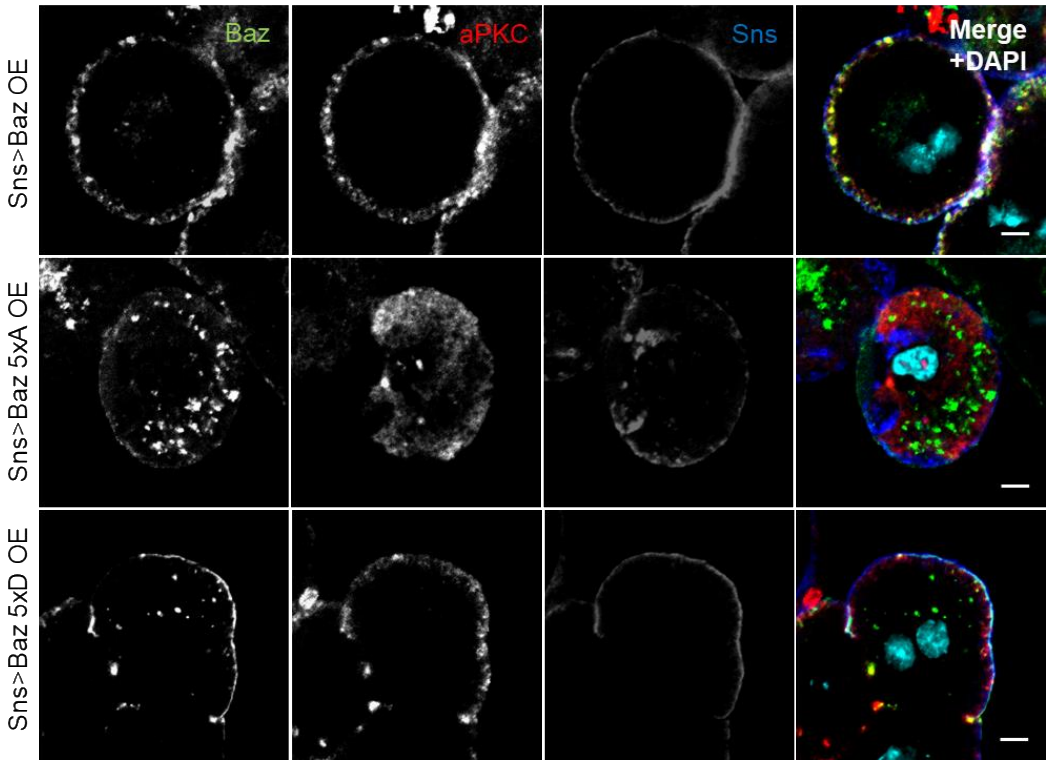

Figure 22: Localization of Baz, aPKC, and Sns in phosphorylation mutants of Bazooka. Normal localization of all proteins with overexpression of wildtype Bazooka and the phosphomimetic Baz_{5xD} (A, C). Overexpression of Baz_{5xA} mutant leads to distorted localization of Baz, aPKC and partly Sns (B). Scale bar = 5 µm

In conclusion, without the phosphorylation of the mutated Baz_{5xA} protein by aPKC, the correct localization of Bazooka itself and aPKC cannot be established. Connected to this disturbed distribution of polarity proteins and interaction partners, the localization of the nephrocyte diaphragm protein Sns is also impaired.

4.3 Functionality assays: GFP accumulation as indicator of functionality in nephrocytes

The unique and crucial function of mammalian podocytes depends on the highly organized cellular configuration as well as the precise signaling within the cell and between neighbouring cells. These structured cellular arrangements emerge, amongst other factors, from polarity cues. Insect nephrocyte cells are organized to function apart from adjacent cells and therefore possess partly a different 3D cell architecture, yet their homoloy to podocytes suggest the same connection between correct polarity establishment and cell function.

Hence, after determining the effects of a Par complex protein knockdown on the localization of their complex interaction partners, the impact of the knockdown on functionality of the cells was investigated as well. If the localization of polarity proteins and their interaction partners is affected in knockdown mutants, it is likely to see differences in functionality as well. The influence of beforementioned knockdown mutants on nephrocyte functionality, the direction and extent of functional differences were measured in GFP accumulation assays.

The functionality assays of this thesis are based on the method described in Zhang et al., 2013b, and were further developed for the specific needs of this study. A ubiquitously produced and secreted ANF-GFP-GFP construct stains the larval hemolymph in a faint greenish color under UV light exposure. In contrast, the pericardial nephrocytes are brightly green since under normal conditions the GFP is taken up and stored abundantly in the nephrocytes. Upon RNAi-knockdown of a specified gene, GFP uptake and accumulation will change accordingly to the importance of the genes involvement in the cells' functionality. Consequently, if GFP uptake/ accumulation in mutant nephrocytes is impaired, the larvae show a brighter hemolymph and less pronounced glowing nephrocyte cells.

Nephrocytes of L3 larvae were dissected and prepared as described in chapter 3.3. The larvae were offspring to standard UAS/Gal4-crossings that produce a RNAi-knockdown of the gene of interest specifically in the nephrocytes. Gene expression was enhanced by keeping the larvae at 29°C prior to dissection.

4.3.1 Knockdown of Par complex components reduces GFP accumulation ability in nephrocytes

In mouse podocytes, the podocyte-specific deletion of apical polarity protein aPKCλ/ι leads to slit diaphragm displacement and is succeeded by foot processes effacement and proteinuria (Huber et al., 2009). The (severe) impact of the deletion of one Par complex component might occur again when other complex proteins are removed separately from the system. Thus, the outcome of single knockdowns of Par complex members were tested in the following experiments.

The Par complex proteins were one by one knocked down via RNAi. As control lines, mCherry-RNAi and kirre-RNAi lines were used. If not described differently, mCherry-RNAi values were set to 100% for representing the normal GFP uptake since mCherry mRNA is neither involved in cell functionality processes nor considered to influence nephrocyte development or their GFP uptake.

Expressing kirre-RNAi leads to an absence of nephrocyte diaphragms (Weavers et al., 2009) and decreases the possibility of GFP uptake and accumulation into the cell via the nephrocyte diaphragms. Therefore, kirre-RNAi was used in this study as control for impaired nephrocyte functionality. Downregulating Kirre, the NEPH1 homolog, leads to a decrease in relative GFP uptake of 91% compared to the mCherry-RNAi control (Fig. 23). Highly impaired uptake is already visible under UV light exposure in the undissected larvae as the remaining GFP engenders a strong green fluorescence of the larval hemolymph.

The knockdown of Bazooka results in an apparent reduction of GFP accumulation, as seen in Fig. 23, but the extent depends on the utilized RNAi-line. GFP accumulation reaches 41% in the baz-RNAi mutant compared to the mCherry RNAi control and only 3% in the baz-RNAi sh2 mutant. The baz-RNAi sh2 efficiently targets the 5'-UTR of baz-mRNA, whereas the baz-RNAi targets the baz-mRNA coding sequence and shows less precision in knockdown and less effect in lethality tests.

In aPKC-RNAi mutants, GFP accumulation in the cells reach 41% compared to mCherry-RNAi control levels. Expressing par6-RNAi in nephrocytes results in a rather mild decrease of GFP accumulation, reaching 59% relative uptake compared to control levels.

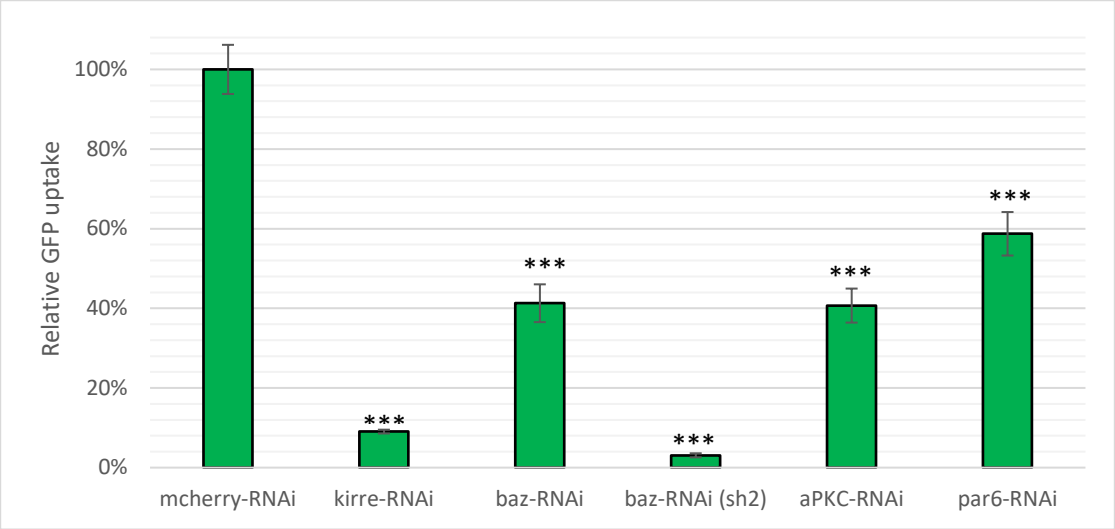

Figure 23: Relative GFP accumulation in Par-complex protein knockdown mutant nephrocytes. MCherry-RNAi (N=59) as control and representative for 100% GFP uptake. Kirre-RNAi (N=18) shows 9% uptake, baz-RNAi R88 (N=21) is diminished to 41%, baz-RNAi sh2 (N=50) is reduced to 3%, aPKC-RNAi (N=34) decreased to 41%, par6-RNAi (N=39) shows an uptake of 59%. All RNAi-lines were crossed to sns::GAL4, ANF-GFP-GFP flies. * $p<0.05$; ** $p<0.01$; *** $p<0.001$; NS=not significant. Error bars = SEM

In previous lethality tests with a ubiquitous daughterless-promoter, the RNAi lines of Bazooka, aPKC and Par6 gave comparable results regarding their knockdown efficiency and impact on development of *Drosophila* offspring. baz-RNAi sh2 showed a more efficient knockdown and effect on the larvae, leading to delayed growth and earlier death. Following these initial findings, the impact of absent aPKC, Bazooka or Par6 on nephrocyte functionality is about of the same extent in each experimental set-up. Removing one component of the Par-complex reduces GFP accumulation by approximately half the capacity. Utilizing an alternative baz-RNAi which eliminates baz-mRNA more efficiently from the cell, GFP accumulation is virtually impossible for the nephrocyte cell.

4.3.2 Overexpression of Bazooka phosphorylation mutant

As described in 4.2.4, the non-phosphorylatable form Baz_{5xA} shows mislocalization of aPKC and Sns in nephrocyte cells. To link this defect in localization to functionality, GFP accumulation assays were performed with overexpression variants of Baz. Females of the sns::GAL4, ANF-GFP-GFP strain were crossed to UAS::Baz_{WT}, UAS::Baz_{5xA}, or UAS::Baz_{5xD} males, respectively. As control, a mCherry-RNAi line was used since the mCherry construct has no effect on nephrocyte development or function.

Overexpression (OE) of the wildtype Bazooka protein leads to a gain-of-function-effect in GFP accumulation, which increases by the factor 1.5 (Fig. 24). Thus, the abundance of functional Bazooka might improve or stabilize the functional properties of nephrocytes. Expressing Baz_{5xA} in the nephrocytes leads to a great loss of functionality of the cell, since GFP uptake is reduced to merely 8%. Consequently, the impaired functionality is not only due to the depletion of Baz in the cell, but more specifically involves the regulation of Baz by aPKC. The phosphomimetic version Baz_{5xD} can only partly rescue GFP accumulation and reaches 48% compared to the control line.

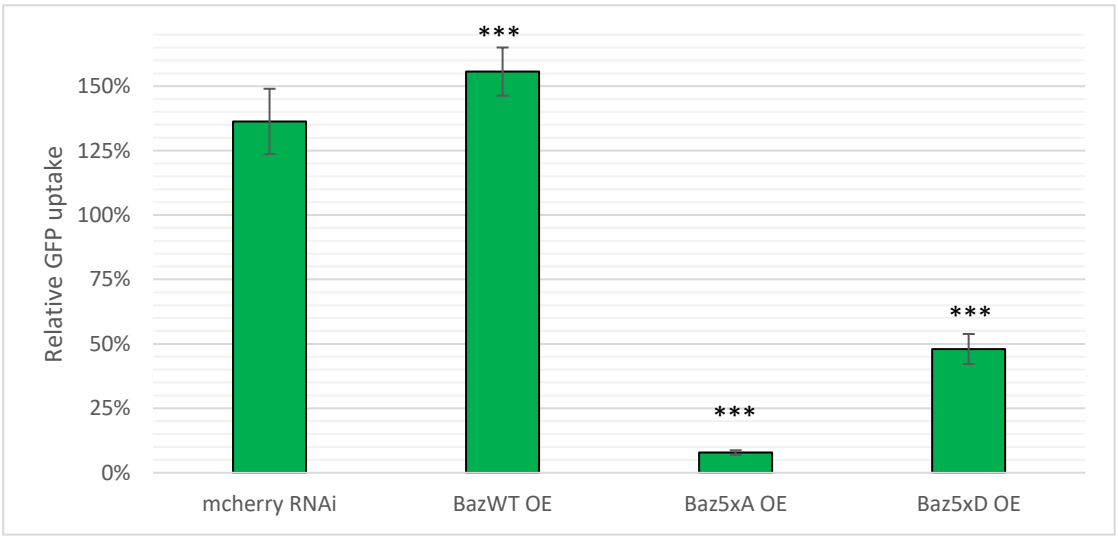

Figure 24: Relative GFP accumulation in Bazooka overexpression variants. mCherry-RNAi (N=45) as control and representative for 100% GFP uptake. Overexpression of wildtype Baz (N=43) increases GFP accumulation to 156%. The phosphorylation mutant Baz_{5xA} (N=47) reduces functionality to 8%, phosphomimetic Baz_{5xD} (N=22) shows impairment in functionality and 48% GFP uptake compared to control level. All RNAi/OE-lines were crossed to sns::GAL4, ANF-GFP-GFP flies. * $p<0.05$; ** $p<0.01$; *** $p<0.001$; NS=not significant. Error bars = SEM

4.3.3 Constitutively expressed aPKC is able to rescue the Baz_{5xA} mutant

Since nephrocytes lose their ability to accumulate molecules like GFP when Baz cannot be phosphorylated by aPKC, it was hypothesized that steadily active aPKC is capable to rescue the phenotype of the Baz_{5xA} phosphorylation mutant. For this experiment, the constitutively active $aPKC_{CAAX}$ was expressed in Baz_{5xA} background nephrocytes. The prenylated aPKC, effectively bound to the apical cell cortex and therfore constantly active, is able to rescue the Baz_{5xA} mutant dysfunctional phenotype completely and restores GFP accumulation to 100% (Fig. 25). Upon introduction of a dominant-negative, kinase-dead aPKC protein ($aPKC_{CAAX}$ DN) in the same Baz_{5xA} background cells, nephrocyte functionality remains impaired (see Fig. 25) and on the same level as the non-phosphorylatable Baz_{5xA} variant.

Taken together, the phosphorylation of Baz by aPKC is important for nephrocyte functionality. In case of this specific phosphorylation mutant, the functional restriction can be circumvented by artifically overexpressing active aPKC in the apical region of the cell.

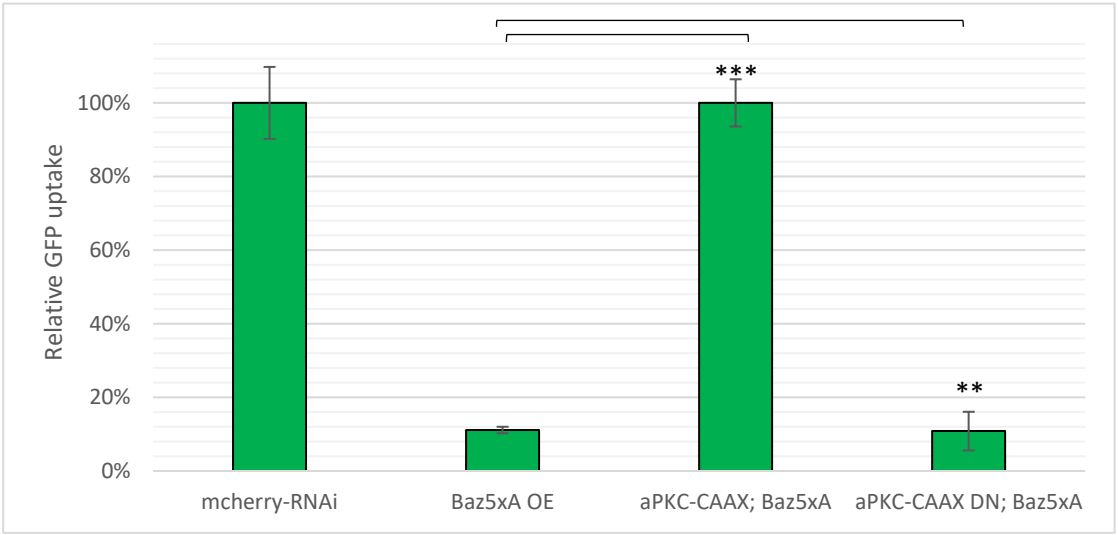

Figure 25: Relative GFP accumulation in Baz_{5xA} and $aPKC_{CAAX}$ rescue. mCherry-RNAi (N=35) representing average wildtype GFP uptake level. Baz5xA mutant (N=47) shows impaired GFP uptake. Constitutively active $aPKC_{CAAX}$ in a Baz_{5xA} background (N=69) restores GFP accumulation to 100%, whereas the kinase-dead version of $aPKC_{CAAX}$ shows impaired functionality with a GFP uptake of 11% (N=53). All RNAi-lines were crossed to sns::GAL4, ANF-GFP-GFP flies. * $p<0.05$; ** $p<0.01$; *** $p<0.001$; NS=not significant. Error bars = SEM

4.3.4 Phosphorylation defective mutant of Bazooka is not able to rescue Baz depletion phenotype

In a next step, the ability of Bazooka variants in rescuing the effect of Bazooka depletion was tested. For these experiments, the fly line sns::GAL4, ANF-GFP-GFP, Baz-RNAi(sh2) was used, where the efficient baz-RNAi sh2 construct (see 4.3.1) was permanently inserted in the sns::GAL4-ANF-GFP-GFP line.

As control, mCherry-RNAi flies were crossed to sns::GAL4, ANF-GFP-GFP as reference for standard GFP accumulation. An additional control was set up with sns::GAL4, ANF-GFP-GFP, Baz-RNAi(sh2) flies crossed to mCherry-RNAi as well. This cross resulted in a reduction of GFP uptake by 78% (see Fig. 26). Compared to similar experiments in chapter 4.3.1., where expression of baz-RNAi(sh2) led to a decrease of 97%, this reduction in functionality is less effective. Most likely, these varying degrees are due to a different genomic surrounding of the genes of interest in the two fly lines and crosses, respectively.

However, the overexpression of wildtype and phosphomimetic Bazooka proteins in *baz*-depleted nephrocytes could partly rescue the phenotype and restore GFP uptake. The expression of Baz_{WT} increased GFP accumulation up to 77% and the Baz_{5xD}-variant displays a rise in GFP uptake to 108% compared to control levels.

In contrast, overexpressing the phosphorylation-mutant variant Baz_{5xA} in cells with a *baz*-knockdown background leads to a GFP uptake in these nephrocytes of 25%, which is effectively no change in GFP accumulation compared to the baz-RNAi(sh2), mCherry-RNAi control. Thus, the capability of Baz to be phosphorylated by aPKC is vital for accurate nephrocyte function regarding endocytosis and accumulation of extracellular molecules.

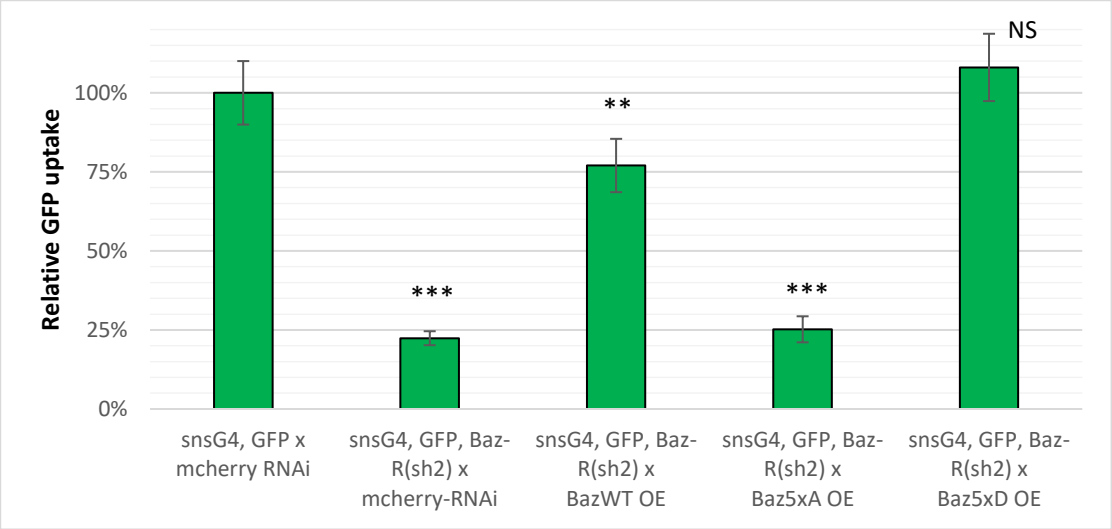

Figure 26: Relative GFP accumulation in Bazooka overexpression variants in Baz-knockdown background. Sns::GAL4, ANF-GFP-GFP x mCherry-RNAi (N=37) as control and representative for 100% GFP uptake. Remaining experiments were performed with Sns::GAL4, ANF-GFP-GFP, baz-RNAi(sh2) flies. mCherry-RNAi control (N=35) reached 22% relative GFP uptake. OE of Baz_{WT} (N=56) leads to 77% rescue of GFP uptake, phosphomimetic Baz_{5xD}-OE (N=26) increases GFP accumulation to 108%. Baz_{5xA} OE (N=59) cannot rescue the baz-RNAi(sh2) knockdown, GFP uptake remains at 25%. * $p<0.05$; ** $p<0.01$; *** $p<0.001$; NS=not significant. Error bars = SEM

4.3.5 Knockdown of basal polarity determinants strongly influences nephrocyte functionality

The knockdown of the basal polarity proteins Lgl (Lethal-giant-larvae), Dlg (Discs-large), and Par1 were also analyzed with regard to their effect on nephrocyte functionality. As these proteins play a significant role in polarity establishment and integrity of the cell, it is likely to obtain an effect on functionality as well when they are removed. Analogous to the previous experiments with the Par complex proteins, the basal polarity proteins were knocked down and investigated individually. All RNAi-lines were crossed to sns::GAL4, ANF-GFP-GFP flies separately and the offspring was raised at 29°C prior to dissection.

mCherry-RNAi was used as control and set as 100% GFP uptake level. Compared to that value, the expression of lgl-RNAi results in a considerable increase of roughly 160% GFP uptake (Fig. 27). Of all tested proteins, Lgl was the only case inducing a significant rise

in GFP accumulation when being partly reduced or deleted in the cell. Therefore, absence of the basolateral Lgl protein leads to changes in intracellular processes involved in functional properties which in turn enhance GFP accumulation in the cell. This result corresponds to previous findings where Lgl depletion in developing Drosophila eye tissue leads to increased Notch signaling and elevated levels of early and recycling endosomes, and other markers of endocytosis (Parsons et al., 2014; Portela et al., 2015).

Several dlg-RNAi lines were tested in regard to their efficiency in knocking down the gene of interest. RNAi lines with a strong effect on larval lethality (i.e. poor to no survival rate of individuals into adulthood) were presumed as most effectual and utilized in functionality assays. The most effective dlg-RNAi line in these assays was subsequently prepared for TEM analysis as well. In Fig. 27, this dlg-RNAi line results in a reduction of GFP accumulation to 3% compared to the mCherry-RNAi control level.

The knockdown of Par1 also causes a decrease of GFP accumulation. The tested par1-RNAi lines show a reduction to only 14% and 25%, respectively, in comparison to the accumulation of the mCherry-RNAi control line. Overall, the effects of a knockdown of basal polarity determinant proteins were even more prominent than those of apical polarity proteins. Loss of Dlg and Par1 diminishes functionality, as measured in GFP accumulation, efficiently by 75-97% whereas on the contrary, lgl-RNAi is increasing functionality.

Endocytosis and cell polarity mechanisms are closely intertwined, though regulation primarily involves apical polarity proteins, and basolateral proteins like Dlg are unaffected when manipulating endosomal markers Rab5 and Rab11 (Eaton et al., 2014; Roeth et al., 2009). Hence, the influence of Dlg- and Par1 knockdown on nephrocyte functionality is most likely of secondary nature.

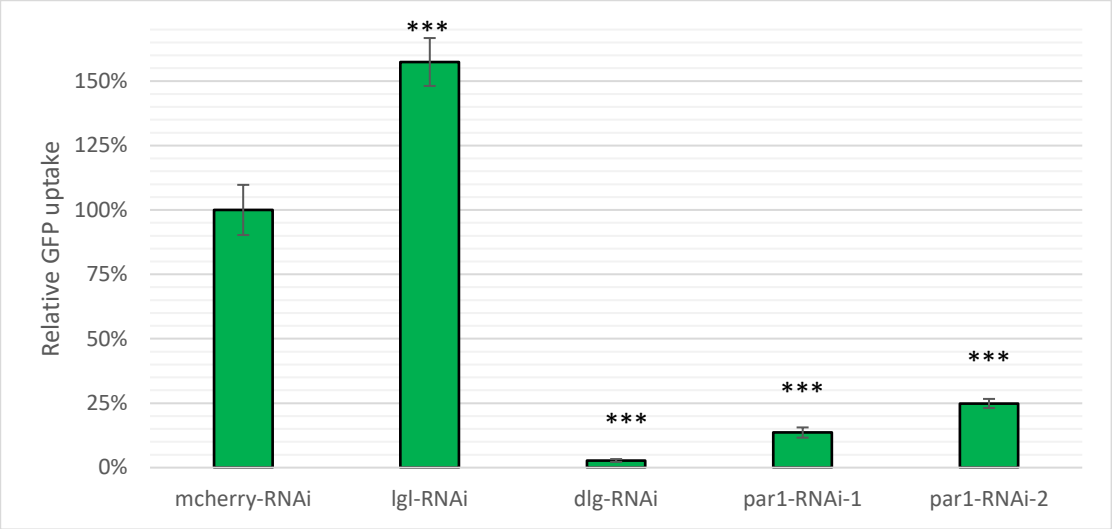

Figure 27: Relative GFP accumulation in basal polarity protein knockdown nephrocytes. mCherry-RNAi (N=20) as control and representative for 100% GFP uptake. lgl-RNAi (N=103) leads to an increase of GFP accumulation of 158%. dlg-RNAi (N=56) reduces GFP uptake to 3%, par1-RNAi-1 (N=85) and par1-RNAi-2 (N=76) decrease GFP accumulation by 86% and 75%, respectively. All RNAi-lines were crossed to sns::GAL4, ANF-GFP-GFP flies. * $p<0.05$; ** $p<0.01$; *** $p<0.001$; NS=not significant. Error bars = SEM

4.4 Ultrastructural changes in polarity protein knockdown mutants

The results from experiments on localization and functionality show that these key features are not necessarily reliant on on each other and both can be influenced by several different aspects. For example, in the *Par6* knockdown, the cells show high distortion in the localization of polarity proteins, but the least reduction in GFP accumulation. As an additional foothold, the interplay between localization and functionality can be evaluated to a certain extent by the ultrastructural features of the cell.

To investigate the effect of polarity protein depletion on nephrocytes in more detail, the ultrastructures of the knockdown mutants were analyzed using electron transmission microscopy (TEM). Females carrying the RNAi-construct of interest under control of a UAS promoter were crossed to sns::GAL4 males. Subsequently, larval Garland nephrocytes of the respective genotypes were prepared for electron microscopy as described in chapters 3.4.1 and 3.5. For comparable results, nephrocyte cell sections containing the nucleus/ nuclei were used and analyzed regarding the ratio of nephrocyte diaphragm (ND) per µm (perimeter) and the development of the peripheral lacuna area at the cortex of the cell.

4.4.1 Drosophila nephrocytes have a highly customized cell ultrastructure

The *Drosophila* nephrocyte possesses a very unique cellular ultrastructure. Wildtype cells measure about 20-30 µm in diameter and are mostly binucleate. The cells' outer layer is pierced with the so-called nephrocyte diaphragms, a homologous structure to the mammalian podocyte slit diaphragm, of roughly 30 nm width. Within the cell, there is a distinct loosened, peripheral labyrinthine system (or lacuna area) with its branchings seemingly disemboguing in the nephrocyte diaphragms.

Typically, this cortical area shows lower electron density than the cytoplasm (see Fig. 28) and appears therefore lighter in the micrograph. The black spots in the cells are mostly condensed residues of various vesicle/ organelle contents. The average number of nephrocyte diaphragms (ND) per µm is 3,19 ND/µm in the wildtype and 2,43 ND/µm in the mCherry-RNAi control.

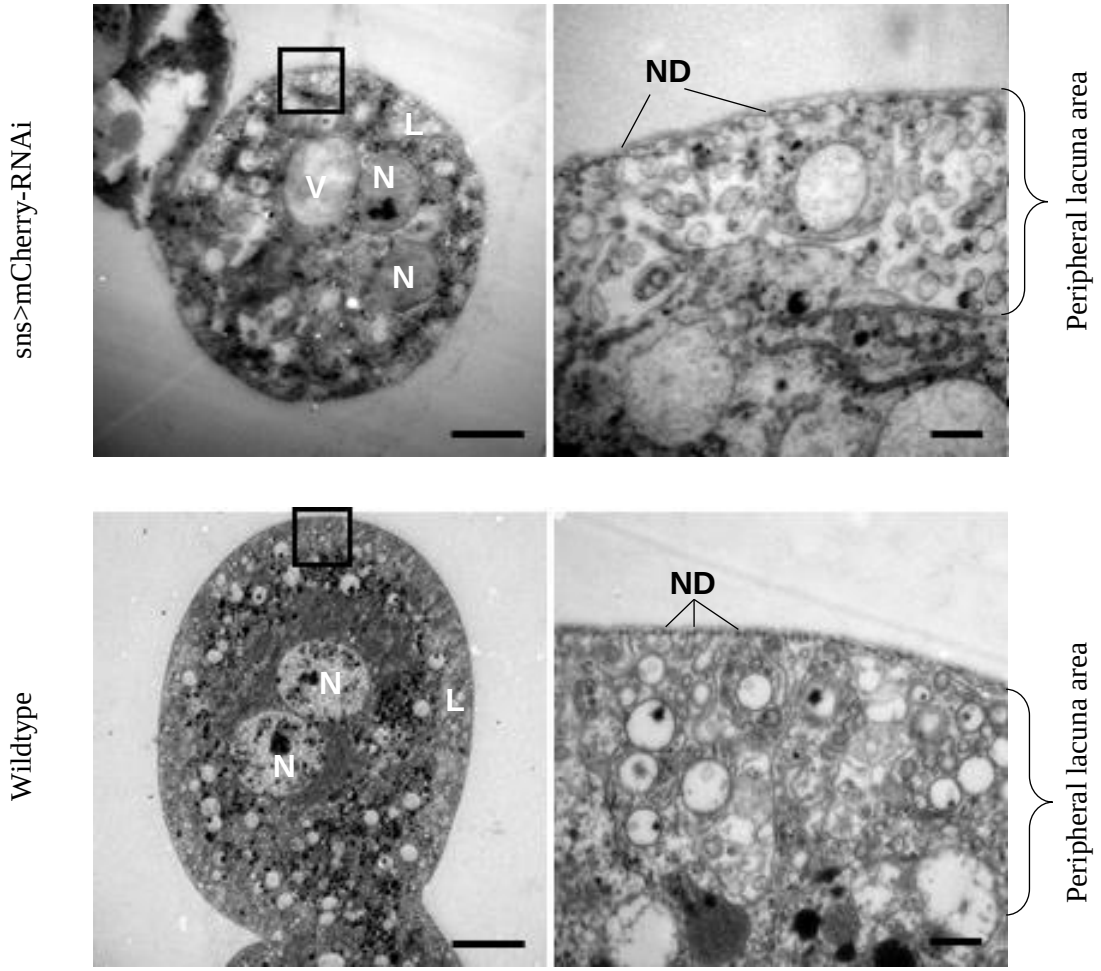

Figure 28: Ultrastructure of sns>mCherry-RNAi and wildtype (attP 28E) nephrocytes. Binucleate cells with labyrinthine like invaginations of the cell membrane. Nephrocyte diaphragms span over the pores and act as filtration barrier and signaling hub. N= Nucleus, L= Lacuna area, V= Vacuole, ND= Nephrocyte diaphragm. Left, overview: 3000x magnification, scale bar = 5µm. Right, detail: 20.000x magnification, scale bar = 500nm

4.4.2 Knockdown of Baz has negligible effect on nephrocyte ultrastructure

Both baz-RNAi lines that were tested in the functionality assays, were analyzed in these ultrastructural studies. Especially visible in the Baz (sh2) mutant, the development of the peripheral lacuna area is not disturbed in the Baz knockdown (see Fig. 29). The width of this area is about 3 µm and comparable to mCherry-RNAi and wildtype control. With 2,6 ND/µm in the baz-RNAi (sh2) mutant, the amount of nephrocytes diaphragms is at control levels or slightly enhanced, respectively (Fig. 31).

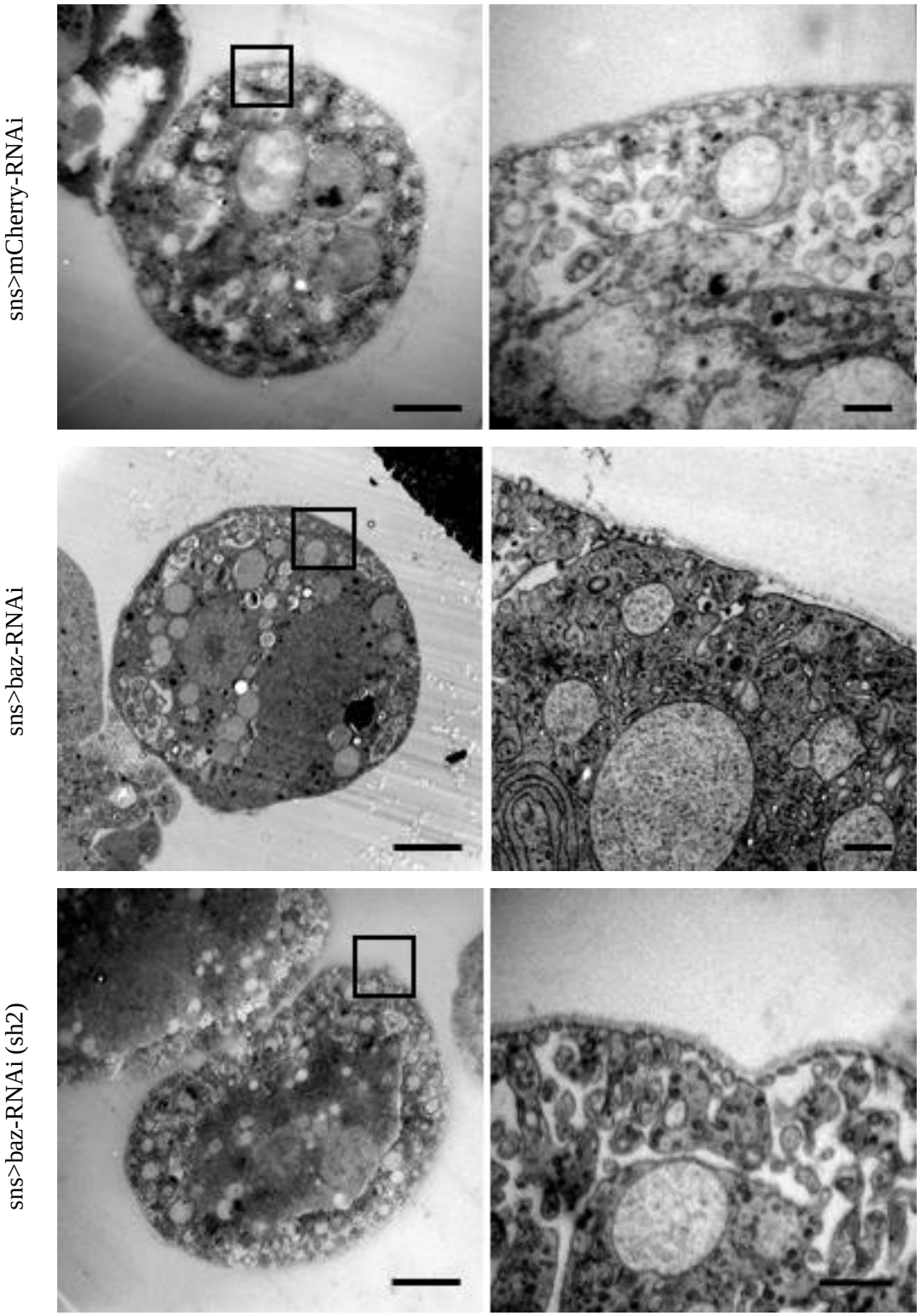

Figure 29: Bazooka knockdown in *Drosophila* nephrocytes. Both lines display well-developed lacuna area and nephrocyte diaphragms. Baz-RNAi shows an under-developed lacuna area and NDs (1,18 ND/µm). Baz-RNAi (sh2) has normal peripheral lacunae and NDs (2,6 ND/µm). Left, overview: 3000x magnification, scale bar = 5µm. Right, detail: 20.000x magnification, scale bar = 500nm

The alternative baz-RNAi line shows a mild effect in the ultrastructure of the cell. Though a well formed peripheral lacuna area is present in parts of the cell, it is missing in other cortical areas. Additionally, the number of diaphragms is reduced to 1,18 ND/µm (Fig. 31). The diverse ultrastructural phenotypes of these two tested baz-RNAi lines might be due to their different targeting of baz-mRNA in early developmental stages of the cell.

Compared to the preceeding functionality tests (chapter 4.3), the impaired filtration capability of the Baz knockdown nephrocytes is partly resulting from the reduced number of NDs and labyrinthine channels in the cortical area, and partly dependent on other, multiple factors to be determined.

4.4.3 Knockdown of aPKC and Par6 leads to decrease in nephrocyte diaphragm development

The absence of the apical polarity protein aPKC results in strong defects in the nephrocyte ultrastructure. Their overall cell size is diminished and they fail to develop the peripheral lacuna area at the cortex (see Fig. 30). Only small invaginations of the cell membrane are present in the vicinity of some nephrocyte diaphragms. The number of diaphragms is also reduced to an average of 0.70 ND/µm, a third of the mCherry-RNAi control (Fig. 31). These results confirm the findings of Huber et al. (2009) reporting of severe effects of loss of aPKCλ/ι in mouse podocytes.

Par6 functions as adaptor protein for aPKC and regulator for aPKC kinase activity (Atwood et al., 2007). Interestingly, the knockdown of Par6 leads to a fully developed labyrinthine system (see Fig. 30), yet the number of nephrocyte diaphragms is also decreased by two thirds to about 0.65 ND/µm (see Fig. 31). These findings suggest that the genesis of the lacuna area and the formation of filtration slits/ nephrocyte diaphragms might be separate or at least partly uncoupled steps in cell development.

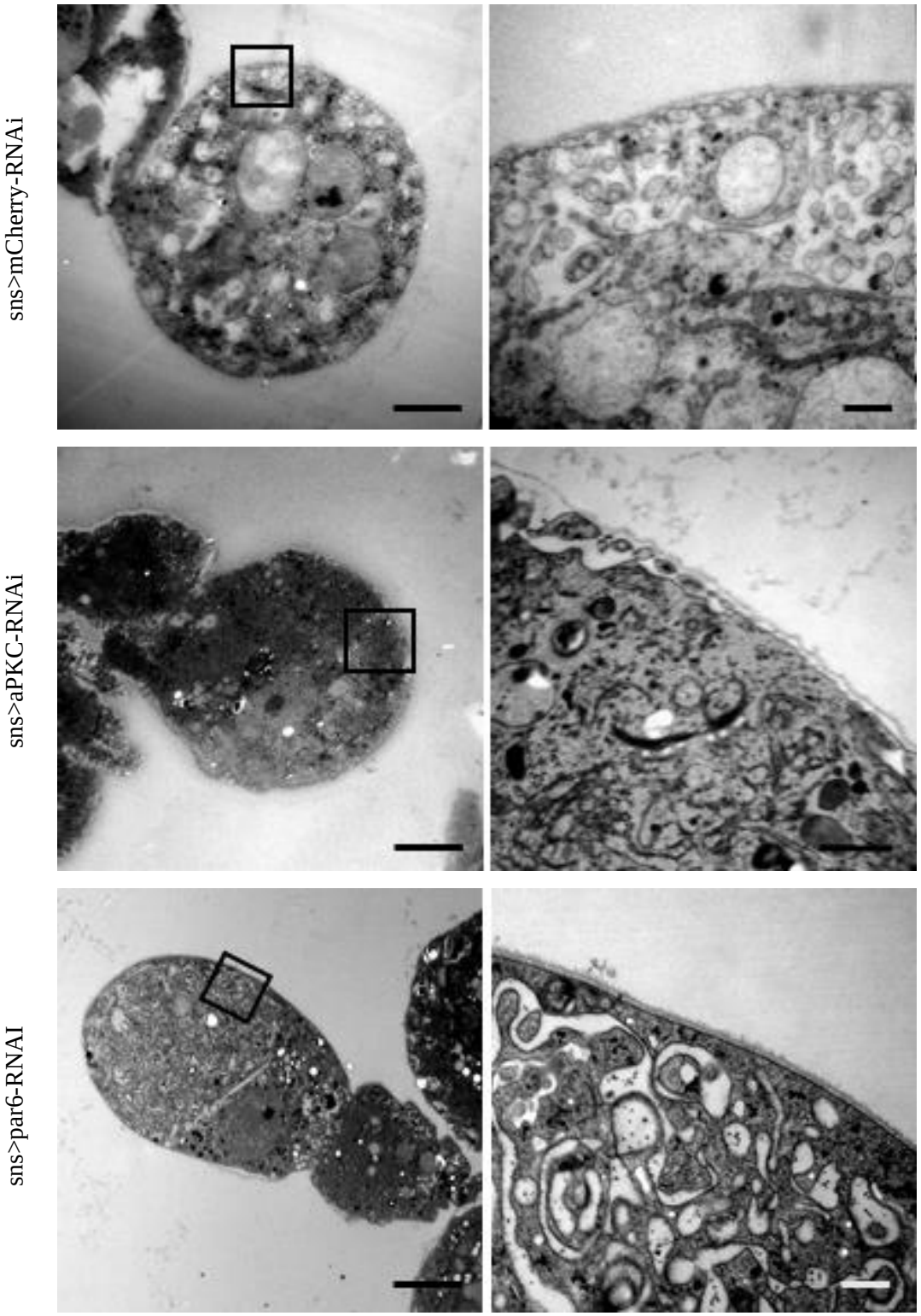

Figure 30: Knockdown of apical polarity proteins aPKC and Par6 in nephrocytes. In the aPKC mutant, the lacuna area and nephrocyte diaphragms are highly reduced. The par6-RNAi nephrocyte reveals a lacuna rich cell, but missing nephrocyte diaphragms on the cell surface. Left, overview: 3000x magnification, scale bar = 5µm. Right, detail: 20.000x magnification, scale bar = 500nm

To summarize, the knockdown of most apical polarity regulators leads to a strong decrease in the number of filtration slits per µm. Deleting the heterodimer complex of aPKC-Par6 by knocking down only one component, the number of occuring nephrocyte diaphragms on the cell surface is more than halved. However, this reduction is not proportional to the decrease in GFP accumulation in the respective genotypes.

Regarding the knockdown of Bazooka, the results are controversial and vary between no changes and half of the control level. Since the used Baz-RNAi lines have different approaches and efficieny of eliminating baz-mRNA from the cell, there might be secondary effects involved.

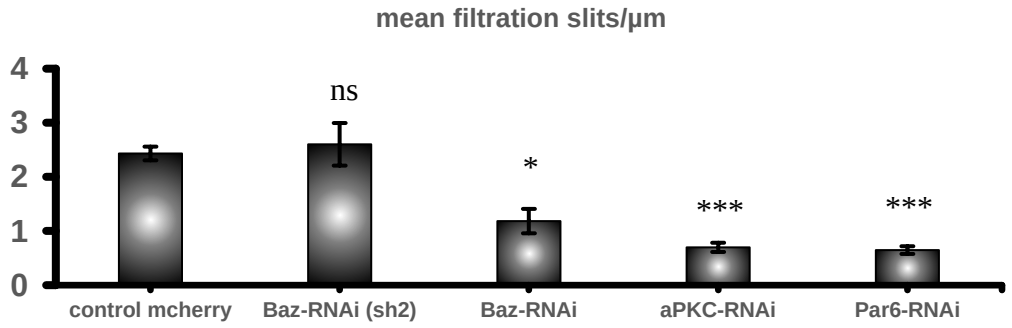

Figure 31: Mean filtration slits/µm in apical polarity protein knockdown nephrocytes. Knocking down one of the Par complex components leads to reduction in the average number of nephrocyte diaphragms per µm. Most knockdown lines lead to a significant lower number of ND/µm in the affected cells: baz-RNAi 1,18, aPKC-RNAi 0.70, par6-RNAi 0.65 ND/µm. baz-RNAi sh2 has no/ a slight enhancing effect on the number of ND: 2.60 ND/µm. mCherry-RNAi control: 2.43 ND/µm. * $p<0.05$; ** $p<0.01$; *** $p<0.001$; NS=not significant. Error bars = SEM.

4.4.4 The Baz_{5xA} phosphorylation mutant is unable to develop normal nephrocyte ultrastructure

The nephrocytes of the phosphorylation variants of Bazooka Baz_{5xA}, Baz_{5xD}, and Baz_{5xA}; $aPKC_{CAAX}$ rescue were prepared for transmission electron microscopy and analyzation. Following the GFP accumulation results, the ultrastructure of the phosphorylation mutant Baz_{5xA} shows the most severe impairments in development. Compared to the wildtype ultrastructure, overexpression of Baz_{WT} and Baz_{5xD} leads to little impact in the cells. The peripheral lacuna area is formed in a normal extent, with some parts of the cortex being more densly packed as in the control (Fig. 32). In both the wildtype and phosphomimetic overexpression, the number of filtration slits is (slightly) reduced to 2,45 and 1,40 ND/µm, respectively (Fig. 34). Thus, abundant wildtype Baz has little effect on ultrastructural development, whereas the actual phosphorylation of Baz possibly plays a role in nephrocyte diaphragm formation.

In contrast, there are ultrastructural detriments upon overexpressing the phosphorylation-mutant Baz_{5xA} in the cell (Fig. 33). Most strikingly, the peripheral labyrinthine channels are shortened and under-developed, and the number of nephrocyte diaphragms is perceptibly decreased to an average of 1,11 ND/µm (Fig. 34). These structural and cellular restrictions are most likely one of the underlying causes of the strong functional deficiencies of this Baz mutant cell.

As in the functionality experiments, the impairments of the Baz_{5xA} mutant can be rescued on the ultrastructural level by introducing an constitutively active $aPKC_{CAAX}$, attached to the apical membrane via its artificial CAAX-motif. Although the overall size of these nephrocytes is smaller compared to wildtype control cells, the lacuna area is restored to a normal width and manifestation (see Fig. 33). Additionally, the number of filtration slits is increased (in comparison to the Baz_{5xA} mutant) to the average of 2,18 ND/µm, which is in the range of control levels. These findings in ultrastructural impacts of the overexpression of Baz mutants complement the previous GFP accumulation data.

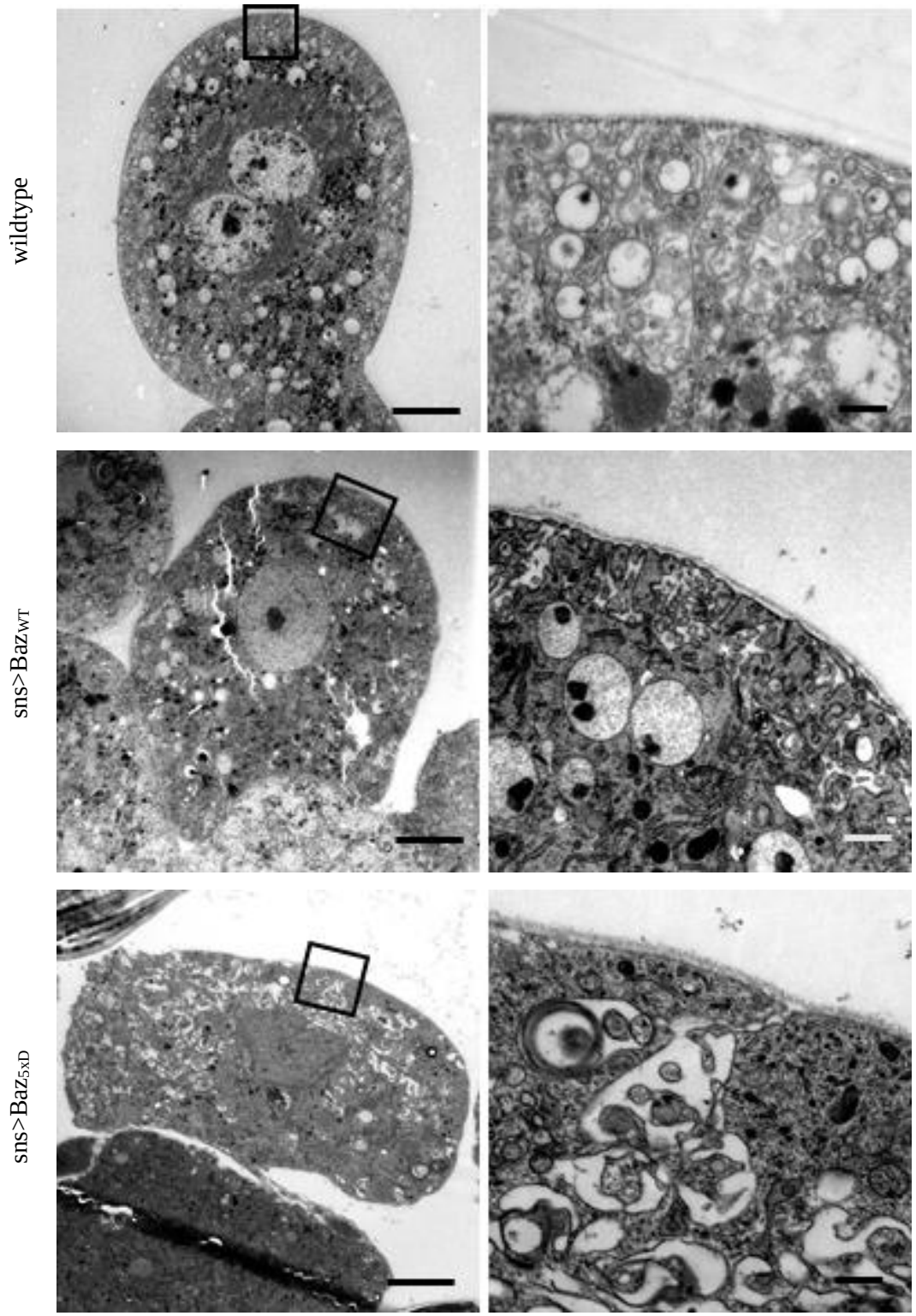

Figure 32: Nephrocyte ultrastructure of Bazooka phosphorylation mutants. Normally developed labyrinthine system and filtration slits in the wildtype cell. Slightly impaired shaping of lacuna area in the Baz_{WT} and phosphomimetic Baz_{5xD} overexpression, accompanied with a mild reduction in nephrocyte diaphragms. Left, overview: 3000x magnification, scale bar = 5µm. Right, detail: 20.000x magnification, scale bar = 500nm

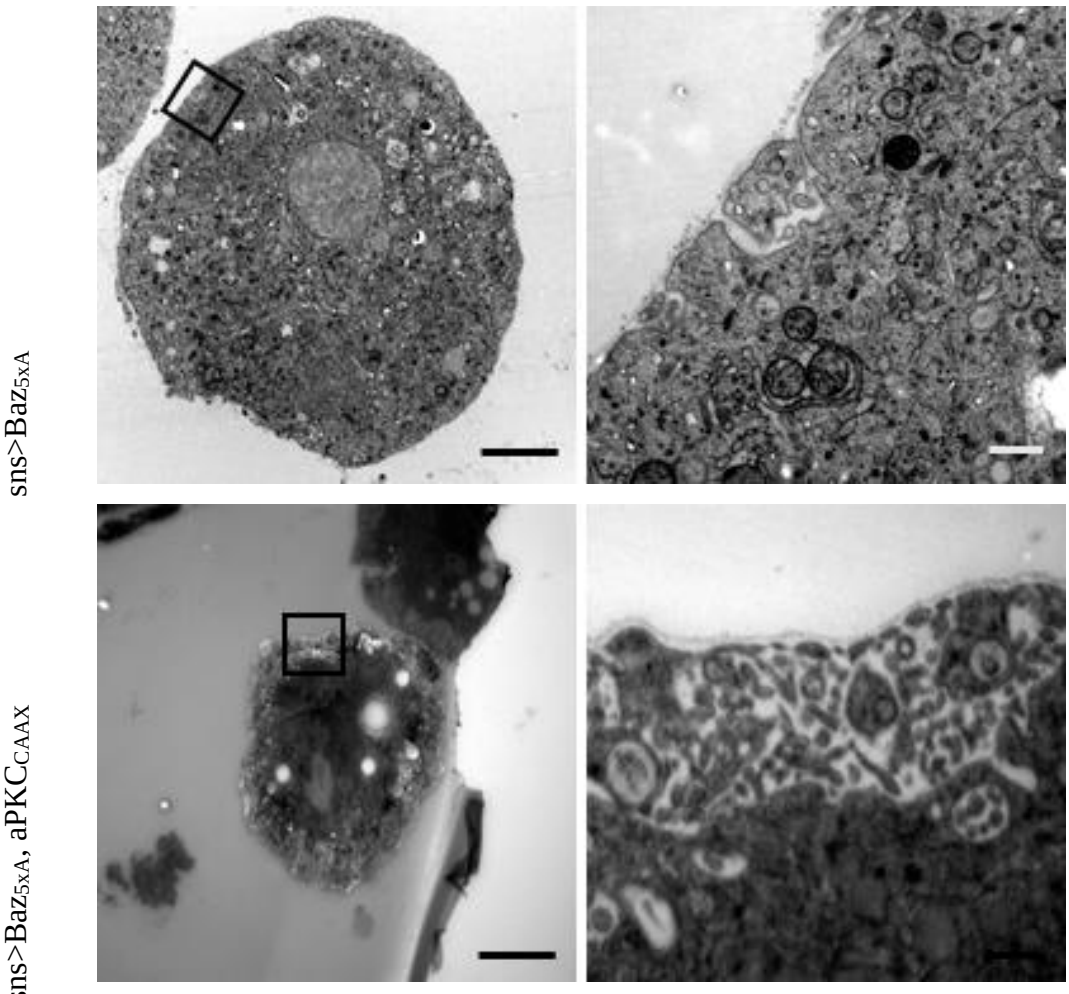

Figure 33: Nephrocyte ultrastructure of Bazooka phosphorylation mutants. Phosphorylation mutant Baz_{5xA} leads to a strong decrease in lacuna channels and filtration slits. This phenotype can be rescued by constitutively active $aPKC_{CAAX}$, labyrinthine channels and nephrocyte diaphragms are restored. Left, overview: 3000x magnification, scale bar = 5µm. Right, detail: 20.000x magnification, scale bar = 500nm

The reduction of nephrocyte diaphragms in overexpressed Bazooka variants are summarized in Fig. 34. While the number of nephrocyte diaphragms is decreased in the phosphorylation-mutant Baz_{5xA} overexpression, this effect is rescued by co-expressing the constitutively active $aPKC_{CAAX}$ protein in the cell. As visible in the functionality assays, the overexpression of phosphomimetic Baz_{5xD} results in a reduction of ND/µm as well and cannot sufficiently compensate wildtype Bazooka properties. Therefore, instead of a stable and continuous (non-)phosphorylation status, the flexibility of changing the

Bazooka phosphorylation status seems to play an important role in the matter of correct protein interaction and function.

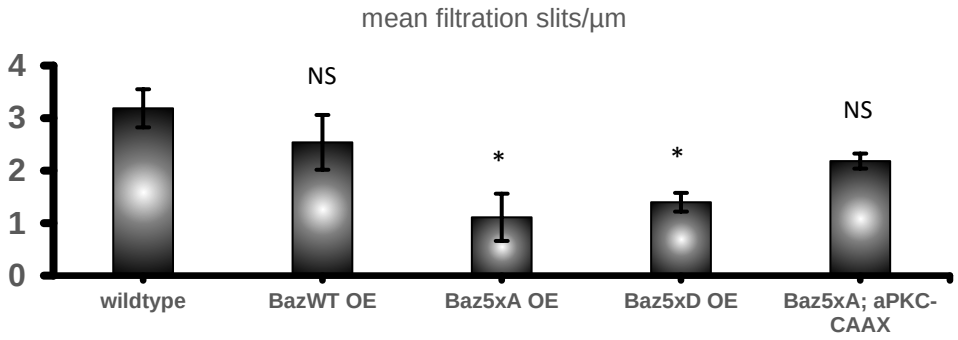

Figure 34: Mean filtration slits/µm in Bazooka mutant nephrocytes. The overexpression of Baz_{5xA} leads to a reduction of filtration slits from 3.19 ND/µm (wildtype) to 1.11 ND/µm. This decrease can be rescued by co-expressing constitutively active aPKC to an average of 2.18 filtration slits/µm. Overexpressing Baz_{WT} shows an average number of 2.54 ND/µm and the phosphomimetic Baz5xD construct a reduction to 1.40 ND/µm. * $p<0.05$; ** $p<0.01$; *** $p<0.001$; NS=not significant. Error bars = SEM.

4.4.5 Downregulation of basal polarity proteins has strong effects on nephrocyte development

For correct establishment of the complex nephrocyte cell structure, the accurate set-up of apical-basal polarity has to be ensured. In chapter 4.3.2, it was shown that the absence of one (out of three examined) basal polarity determinant has an impact on nephrocyte functionality, either significantly reducing or enhancing the cells' ability to accumulate GFP.

The knockdown of apical polarity proteins influences the nephrocyte ultrastructure to various extents, but only partly coherent with their influence on functionality. For analyzing the effects of basal polarity regulator depletion on cellular development, the proteins Dlg (Discs-large) and Par1 (partitioning-defective 1) were downregulated via RNAi in nephrocytes (see Fig. 35).

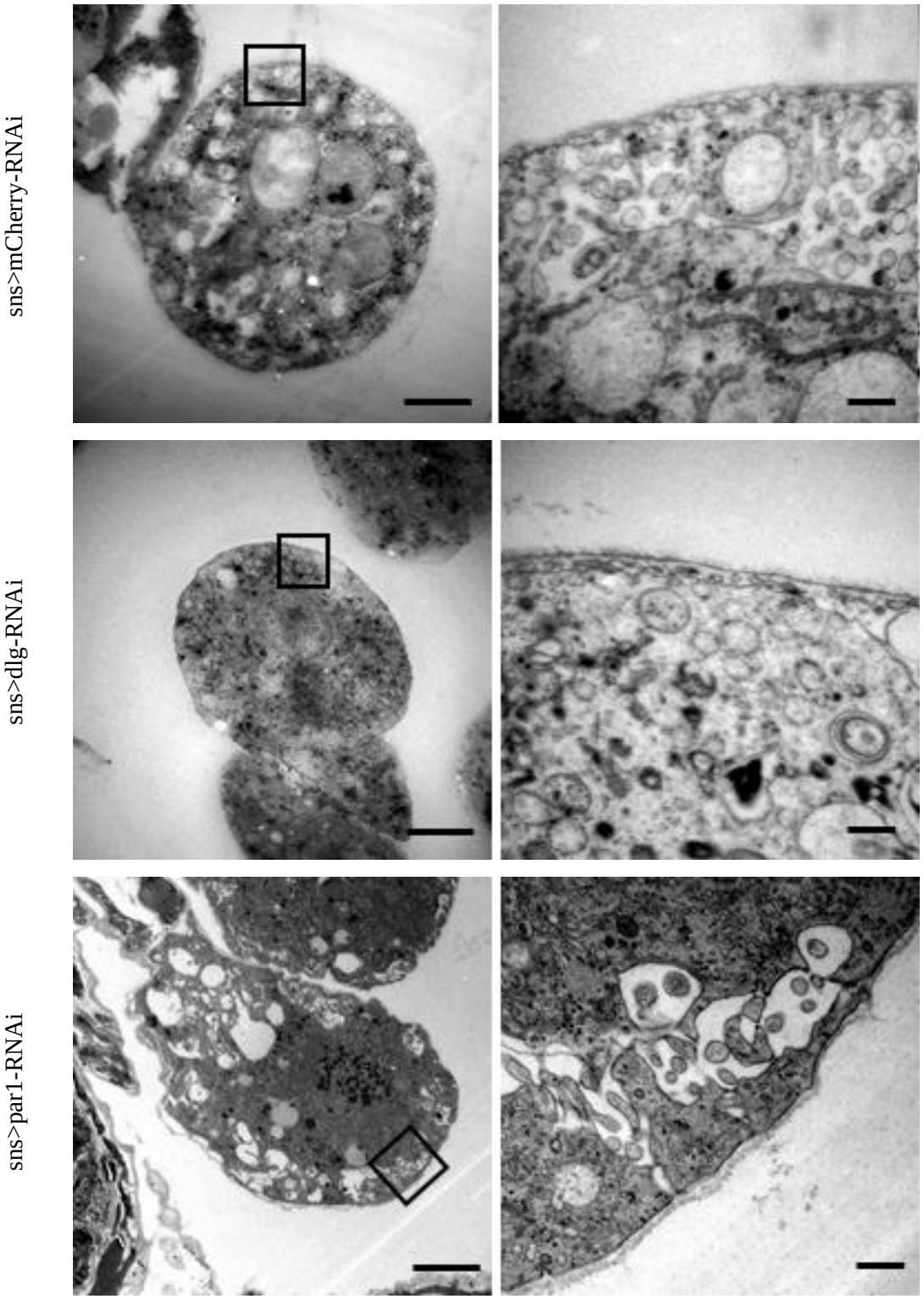

Figure 35: Nephrocyte ultrastructure of Dlg- and Par1-knockdown cells. In Dlg-knockdown nephrocytes, both the peripheral lacuna area and nephrocyte diaphragms are under-developed and missing in the greater part of the cell. Par1-RNAi nephrocytes display a loosened, nevertheless apparent lacuna area, but simultaneously a reduced number of filtration slits on the cell surface. Left, overview: 3000x magnification, scale bar = 5µm. Right, detail: 20.000x magnification, scale bar = 500nm

In the micrographs of Dlg-knockdown nephrocytes, the ultrastructure shows lacunae area effacement and a strong reduction in nephrocyte diaphragms (see Fig. 35). The distinct peripheral channel system is, with few exceptions, not developed. The number of filtration slits is decreased by 80% to 0.54 ND/µm. In general, the overall nephrocyte structure in this mutant is not very well defined.

Knocking down the basal polarity determinant Par1 has mild effects on the lacuna area. The inner, more dense cytoplasm and the peripheral channel system can be well distinguished (see Fig. 35), although the channels appear broader and loosened, with wider channel lumina than in the mCherry-RNAi control. Nephrocyte diaphragms are developed and visible in the micrographs, but their number is diminished by about 70% to 0.68 filtration slits per µm, compared to 2.43 in the control (Fig. 36).

Figure 36 summarizes the implications of reducing basal polarity protein activity on nephrocyte diaphragm development. The average number of filtration slits is reduced to about 23% in the Dlg-knockdowns and to 30% in the Par1-knockdown. Depletion of either tested basal polarity protein had a strong effect on the number of nephrocyte diaphragms, but only dlg-RNAi influenced the formation of the outer lacuna area as well. This finding is another indication on how the development of these two typical nephrcaote features might be regulated via separate paths.

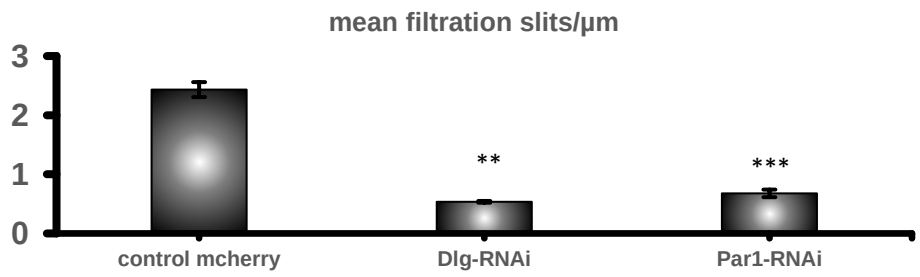

Figure 36: Mean filtration slits/µm in Dlg and Par1 knockdown nephrocytes. Both knockdowns have an under-developed number of nephrocyte diaphragms (ND): dlg-RNAi nephrocytes reach only 0.54 ND/µm, par1-RNAi cells 0.68 ND/µm. Control: mCherry-RNAi, 2. 43 ND/µm. * p<0.05; ** p<0.01; *** p<0.001; NS=not significant. Error bars = SEM.

5 DISCUSSION

Nephrocytes in *Drosophila melanogaster* represent a particularly suitable model system for a unique cell type in mammals, the podocyte. Their striking homology to podocytes predestine these insect cells for extensive research regarding nephrocyte/ podocyte structure and function. Valuable and clinically relevant insights can be generated and help to understand and ultimately even alleviate kidney disease.

Since both podocytes and nephrocytes have a very specific cell structure, the correct establishment of apical-basal polarity is a crucial step for proper cell function. The definition of cell poles and particular membrane compartements via polarity protein complexes is closely connected to the formation of slit or nephrocyte diaphragms, a highly specialized cell junction and important signaling hub (Hartleben et al., 2008; New et al., 2014; Simons et al., 2009).

In this study, the role of apical-basal polarity determinants in *Drosophila* nephrocytes and their impact on functionality and ultrastructure was analyzed. The loss of apical polarity regulator aPKC was examined in podocytes before (Hirose et al., 2009; Huber et al., 2009; Satoh et al., 2014), but the effects of other polarity proteins have been less acknowledged. Here, it was shown that apart from aPKC, the Par complex components Par6 and Bazooka/Par3 are in fact involved in correct nephrocyte development and function as well as their polarity counterparts, Dlg and Par1.

By knocking down single components of the apical Par complex formed by aPKC/Par6/Bazooka, it could be shown that the remaining polarity proteins and interaction partners are affected in their localization and distribution to various extents. Additionally, the most relevant aspect of nephrocyte functionality, their filtration ability, was reduced. In an ultrastructural approach, the impact of missing apical polarity proteins was apparent in impaired development of the typical nephrocte structures, the nephrocyte diaphragms and lacuna-like, labyrinthine channels. The knockdown of Par complex proteins results in an insufficient expansion of the peripheral lacunae and/or a decrease in the average number of nephrocyte diaphragms per µm.

The share of basal polarity proteins in nephrocyte and podocyte development has not been adequately assessed so far. The knockdown of the basal polarity regulators Dlg (Discs-large) and Par1 (partitioning-defective 1) leads to high reduction in nephrocyte functionality. Moreover, the Dlg-depleted nephrocyte cell displays severe ultrastructural impairments regarding the low number of nephrocyte diaphragms and the mostly missing peripheral lacuna area. Similar to dlg-RNAi, Par1 knockdown leads to a blatant decrease in filtrations slits, which points to the contribution of these proteins in junction establishment. The peripheral labyrinthine system, on the other hand, seems to be not much influenced in Par1 depleted nephrocytes.

In contrast, the knockdown of Lgl results in a gain-of-function effect in nephrocyte accumulation function. It has been shown that Lgl regulates endocytosis and Notch-signaling independently of the aPKC/Par6/Baz complex (Parsons et al., 2014). Besides filtration, endocytosis is another important factor in nephrocyte functionality (Harrison & Foelix, 1999; Ivy et al., 2015; Kerkut, 1985)

5.1 Localization of Par complex proteins in Drosophila nephrocytes

5.1.1 Par complex proteins co-localize in nephrocytes

The Par complex proteins aPKC, Par6 and Baz/Par3 belong to one of the major protein complexes establishing apical-basal polarity in epithelial cells. By mutual binding and/or phosphorylation within the Par complex and more interaction partners outside of the complex, they play an important role in setting up the apical membrane domain. The localization of the Par complex proteins in epithelial cells has been studied intensively and shows a specific pattern. The binding of Baz/Par3 to the dimer aPKC/Par6 results initially in the recruitment of aPKC/Par6 to the apical membrane (Goldstein & Macara, 2007; Harris & Peifer, 2005; Horikoshi et al., 2009). Secondly, the phosphorylation of Baz/Par3 by aPKC within the trimeric complex leads to the release of Baz/Par3 and its positioning at the site of AJ, whereas aPKC/Par6 remain placed more apically at the apical membrane (Morais-de-Sá et al., 2010; Walther & Pichaud, 2010).

It has been shown that aPKC and Baz/Par3 co-localize in mammalian podocytes at the site of slit diaphragms (Hartleben et al., 2008). Nephrocytes are an insect model for podocytes and share high similarities in structure and function. However, there are some differences in cell structure due to the fact that podocyte foot processes and slit diaphragms function as filtration barriers, whereas nephrocytes filtrate and accumulate molecules within the cell.

This study presents the co-localization of the Par complex proteins at the nephrocyte membrane and cortical zone together with the nephrocyte diaphragm proteins Sns (Sticks-and-stones) and Kirre (Kin-of-Irre), the *Drosophila* homologs of slit diaphragm proteins Nephrin and NEPH1. Sns and Kirre form both hetero- and homo-dimers and constitute the main protein bridge spanning the pores of the nephrocyte surface. Hence, they are used as markers for nephrocyte diaphragms and the cell boundary as well as indicators for correct diaphragm establishment.

Both Baz und Par6 reside in a well defined line at the cell membrane, whereas aPKC extends slightly, but apparent, to the cytoplasm. The detail penal in Figure 14 A (chapter 4.1) displays Baz and aPKC localized in two distinct layers at the cell cortex with occasional overlaps. This stratified pattern is also seen in *Drosophila* embryonic epithelial cells, where it describes the segregation of Baz localization at the lower AJ region and aPKC positioning in the apical membrane domain above (Harris & Peifer, 2005). In the case of the nephrocytes, aPKC localizes at the cortical region of the labyrinthine cannels, seemingly below Baz. The explicit cortical distribution of aPKC in the nephrocyte, divergent in width from other apical polarity proteins, suggests an imperative necessity of aPKC activity in this defined cell region.

In a deviant behavior from epithelial cells, Par6 co-localizes with Baz and Sns at the nephrocyte membrane instead of joining aPKC in the separate inner layer (see Figure 14, chapter 4.1). Thus, Par6 activity might play a greater role at the direct vicinity of the nephrocyte diaphragms as in the peripheral lacuna area.

In this work we focused on the effects on the main/direct interaction partners upon single knockdown of polarity proteins. In a next step, it would be interesting to study the localization of the respective, antagonistic polarity proteins in those single knockdowns. Additionally, the localization and expression pattern of further interaction partners of

polarity proteins should be examined. For example, aPKC as part of the Par complex controls cell polarity and cell fate by phosphorylating a number of downstream targets, therefore assigning those targets a cortical or cytoplasmic position depending on their phosphorylation status (Drummond & Prehoda, 2016; Prehoda, 2009). aPKC/Par3 also regulates Tiam1, an important activator of the small GTPase Rac (Matsuzawa et al., 2016). GTPases (Rac and Rho family) act as molecular switches and are crucial factors in cell signalling pathways. Similar important interactions, targets and regulations can be found for any of the polarity proteins examined in this study. Hence, the implications of depleting (or also overexpressing) single polarity proteins on multiple interaction partners or targets should be addressed in proceeding experiments.

To investigate the localization and distribution pattern in more detail, there are images of a higher resolution and more sharp footage of the cortical zone required. This could be achieved by applying, for example, z-stack images of immunohistochemistry stainings using optimized laser parameters. Supreme resolution can be accomplished by electron microscopy. Transmission electron microscopy offers the possibility of gold-immunostaining, targeting the GFP-tagged protein of interest. Unfortunately, with this specific method, only one protein per sample can be studied, which could lead to difficulties setting multiple proteins in relation to each another.

5.1.2 aPKC and Par6 show mutual dependence in establishing their localization

The exact chronological order of apical-basal polarity establishment in epithelial cells is not completely elucidated so far, since a variety of proteins and molecules are involved in this complicated process.

Bazooka activity is important for AJ assembly and polarization, working together with aPKC/Par6 or also acting independently from the Par complex. Baz is first positioned at the site of newly forming AJs in a cytoskeletal networks-dependent manner. Apart from its scaffolding properties of other interaction partners, Baz binds to Par6/aPKC and subsequently recruits this heterodimer to the apical domain of epithelial cells (Harris & Peifer, 2005; Horikoshi et al., 2009). aPKC phosphorylation of Baz confirms the specific localization of the Par-complex members at the apical and AJ region. Therefore,

removing one player in this fine-tuned machinery impacts the correct distribution and positioning of the other protein complex members.

The knockdown of either aPKC or Par6 affects the localization of the remaining dimeric binding partner. Missing aPKC leads to the reallocation of Par6 from the cell membrane into the cytoplasm or assembling of Par6 in concentrated spots instead of being evenly distributed along the cell membrane (see chapter 4.2.1, Figures 16 and 17). The interaction of Par6 with other polarity proteins presumably moderates Par6 misplacement in the aPKC knockdown mutant. It has been demonstrated in mammalian cells that Par6 can also bind to Lgl, though this interaction requires again aPKC activity (Plant et al., 2003; Yamanaka et al., 2003). Moreover, Par6 was found to associate with Pals1/Stardust (Sdt) via a conserved region in the amino terminus of Pals1 (Hurd et al., 2003; Wang et al., 2004). Pals1 is part of another multiprotein polarity complex consisting of Crumbs, Pals1/Sdt and PATJ. Par6 localization is also mediated by Sdt (Bulgakova et al., 2008).

In conclusion, although other factors are partially interacting with Par6 and therefore recruit the protein to distinct regions in the cell to complete this interaction, aPKC binding and establishing the Par complex with Baz seems to play a vital role in correct Par6 positioning at the apical domain.

In Par6 knockdown nephrocytes, the localization of aPKC and Baz is severly distorted. Par6 functions as binding partner for firstly aPKC in the dimeric aPKC/Par6 complex and secondly Baz/Par3 in the Par complex. aPKC regulates as an upstream factor a greater quantity of other proteins, but itself depends on the Par6 interaction for correct distribution in the cell. Hence, without being able to bind to Par6, the correct aPKC positioning and activity is lost in the nephrocyte. Also the binding of Baz to Par6 and the consequential phosphorylation by aPKC seems to be crucial for accurate Baz positioning in the cell. Without the linker protein Par6, Baz localization is no longer ultimately defined by aPKC, which leads to an off-balance of all involved proteins (see chapter 4.2.2, Fig. 18 and 19).

The effects of aPKC or Par6 knockdown of the filtration slit proteins Sns and Kirre are, according to results of immunostainings, apparent but not as grave as on the investigated remaining polarity proteins themselves. The stainings of either knockdown mutant reveal the constriction of both Sns and Kirre to a spot-like pattern along the nephrocyte

membrane. Loss of aPKC or Par6 presumably impaires an accurate assembly of adherens junction-like structures that eventually would lead to slit diaphragm establishment.

Bazooka knockdown displays rather mild effects on the localization of aPKC, Par6 and the nephrocyte diaphragm proteins. Though the distribution of all investigated proteins appears much more vage and less accurately defined at the cell boundary, all protein complex components are present at their actual location none the less. In epithelial cells, Baz acts upstream of aPKC/Par6 and recruits the dimer to the apical domain. Although this is regarded as the key aspect in aPKC/Par6 positioning, there are more subtle conducts possible. Apart from interacting with Baz through direct PDZ-PDZ binding, Par6 binds to RhoGTPase Cdc42 via its semi-CRIB motif. (Activated) Cdc42 is a membrane-bound molecular switch with a variety of downstream effectors and controlling cell polarity (Johnson, 1999). Since Cdc42 is enriched at cortical domains, its binding to Par6 feasible connects Par6 to the membrane (Atwood et al., 2007), pulling aPKC to the membrane as well. However, without the coordination interaction of aPKC and Baz, aPKC/Par6 localization remains more or less apically, yet unrestrained.

The impact of Baz depletion is more apparent in abberant Sns and Kirre localization. The role of Baz in the establishment of cell junctions, the platform for filtration slit assembly, seems to have greater influence than regulating aPKC/Par6 positioning. Compensating disturbed junction formation, the diaphragm proteins might sidestep to alternative interaction mechanism. Sns and Kirre are putatively associated with aPKC, analogous to Nephrin and Neph1 in mammalian podocytes (Hartleben et al., 2008). Hence, the binding of Sns and Kirre to the slightly mislocalized aPKC results in abundant assembly of nephrocyte diaphragms not only at the outer cell cortex, but also further in the cytoplasm, that means alongside the walls of the lacuna channels reaching into the cytoplasm (see chapter 4.2.3, Fig. 20 and 21).

5.2 Dysfunctional Par complex leads to ultrastructural and functional inadequacies in nephrocytes

The importance of podocyte health becomes evident in numerous studies on kidney disease. Looking at various forms of human and experimental glomerular diseases such as focal segmental glomerulosclerosis, membranous glomerulopathy, minimal change disease, diabetes mellitus and lupus nephritis, podocytes are found to be injured (Kerjaschki, 2001; Somlo & Mundel, 2000). Damage starts subtle in changes in the molecular composition of the slit diaphragm and progress visibly to major alterations in the structure of foot processes and filtration slits (Asanuma & Mundel, 2003; Kerjaschki, 2001; Somlo & Mundel, 2000). Most studies concentrated on the role of actin dynamics and actin network - associated proteins/components like synaptopodin and non-muscle myosin heavy chain II (Arrondel et al., 2002; Asanuma et al., 2007; Garovic et al., 2007; Ghiggeri et al., 2003; Mundel et al., 1997) in the investigation of functional impaired podocyte cells.

There are not many studies on the consequences of polarity distortion on podocyte fitness. So far, the effects of loss of polarity protein aPKC in podocytes has been primarily described (Hartleben et al., 2008; Hirose et al., 2009; Huber et al., 2009). Therefore, the significance of cell polarity in podocytes ought to be further analyzed in the model system of *Drosophila* nephrocytes.

Depleting the nephrocyte cell of either of the Par complex components Baz, aPKC, or Par6 results in a decrease in accumulation functionality of 40% to 60% compared to a mCherry-RNAi control (see chapter 4.3.1, Fig 23.). Interestingly, there is no clear direct correlation between the functionality of the nephrocyte and the developmental state of its ultrastructure. aPKC- and baz-RNAi nephrocytes have the same level of functionality defects, but while the aPKC mutant cell contains almost no peripheral lacuna network and a highly decreased number of filtration slits, baz-RNAi nephrocytes are less confined and develop about the half of the normally available lacuna channels and nephrocyte slits. Par6 mutant nephrocytes have elaborate lacuna channels, but filtration slits are mostly missing at the cell surface (see chapter 4.4., Fig. 29-31). Most likely, the functional performance of nephrocytes relates partly with filtration capacity or the number of filtrations slits, respectively, but depends on other processes like endocytosis as well.

However, all apical polarity proteins have their distinct effect on nephrocyte development. The severe ultrastructural malformation in the aPKC-knockdown cells indicate the importance of aPKC kinase activity in the developmental process in nephrocytes. aPKC, the atypical protein kinase C, belongs to the PKC family of Ser/Thr kinases that shares a highly conserved carboxy-terminal kinase domain. By interaction of their PB1 domain with the Par6/Cdc42 complex, activated aPKC acts as crucial factor in specifying apical-basal cell polarity (Suzuki et al., 2001). aPKC interaction is not restricted to Par6 and Baz, but extends to, amongst others, basal polarity proteins Lgl and Par1 (Hurov et al., 2004; Plant et al., 2003) and asymmetric cell division proteins Numb and Miranda (Atwood & Prehoda, 2009; Smith et al., 2007). Phosphorylation of these proteins by aPKC lays tracks to precise (asymmetric) polarization of different cell types, a crucial event in the development and organisation of cells and tissues. The exact mechanisms of aPKC activity and interaction in the specialized nephrocyte are yet to be elucidated, but they apparently play an important role in correct functionality of these cells.

Depleting the nephrocytes of aPKC-binding partner and -activator Par6 leads to a similar reduction of nephrocyte diaphragms per µm as in the aPKC-RNAi mutants, but the peripheral lacuna area remains properly shaped. The cells' functionality is fairly compromised to about 60% GFP accumulation compared to control capacities. The process behind lacuna channel branching is sparsely affected by a decreased Par6 activity as the lacuna area appears well-developed (see chapter 4.4.3, Fig. 30). These results suggest the main function of Par6 in the nephrocyte in the structural estalishment of apical membrane affiliated with junction assembly. In mammalian epithelial cells, the relevance of Par6 in junction establishment has been described before. Apart from the close interaction with aPKC, Par6 cooperates with PALS1/Stardust and Crumbs (CRB3) in enforcing the apical membrane domain by tight junction assemblage in mammalian epithelial cells (Hurd et al., 2003; Lemmers et al., 2003; Wang et al., 2004). Equally in several *Drosophila* tissues, the (direct) interaction of Par6 and Crb is a vital factor in polarization of membrane regions and adherens junction organisation (Fletcher et al., 2012; Nam, 2003). Regarding the insect nephrocyte cell and its particular cell architecture, the consequences of losing the protein Par6 in this interplay is visible in the reduced number of filtration slits in the nephrocytes followed by functional restrictions.

This underlines the importance of correct and abundant junction assembly in this unique cell type.

Knocking down Bazooka in the nephrocyte cell showed varying effects depending on the utilized RNAi-line. Both lines cause functionality defects in the GFP accumulation assay. Interestingly, the RNAi line showing the milder reduction of GFP accumulation to about 40% GFP uptake also displayed alterations in the ultrastructure of the cell (see chapter 4.3.1, Fig. 23 and chapter 4.4.2, Fig. 29). The maturation of the lacuna channel system appears impaired and the number of nephrocyte diaphragm is reduced. In this case, removing Baz clearly interferes with correct establishment of specific nephrocyte structures dependent on polarity and junction assembly. The crucial role of Baz in apicobasal polarization has been stated before (reviewed in Macara, 2004b; Suzuki & Ohno, 2006; Tepass, 2012). However, the alternative baz-RNAi sh2, designed for a different target of baz-mRNA, exhibits no ultrastructural changes or even a slight enrichment in forming the lacunae area and establishing filtration slits. At the same time, the ability to take up GFP is lost (see chapter 4.3.1, Fig. 23 and chapter 4.4.2, Fig. 29). In this baz mutant, there appears no direct correlation between ultrastructural conditions and nephrocyte functionality, which poses numerous further questions. Hereinafter, the actual molecular interactions of the different RNAi variants have to be investigated on their impact on Baz protein levels and other alterations in the cell. Additionally, the exact mechanisms of Baz activity in nephrocytes and possible unique interaction partners have to be determined in subsequent biochemical approaches. These experiments are necessary to understand the Par complex-regulated pathways of establishing the elaborate cell architecture of nephrocytes in detail.

5.3 Baz phosphorylation is crucial for correct nephrocyte development

The phosphorylation of Baz/Par3 by aPKC depicts a key event in cellular polarity establishment. The fine adjustments in positioning Baz and aPKC (together with Par6) at the apical region constitutes a landmark in the apical-basal polarization process. To gain a further look into the mechanisms of the correlation between cell polarity and correct nephrocyte development and functionality, the phosphorylation-mutant variant Baz_{5xA} was therefore examined in its impact on localization, ultrastructure and functionality.

Immunohistochemistry experiments showed that upon Baz_{5xA} expression in nephrocytes, the localization of Baz_{5xA} itself and aPKC is rather distorted and shifts from clear lines at the cell cortex to diffuse dispersion in the cytoplasm. Therefore, phosphorylation of Baz by aPKC seems crucial for the defined positioning of both proteins in membrane vicinity. The nephrocyte diaphragm protein Sns was also affected in the phosphorylation mutant, yet to a much lesser extent. Sns immunostaining appears more irregular than in the overexpression of Baz wildtype, but remains mostly at it the actual localization at the cell membrane (see chapter 4.2.4, Fig.22). In comparison, overexpressing the phospho-mimetic variant Baz_{5xD} in the nephrocytes lead to no visible alterations in the localization of Baz_{5xD}, aPKC or Sns.

Furthermore, the GFP accumulation performance of Baz_{5xA} mutant cells collapsed to 8% and reveals the severe impairment of functionality by non-phosphorylatable Baz_{5xA} in the nephrocyte. This is mirrored on the ultrastructural level, where these cells show an under-developed peripheral labyrinthine network and a reduction of nephrocyte diaphragms to 1.11 ND/µm (see chapter 4.4.4, Fig, 33 and 34). Summarized, the Baz_{5xA} variant apparently interferes heavily in accurate structural development of the highly specialized nephrocyte cell.

Expressing Baz wildtype, GFP accumulation is normal compared to control levels, whereas the phospho-mimetic Baz_{5xD} could only mildly compensate the actual phosphorylation status required for full functionality. This functional impairment reflects partly in the ultrastructure of Baz_{5xD} nephrocytes. While their lacuna area appears normally elaborated, the number of filtration slits is decreased by about half to 1.40 ND/µm. Therefore, the static phosphorylation of the Baz protein represented in the 5xD alterations is able to at least partly balance the genuine phosphorylation, but the

dynamics in protein (de-)phosphorylation seem to play a major role in overall cell activities.

In a next step, there were rescue experiments performed to see if insufficient Baz function can be compensated by hyperactivated aPKC. The $aPKC_{CAAX}$ construct is effectivly bound to the apical cell membrane via its artifical prenylation motif CAAX and hence constitutively active. This coerced overexpression of aPKC in Baz_{5xA} nephrocytes could sufficiently rescue the non-phosphorylatable phenotype in functionality as well as in ultrastructure. In theses cells, the capability of GFP accumulation was completely restored and a wildtypic manifestation of lacuna channels and nephrocyte diaphragms was reached. Concurring with these results, a dominant-negative, kinase-dead variant of $aPKC_{CAAX}$ failed to rescue Baz_{5xA} generated indispositions (see chapter 4.3.4, Fig. 25).

In another experiment, the ability of the Baz_{5xA} and Baz_{5xD} mutations to rescue Baz depletion were tested in GFP accumulation assays (see chapter 4.3.5, Fig. 26). Here, flies carrying sns::GAl4, ANF-GFP-GFP, and UAS::baz-RNAi sh2 were crossed to flies carrying three different Baz variants (wildtype, 5xA- and 5xD-mutation). This set-up leads to the elimination of endogenous Baz protein, which is replaced by the rescue constructs. Again, the phosphorylation mutant Baz_{5xA} protein was not able to rescue the nephrocyte accumulation capability, as the level of GFP uptake remained at the level of the baz-RNAi sh2 control. The wildtype Baz construct was able to rescue the phenotype up to 75%, and the phosphomimetic variant Baz_{5xD} even showed a gain-of-function effect. This feigned, continuously phosphorylated Baz as the only available option seems to enhance nephrocyte functionality, other than in previous experiments with overexpressing Baz_{5xD} in an enviroment with residual endogenous Baz protein.

Hence, the specific interaction of aPKC and Bazooka, and adaptable phosphorylation of the latter is required to ensure accurate nephrocyte development. The explicit phosphorylation of Baz by aPKC was shown in previous works (Morais-de-Sá, Mirouse, & St Johnston, 2010b) and more putative phosphorylations sites for aPKC were analyzed in preceding experiments in different cell types (Krahn lab, see chapter 4.2.4). Due to technical restriction in dissection and therefore limited availability of single isolated nephrocyte cells, it is difficult to perform descriptive biochemical assays with isolated proteins from nephrocytes. Instead, purified recombinant proteins have to be utilized in

follow-up biochemical assays. The specific mutations in the Baz_{5xA} variant seem to corrupt vital information for developing accurate nephrocyte structures. In the next steps, the targets and mechanisms laying downstream of this Baz phosphorylation and that are regulating lacuna channel branching and nephrocyte diaphragm establishment have to be clarified.

In the course of this study, attempts were made to determine alternative substrates (apart from Baz) for aPKC phosphorylation. It has been shown before that in mammalian podocytes, Nephrin/ Neph1 and the Par complex are co-localizing and interacting at the nephrocyte diaphragm. The direct binding of diaphragm proteins Neph1 and Nephrin to Par3 via their PDZ motifs has been verified *in vitro* and *in vivo* (Hartleben et al., 2008). The close vicinity of aPKC and the Neph proteins at the slit or nephrocyte diaphragm suggests a possible phosphorylation of either Neph1, Nephrin or Podocin. *In silico* analysis proposed several aPKC phosphorylation sites for the *Drosophila* homologs Kirre and Rst (Neph1), Sns or Hbs (Nephrin), and Mec2 (Podocin). To find one or more actual phosphorylation site in these proteins, recombinant proteins were generated lacking these putative phosphorylation sites in a particular pattern. However, initial kinase assays showed no resilient results for aPKC phosphorylation of these proteins. Either there was no phosphorylation detectable or recombinant protein with single deleted aPKC phosphorylation sites showed no changes in the phosphorylation status, leaving Baz as the core protein in the supramolecular diaphragm complex that is regulated by aPKC.

5.4 Basal polarity proteins are important factors in nephrocyte functionality

Hartleben et al. (2012) described the expansion of the apical domain of podocytes during glomerulus maturation, leaving the baso-lateral domain reduced to a fraction of the whole cell facing the glomerular basement membrane and endothelial capillary. In podocytes, the slit diaphragms constitute part of the filtration barrier and filtration is a passing process. In contrast, filtration/ accumulation is a inbound process in nephrocytes, leading to an inverted filtration model of the podocyte. Projected to the single nephrocyte cell, this would suggest that the basolateral region is pushed back between the nephrocyte diaphragms, leaving the apical region at the nephrocyte diaphragms and just below in the cortical area. This would display a contrary situation to most polarized epithelial cells where the apical membrane is restricted and the basolateral domain expands to the majority of the cell.

However, immunostainings of basolateral proteins have revealed a rather unspecific localization in the nephrocyte cytosplasm with a slight accentuation in the zone of the cortical lacuna area. Since the *Drosophila* nephrocytes present a quite unique cell form that has to meet specific requirements, they might obtain a particular distribution of polarity proteins. Nevertheless, both apical and basolateral polarity proteins demonstrate substantial participation in the establishment of functional nephrocyte cells.

In general, the interaction of apical and basal polarity proteins is mandatory for correct cell polarization. For example, loss of one of the basal regulator complex proteins Scrib, Lgl or Dlg leads to the basolateral mislocalization of apical proteins in *Drosophila*, and the affected cells fail to form adherens junctions and eventually the zonula adherens (Bilder et al., 2000; Bilder & Perrimon, 2000). As the knockout phenotypes of either of the Scribble complex proteins exhibit similar abberations, a strong genetic interaction in a common pathway is suggested (Bilder et al., 2000). In *Drosophila* epithelial tissues, they are considered to regulate tissue architecture, since mutations in *scrib*, *lgl* or *dlg* result in tumorous cells characterized by loss of polarity, differentiation and proliferation control (Elsum et al., 2012; Humbert et al., 2008). The basal determinant Par1 acts as counterbalance to apical regulator Baz/Par3, whose homo-oligomerization and therefore clustering is inhibited by Par1 and 14-3-3 interference (Benton & St Johnston, 2003).

Removal of the basal protein Dlg in nephrocytes leads to significant impairments in ultrastructure and function. In the dlg-RNAi cells, GFP accumulation ability collapses almost completely and the development of the peripheral lacuna area and nephrocyte diaphragm formation is severely disturbed.

The role of Dlg in *Drosophila* epithelial cells is crucial for apicobasal polarity and cell proliferation control. It is localized at the septate junctions and promotes junction structure (Woods et al., 1996; Woods & Bryant, 1991). As a member of the MAGUK (membrane-associated guanylate kinase) superfamily, Dlg possess three PDZ domains, a SH3 (Src homology 3) domain and a GUK (guanylate kinase-like) domain, and acts as a scaffolding protein involved in stabilizing membrane structures, adhesion and signalling (Pan et al., 2011). At *Drosophila* synapses, Dlg co-localizes basolaterally with Scrib, mediated by adapter protein GUK-holder (Mathew et al., 2002) and for mammalian Lgl2 and Dlg4, a direct interaction promoted by aPKC-phosphorylation of Lgl2 has been shown (Zhu et al., 2014). The actual specific biochemical mechanisms and interactions of Dlg in nephrocytes have yet to be further examined, but the results from the first functional and ultrastructural analyses indicate a key position of Dlg in nephrocyte development.

The Par1-knockdown in nephrocytes resulted in a significant decrease in functionality and structural alterations as well. In this mutant, the peripheral labyrinthine channels are less elaborate and the number of diaphragm nephrocytes per µm is reduced. Par1 kinase is described as polarity protein and neoplastic tumour suppressor, regulating polarity establishment, growth and proliferation control. In these functions, Par1 interacts with aPKC and Par3/Baz. In the process of polarization, basal polarity proteins Par1 and Lgl are phosphorylated by aPKC to avert them from associating with the apical membrane domain (Betschinger et al., 2003; Hurov et al., 2004; Kusakabe & Nishida, 2004; Plant et al., 2003; Suzuki et al., 2004). Par1 in turn was found to phosphorylate Baz to prevent a basolateral orientation of the apical aPKC/Par6/Baz complex (Benton & St Johnston, 2003). The phosphorylation of Baz at two residues (S151 and S1085) creates binding sites for 14-3-3/Par5, which blocks Baz oligomerization and the binding to aPKC, respectively, maintaining the balance of polarity protein distribution at their corresponding cell poles (Benton & St Johnston, 2003).

Reducing Par1 activity in the cell might lead to excessive Baz distribution and activity. Since Baz and downstream functions regulated by Baz seem to entail major contribution to nephrocyte development, Par1 might be rather important to restrict Baz activity to the correct localization. Secondly, Par1 phosphorylates Dlg and controls its synaptic targeting in *Drosophila* synapses (Zhang et al., 2007). Similar regulatory events of Dlg might take place in the nephroycte as well. Although more detailed analysis will be required, Dlg and Par were found to localize both in the nephrocyte cytosplasm, indicating putative interaction of these proteins. Moreover, Par1 regulates stability and apical-basal organisation of microtubules in *Drosophila* follicular epithelium (Doerflinger et al., 2003), suggesting analog functions for Par1 in forming the nephrocyte inner structure.

In this study, the effect of Lgl-knockdown on nephrocytes cells presented a hyperactivity in functionality, resulting in a strong increase GFP accumulation rate (see chapter 4.3.2, Fig. 23). Of all tested RNAi lines, lgl-RNAi was the only one showing a gain-of-function effect. Lgl is a key determinant of basal polarity by its mutual antagonism with apical regulator aPKC. Lgl binding to the Par complex, Lgl phosphorylation, and activation via aPKC defines and stabilizes apical membrane domains in *Drosophila* cells (Betschinger et al., 2003; Wirtz-Peitz & Knoblich, 2006; Yamanaka et al., 2003, 2006). Additionally, Lgl is linked to the cytoskeletal network via its interaction with non-muscle mysosin II, in cooperation with aPKC phosphorylation activity (Betschinger, Mechtler, & Knoblich, 2003; Kalmes et al., 1996; Strand et al., 1994). Analyses in *Drosophila* mutant embryos have shown the necessity of Lgl in controlling cell shape during development *in vivo* in certain epithelial cells (Manfruelli et al., 1996). A specialized cell architecture is the hallmark of nephrocyte and podocyte cells, underlining the importance of accurate establishment of the particular cell structures like membrane invaginations or protruding processes, respectively. The impact on localization of polarity proteins and ultrastructure in *lgl*-mutant cells could not be stated yet, therefore performing immunostainings and TEM analysis will clarify the contribution of Lgl in nephrocyte (and podocyte) development and functionality in the future.

Using confocal laser microscopy with immunohistochemical stainings is a fast method to evaluate localization of several proteins in parallel in nephrocytes. In the case of the basal polarity proteins, their influence on their apical counterparts should also be investigated further in RNAi-knockdown mutant cells. The effects of absent basal polarity proteins on

the localization and behavior of apical polarity proteins could support undesirable development of nephrocyte cells. Additionally, more detailed results of single protein localization could be obtained from gold-immunostainings of high-pressure frozen, epoxy resin-embedded cells. GFP-tagged proteins in the specimen can be precisely located by a gold secondary antibody targeting GFP.

The data acquired in this study suggest that apical-basal polarity proteins play a crucial role in the correct development and establishment of *Drosophila* nephrocyte cells. Knocking down either of the apical polarity determinants aPKC, Par6 and Baz, or the basal polarity regulators Lgl, Dlg and Par1 results in the mislocalization of other polarity and nephrocyte-specific proteins, in mild to severe impairments in ultrastructrural development, and subsequently in a varying decrease (or seldom increase) of functionality. Phosphorylation activity of aPKC, supported by Par6, and the capability of Baz to be phosphorylated are closely connected to nephrocyte development. The participation of basal polarity proteins is mainly unexplored in nephrocytes. However, first functional and ultrastructural experiments showed that they are involved in and required for accurate nephrocyte development. Further investigation of polarity proteins in nephrocytes will be neccessary and needs to be addressed in various approaches. One important factor is the limited access to actual isolated *Drosophila* (Garland or pericardial) nephrocytes to perform gene expression arrays or protein expression blots. The current dissection method includes a large portion of unspecific gut tissue attached to the Garland nephrocytes to be able to handle the fragile nephrocyte cells in immunostainings and TEM sample preparation. This gut tissue would falsify any detailed comparative expression experiments on mRNA or protein levels. Next to localization, functional and ultrastructural studies, experiments such as kinase assays and co-immunoprecipitation should be set up. As long as protein isolation from nephrocytes is not sufficient enough yet, samples for biochemical assays have to be obtained from recombinant proteins. In particular, the exact biochemical interactions of polarity proteins and nephrocyte/ slit diaphragm proteins will elucidate the mechanisms in this unique cell type and eventually promote progress in mammalian podocyte and kidney disease research.

6 BIBLIOGRAPHY

Arrondel, C., Vodovar, N., Knebelmann, B., Grünfeld, J.-P., Gubler, M.-C., Antignac, C., & Heidet, L. (2002). Expression of the nonmuscle myosin heavy chain IIA in the human kidney and screening for MYH9 mutations in Epstein and Fechtner syndromes. *Journal of the American Society of Nephrology : JASN*, *13*(1), 65–74. Retrieved from http://www.ncbi.nlm.nih.gov/pubmed/11752022

Artero, R. D., Castanon, I., & Baylies, M. K. (2001). The immunoglobulin-like protein Hibris functions as a dose-dependent regulator of myoblast fusion and is differentially controlled by Ras and Notch signaling. *Development (Cambridge, England)*, *128*(21), 4251–64. Retrieved from http://www.ncbi.nlm.nih.gov/pubmed/11684661

Asanuma, K., & Mundel, P. (2003). The role of podocytes in glomerular pathobiology. *Clinical and Experimental Nephrology*. https://doi.org/10.1007/s10157-003-0259-6

Asanuma, K., Yanagida-Asanuma, E., Takagi, M., Kodama, F., & Tomino, Y. (2007). The role of podocytes in proteinuria. In *Nephrology* (Vol. 12, pp. S15–S20). Blackwell Publishing Asia. https://doi.org/10.1111/j.1440-1797.2007.00876.x

Ashburner, M. (1989). *Drosophila*. Cold Spring Harbor Laboratory.

Assémat, E., Bazellières, E., Pallesi-Pocachard, E., Le Bivic, A., & Massey-Harroche, D. (2008). Polarity complex proteins. *Biochimica et Biophysica Acta - Biomembranes*. https://doi.org/10.1016/j.bbamem.2007.08.029

Atwood, S. X., Chabu, C., Penkert, R. R., Doe, C. Q., & Prehoda, K. E. (2007). Cdc42 acts downstream of Bazooka to regulate neuroblast polarity through Par-6 aPKC. *Journal of Cell Science*, *120*(18), 3200–3206. https://doi.org/10.1242/jcs.014902

Atwood, S. X., & Prehoda, K. E. (2009). aPKC Phosphorylates Miranda to Polarize Fate Determinants during Neuroblast Asymmetric Cell Division. *Current Biology*, *19*(9), 723–729. https://doi.org/10.1016/j.cub.2009.03.056

Bachmann, A., & Knust, E. (2008). The Use of P-Element Transposons to Generate Transgenic Flies. In *Methods in molecular biology (Clifton, N.J.)* (Vol. 420, pp. 61–77). https://doi.org/10.1007/978-1-59745-583-1_4

Barletta, G.-M., Kovari, I. A., Verma, R. K., Kerjaschki, D., & Holzman, L. B. (2003). Nephrin and Neph1 co-localize at the podocyte foot process intercellular junction and form cis hetero-oligomers. *The Journal of Biological Chemistry*, *278*(21), 19266–71. https://doi.org/10.1074/jbc.M301279200

Beatty, A., Morton, D. G., & Kemphues, K. (2013). PAR-2, LGL-1 and the CDC-42 GAP CHIN-1 act in distinct pathways to maintain polarity in the C. elegans embryo. *Development*, *140*(9), 2005–2014. https://doi.org/10.1242/dev.088310

Beatty, A., Morton, D., & Kemphues, K. (2010). The C. elegans homolog of Drosophila Lethal giant larvae functions redundantly with PAR-2 to maintain polarity in the early embryo. *Development*, *137*(23), 3995–4004.

https://doi.org/10.1242/dev.056028

Beltcheva, O., Martin, P., Lenkkeri, U., & Tryggvason, K. (2001). Mutation spectrum in the nephrin gene (NPHS1) in congenital nephrotic syndrome. *Human Mutation*, *17*(5), 368–373. https://doi.org/10.1002/humu.1111

Benton, R., & St Johnston, D. (2003). Drosophila PAR-1 and 14-3-3 inhibit Bazooka/PAR-3 to establish complementary cortical domains in polarized cells. *Cell*, *115*(6), 691–704. Retrieved from http://www.ncbi.nlm.nih.gov/pubmed/14675534

Bergstralh, D. T., & St Johnston, D. (2012). Epithelial cell polarity: what flies can teach us about cancer. *Essays In Biochemistry*, *53*. Retrieved from http://essays.biochemistry.org/content/53/129

Betschinger, J., Mechtler, K., & Knoblich, J. A. (2003). The Par complex directs asymmetric cell division by phosphorylating the cytoskeletal protein Lgl. *Nature*, *422*(6929), 326–330. https://doi.org/10.1038/nature01486

Bierzynska, A., Soderquest, K., & Koziell, A. (2014, January 23). Genes and podocytes - new insights into mechanisms of podocytopathy. *Frontiers in Endocrinology*. https://doi.org/10.3389/fendo.2014.00226

Bilder, D. (2004, August 15). Epithelial polarity and proliferation control: Links from the Drosophila neoplastictumor suppressors. *Genes and Development*. https://doi.org/10.1101/gad.1211604

Bilder, D., Birnbaum, D., Borg, J.-P., Bryant, P., Huigbretse, J., Jansen, E., … Sinha, P. (2000). Collective nomenclature for LAP proteins. *Nat Cell Biol*, *2*(7), E114–E114. Retrieved from http://dx.doi.org/10.1038/35017119

Bilder, D., Li, M., & Perrimon, N. (2000). Cooperative Regulation of Cell Polarity and Growth by Drosophila Tumor Suppressors. *Science*, *289*(5476), 113 LP-116. Retrieved from http://science.sciencemag.org/content/289/5476/113.abstract

Bilder, D., & Perrimon, N. (2000). Localization of apical epithelial determinants by the basolateral PDZ protein Scribble. *Nature*, *403*(6770), 676–680. https://doi.org/10.1038/35001108

Bischof, J., Maeda, R. K., Hediger, M., Karch, F., & Basler, K. (2007). An optimized transgenesis system for Drosophila using germ-line-specific C31 integrases. *Proceedings of the National Academy of Sciences*, *104*(9), 3312–3317. https://doi.org/10.1073/pnas.0611511104

Bour, B. A., Chakravarti, M., West, J. M., & Abmayr, S. M. (2000). Drosophila SNS, a member of the immunoglobulin superfamily that is essential for myoblast fusion. *Genes & Development*, *14*(12), 1498–511. Retrieved from http://www.ncbi.nlm.nih.gov/pubmed/10859168

Boute, N., Gribouval, O., Roselli, S., Benessy, F., Lee, H., Fuchshuber, A., … Antignac, C. (2000). NPHS2, encoding the glomerular protein podocin, is mutated in autosomal recessive steroid-resistant nephrotic syndrome. *Nature Genetics*, *24*(4), 349–54. https://doi.org/10.1038/74166

Boyd, L., Guo, S., Levitan, D., Stinchcomb, D. T., & Kemphues, K. J. (1996). PAR-2 is asymmetrically distributed and promotes association of P granules and PAR-1 with the cortex in C. elegans embryos. *Development (Cambridge, England)*, *122*(10), 3075–84. Retrieved from http://www.ncbi.nlm.nih.gov/pubmed/8898221

Bryant, D. M., & Mostov, K. E. (2008). From cells to organs: building polarized tissue. *Nature Reviews. Molecular Cell Biology*, *9*(11), 887–901. https://doi.org/10.1038/nrm2523

Bulgakova, N. A., Kempkens, Ö., & Knust, E. (2008). Multiple domains of Stardust differentially mediate localisation of the Crumbs-Stardust complex during photoreceptor development in Drosophila. *Journal of Cell Science*, *121*(12). Retrieved from http://jcs.biologists.org/content/121/12/2018.figures-only

Caplan, M. J., Seo-Mayer, P., & Zhang, L. (2008). Epithelial junctions and polarity: complexes and kinases. *Current Opinion in Nephrology and Hypertension*, *17*(5), 506–12. https://doi.org/10.1097/MNH.0b013e32830baaae

Chen, J., & Zhang, M. (2013). The Par3/Par6/aPKC complex and epithelial cell polarity. *Experimental Cell Research*. https://doi.org/10.1016/j.yexcr.2013.03.021

Cheng, J., Türkel, N., Hemati, N., Fuller, M. T., Hunt, A. J., & Yamashita, Y. M. (2008). Centrosome misorientation reduces stem cell division during ageing. *Nature*, *456*(7222), 599–604. https://doi.org/10.1038/nature07386

Coradini, D., Casarsa, C., & Oriana, S. (2011). Epithelial cell polarity and tumorigenesis: new perspectives for cancer detection and treatment. *Acta Pharmacologica Sinica*, *32*(5), 552–64. https://doi.org/10.1038/aps.2011.20

Cuenca, A. A., Schetter, A., Aceto, D., Kemphues, K., & Seydoux, G. (2003). Polarization of the C. elegans zygote proceeds via distinct establishment and maintenance phases. *Development (Cambridge, England)*, *130*(7), 1255–65. Retrieved from http://www.ncbi.nlm.nih.gov/pubmed/12588843

Demerec, M. (1950). *Biology of Drosophila*. Cold Spring Harbor Laboratory Press. https://doi.org/10.1038/168803a0

Denholm, B., & Skaer, H. (2009). Bringing together components of the fly renal system. *Current Opinion in Genetics & Development*, *19*(5), 526–32. https://doi.org/10.1016/j.gde.2009.08.006

Doerflinger, H., Benton, R., Shulman, J. M., & St Johnston, D. (2003). The role of PAR-1 in regulating the polarised microtubule cytoskeleton in the Drosophila follicular epithelium. *Development (Cambridge, England)*, *130*(17), 3965–75. Retrieved from http://www.ncbi.nlm.nih.gov/pubmed/12874119

Doerflinger, H., Vogt, N., Torres, I. L., Mirouse, V., Koch, I., Nusslein-Volhard, C., & St Johnston, D. (2010). Bazooka is required for polarisation of the Drosophila anterior-posterior axis. *Development*, *137*(10), 1765–1773. https://doi.org/10.1242/dev.045807

Donoviel, D. B., Freed, D. D., Vogel, H., Potter, D. G., Hawkins, E., Barrish, J. P., … Powell, D. R. (2001). Proteinuria and perinatal lethality in mice lacking NEPH1, a novel protein with homology to NEPHRIN. *Molecular and Cellular Biology*, *21*(14), 4829–36. https://doi.org/10.1128/MCB.21.14.4829-4836.2001

Drenckhahn, D., & Franke, R. P. (1988). Ultrastructural organization of contractile and cytoskeletal proteins in glomerular podocytes of chicken, rat, and man. *Laboratory Investigation; a Journal of Technical Methods and Pathology*, *59*(5), 673–82. Retrieved from http://www.ncbi.nlm.nih.gov/pubmed/3141719

Drummond, M. L., & Prehoda, K. E. (2016). Molecular Control of Atypical Protein Kinase C: Tipping the Balance between Self-Renewal and Differentiation. *Journal of Molecular Biology*, *428*(7), 1455–1464. https://doi.org/10.1016/J.JMB.2016.03.003

Eaton, S., & Martin-Belmonte, F. (2014). Cargo sorting in the endocytic pathway: a key regulator of cell polarity and tissue dynamics. *Cold Spring Harbor Perspectives in Biology*, *6*(10), a016899. https://doi.org/10.1101/cshperspect.a016899

Ebarasi, L., He, L., Hultenby, K., Takemoto, M., Betsholtz, C., Tryggvason, K., & Majumdar, A. (2009). A reverse genetic screen in the zebrafish identifies crb2b as a regulator of the glomerular filtration barrier. *Developmental Biology*, *334*(1), 1–9. https://doi.org/10.1016/j.ydbio.2009.04.017

Ebnet, K., Suzuki, A., Horikoshi, Y., Hirose, T., Meyer Zu Brickwedde, M. K., Ohno, S., & Vestweber, D. (2001). The cell polarity protein ASIP/PAR-3 directly associates with junctional adhesion molecule (JAM). *The EMBO Journal*, *20*(14), 3738–48. https://doi.org/10.1093/emboj/20.14.3738

Elsum, I., Yates, L., Humbert, P. O., & Richardson, H. E. (2012). The Scribble–Dlg–Lgl polarity module in development and cancer: from flies to man. *Essays In Biochemistry*, *53*. Retrieved from http://essays.biochemistry.org/content/53/141.long

Feicht, S. U. K. (2017). Impact of Baz/PAR-3 phosphorylation by aPKC on cell polarity. Retrieved from https://epub.uni-regensburg.de/35943/

Feng, Y., Ueda, A., & Wu, C.-F. (2004). A MODIFIED MINIMAL HEMOLYMPH-LIKE SOLUTION, HL3.1, FOR PHYSIOLOGICAL RECORDINGS AT THE NEUROMUSCULAR JUNCTIONS OF NORMAL AND MUTANT DROSOPHILA LARVAE. *J. Neurogenetics*, *18*, 377–402. https://doi.org/10.1080=01677060490894522

Fischbach, K. F., Linneweber, G. A., Felix Malte Andlauer, T., Hertenstein, A., Bonengel, B., & Chaudhary, K. (2009, January 11). The irre cell recognition module (IRM) proteins. *Journal of Neurogenetics*.

https://doi.org/10.1080/01677060802471668

Fletcher, G. C., Lucas, E. P., Brain, R., Tournier, A., & Thompson, B. J. (2012). Positive feedback and mutual antagonism combine to polarize crumbs in the drosophila follicle cell epithelium. *Current Biology*, *22*(12), 1116–1122. https://doi.org/10.1016/j.cub.2012.04.020

Garovic, V. D., Wagner, S. J., Petrovic, L. M., Gray, C. E., Hall, P., Sugimoto, H., … Grande, J. P. (2007). Glomerular expression of nephrin and synaptopodin, but not podocin, is decreased in kidney sections from women with preeclampsia. *Nephrology Dialysis Transplantation*, *22*(4), 1136–1143. https://doi.org/10.1093/ndt/gfl711

Garrard, S. M., Capaldo, C. T., Gao, L., Rosen, M. K., Macara, I. G., & Tomchick, D. R. (2003). Structure of Cdc42 in a complex with the GTPase-binding domain of the cell polarity protein, Par6. *The EMBO Journal*, *22*(5), 1125–1133. https://doi.org/10.1093/emboj/cdg110

Gelberg, H., Healy, L., Whiteley, H., Miller, L. A., & Vimr, E. (1996). In vivo enzymatic removal of alpha 2-->6-linked sialic acid from the glomerular filtration barrier results in podocyte charge alteration and glomerular injury. *Laboratory Investigation; a Journal of Technical Methods and Pathology*, *74*(5), 907–20. Retrieved from http://www.ncbi.nlm.nih.gov/pubmed/8642786

George, B., & Holzman, L. B. (2012). Signaling from the podocyte intercellular junction to the actin cytoskeleton. *Seminars in Nephrology*, *32*(4), 307–18. https://doi.org/10.1016/j.semnephrol.2012.06.002

Gerke, P., Huber, T. B., Sellin, L., Benzing, T., & Walz, G. (2003). Homodimerization and heterodimerization of the glomerular podocyte proteins nephrin and NEPH1. *Journal of the American Society of Nephrology : JASN*, *14*(4), 918–26. https://doi.org/10.1097/01.ASN.0000057853.05686.89

Ghiggeri, G. M., Caridi, G., Magrini, U., Sessa, A., Savoia, A., Seri, M., … Balduini, C. L. (2003). Genetics, clinical and pathological features of glomerulonephrites associated with mutations of nonmuscle myosin IIA (Fechtner syndrome). *American Journal of Kidney Diseases*, *41*(1), 95–104. https://doi.org/10.1053/ajkd.2003.50028

Goldstein, B., & Macara, I. G. (2007). The PAR Proteins: Fundamental Players in Animal Cell Polarization. *Developmental Cell*. https://doi.org/10.1016/j.devcel.2007.10.007

Grahammer, F., Wigge, C., Schell, C., Kretz, O., Patrakka, J., Schneider, S., … Huber, T. B. (2016). A flexible, multilayered protein scaffold maintains the slit in between glomerular podocytes. *JCI Insight*, *1*(9). https://doi.org/10.1172/jci.insight.86177

Haraldsson, B., Nyström, J., & Deen, W. M. (2008). Properties of the glomerular barrier and mechanisms of proteinuria. *Physiological Reviews*, *88*(2), 451–87. https://doi.org/10.1152/physrev.00055.2006

Harris, T. J. C., & Peifer, M. (2005). The positioning and segregation of apical cues during epithelial polarity establishment in *Drosophila*. *The Journal of Cell Biology*, *170*(5), 813–823. https://doi.org/10.1083/jcb.200505127

Harrison, F. W., & Foelix, R. F. (1999). Microscopic anatomy of invertebrates. In *Vol. 8A: Chelicerate arthropoda* (p. 508). Wiley-Liss. https://doi.org/10.1002/iroh.19890740316

Hartleben, B., Schweizer, H., Lübben, P., Bartram, M. P., Möller, C. C., Herr, R., … Huber, T. B. (2008). Neph-Nephrin proteins bind the Par3-Par6-atypical protein kinase C (aPKC) complex to regulate podocyte cell polarity. *The Journal of Biological Chemistry*, *283*(34), 23033–8. https://doi.org/10.1074/jbc.M803143200

Hartleben, B., Widmeier, E., Wanner, N., Schmidts, M., Kim, S. T., Schneider, L., … Huber, T. B. (2012). Role of the polarity protein Scribble for podocyte differentiation and maintenance. *PloS One*, *7*(5), e36705. https://doi.org/10.1371/journal.pone.0036705

Hartley, J. L., Temple, G. F., & Brasch, M. A. (2000). DNA cloning using in vitro site-specific recombination. *Genome Research*, *10*(11), 1788–95. Retrieved from http://www.ncbi.nlm.nih.gov/pubmed/11076863

Helmstädter, M., Lüthy, K., Gödel, M., Simons, M., Ashish, Nihalani, D., … Huber, T. B. (2012). Functional study of mammalian Neph proteins in Drosophila melanogaster. *PloS One*, *7*(7), e40300. https://doi.org/10.1371/journal.pone.0040300

Hirabayashi, S., Mori, H., Kansaku, A., Kurihara, H., Sakai, T., Shimizu, F., … Hata, Y. (2005). MAGI-1 is a component of the glomerular slit diaphragm that is tightly associated with nephrin. *Laboratory Investigation; a Journal of Technical Methods and Pathology*, *85*(12), 1528–43. https://doi.org/10.1038/labinvest.3700347

Hirose, T., Satoh, D., Kurihara, H., Kusaka, C., Hirose, H., Akimoto, K., … Ohno, S. (2009). An essential role of the universal polarity protein, aPKClambda, on the maintenance of podocyte slit diaphragms. *PloS One*, *4*(1), e4194. https://doi.org/10.1371/journal.pone.0004194

Holzman, L. B., & Garg, P. (2009). Initial insight on the determinants of podocyte polarity. *Journal of the American Society of Nephrology : JASN*, *20*(4), 683–5. https://doi.org/10.1681/ASN.2009020217

Horikoshi, Y., Suzuki, A., Yamanaka, T., Sasaki, K., Mizuno, K., Sawada, H., … Ohno, S. (2009). Interaction between PAR-3 and the aPKC-PAR-6 complex is indispensable for apical domain development of epithelial cells. *Journal of Cell Science*, *122*(10), 1595–1606. https://doi.org/10.1242/jcs.043174

Huber, T. B., Hartleben, B., Winkelmann, K., Schneider, L., Becker, J. U., Leitges, M., … Schiffer, M. (2009). Loss of podocyte aPKClambda/iota causes polarity defects and nephrotic syndrome. *Journal of the American Society of Nephrology : JASN*, *20*(4), 798–806. https://doi.org/10.1681/ASN.2008080871

Huber, T. B., Kottgen, M., Schilling, B., Walz, G., & Benzing, T. (2001). Interaction with podocin facilitates nephrin signaling. *The Journal of Biological Chemistry*, *276*(45), 41543–6. https://doi.org/10.1074/jbc.C100452200

Hull, R. P., & Goldsmith, D. J. A. (2008). Nephrotic syndrome in adults. *BMJ (Clinical Research Ed.)*, *336*(7654), 1185–9. https://doi.org/10.1136/bmj.39576.709711.80

Humbert, P. O., Grzeschik, N. A., Brumby, A. M., Galea, R., Elsum, I., & Richardson, H. E. (2008). Control of tumourigenesis by the Scribble/Dlg/Lgl polarity module. *Oncogene*, *27*(55), 6888–6907. https://doi.org/10.1038/onc.2008.341

Hurd, T. W., Fan, S., Liu, C. J., Kweon, H. K., Hakansson, K., & Margolis, B. (2003). Phosphorylation-dependent binding of 14-3-3 to the polarity protein Par3 regulates cell polarity in mammalian epithelia. *Current Biology : CB*, *13*(23), 2082–90. Retrieved from http://www.ncbi.nlm.nih.gov/pubmed/14653998

Hurd, T. W., Gao, L., Roh, M. H., Macara, I. G., & Margolis, B. (2003). Direct interaction of two polarity complexes implicated in epithelial tight junction assembly. *Nature Cell Biology*, *5*(2), 137–142. https://doi.org/10.1038/ncb923

Hurov, J. B., Watkins, J. L., & Piwnica-Worms, H. (2004). Atypical PKC Phosphorylates PAR-1 Kinases to Regulate Localization and Activity. *Current Biology*, *14*(8), 736–741. https://doi.org/10.1016/j.cub.2004.04.007

Hutterer, A., Betschinger, J., Petronczki, M., & Knoblich, J. A. (2004). Sequential Roles of Cdc42, Par-6, aPKC, and Lgl in the Establishment of Epithelial Polarity during Drosophila Embryogenesis. *Developmental Cell*, *6*(6), 845–854. https://doi.org/10.1016/j.devcel.2004.05.003

Inoue, T., Yaoita, E., Kurihara, H., Shimizu, F., Sakai, T., Kobayashi, T., … Yamamoto, T. (2001). FAT is a component of glomerular slit diaphragms. *Kidney International*, *59*(3), 1003–12. https://doi.org/10.1046/j.1523-1755.2001.0590031003.x

Ivy, J. R., Drechsler, M., Catterson, J. H., Bodmer, R., Ocorr, K., Paululat, A., & Hartley, P. S. (2015). Klf15 Is Critical for the Development and Differentiation of Drosophila Nephrocytes. *PloS One*, *10*(8), e0134620. https://doi.org/10.1371/journal.pone.0134620

Jefferson, J. A., Shankland, S. J., & Pichler, R. H. (2008). Proteinuria in diabetic kidney disease: A mechanistic viewpoint. *Kidney International*, *74*(1), 22–36. https://doi.org/10.1038/ki.2008.128

Joberty, G., Petersen, C., Gao, L., & Macara, I. G. (2000). The cell-polarity protein Par6 links Par3 and atypical protein kinaseC to Cdc42. *Nature Cell Biology*, *2*(8), 531–539. https://doi.org/10.1038/35019573

Johnson, D. I. (1999). Cdc42: An essential Rho-type GTPase controlling eukaryotic cell polarity. *Microbiology and Molecular Biology Reviews : MMBR*, *63*(1), 54–105. https://doi.org/citeulike-article-id:13113720

Kalmes, A., Merdes, G., Neumann, B., Strand, D., & Mechler, B. M. (1996). A serine-kinase associated with the p127-l(2)gl tumour suppressor of Drosophila may regulate the binding of p127 to nonmuscle myosin II heavy chain and the attachment of p127 to the plasma membrane. *Journal of Cell Science*, *109 (Pt 6)*, 1359–68. Retrieved from http://www.ncbi.nlm.nih.gov/pubmed/8799824

Kemphues, K. (2000). PARsing Embryonic Polarity Minireview embryonic polarity. The polarity genes with the strong. *Cell*, *101*, 345–348.

Kerjaschki, D. (1994). Dysfunctions of cell biological mechanisms of visceral epithelial cell (podocytes) in glomerular diseases. *Kidney International*, *45*(2), 300–13. Retrieved from http://www.ncbi.nlm.nih.gov/pubmed/8164413

Kerjaschki, D. (2001, December). Caught flat-footed: Podocyte damage and the molecular bases of focal glomerulosclerosis. *Journal of Clinical Investigation*. American Society for Clinical Investigation. https://doi.org/10.1172/JCI200114629

Kerkut, G. A. (1985). *Comprehensive insect physiology, biochemistry and pharmacology*. Pergamon Press.

Kestilä, M., Lenkkeri, U., Männikkö, M., Lamerdin, J., McCready, P., Putaala, H., … Tryggvason, K. (1998). Positionally Cloned Gene for a Novel Glomerular Protein—Nephrin—Is Mutated in Congenital Nephrotic Syndrome. *Molecular Cell*, *1*(4), 575–582. https://doi.org/10.1016/S1097-2765(00)80057-X

Khoshnoodi, J., Sigmundsson, K., Ofverstedt, L.-G., Skoglund, U., Obrink, B., Wartiovaara, J., & Tryggvason, K. (2003). Nephrin promotes cell-cell adhesion through homophilic interactions. *The American Journal of Pathology*, *163*(6), 2337–46. https://doi.org/10.1016/S0002-9440(10)63590-0

Klowden, M. J. (2007). *Physiological Systems in Insects* (2nd editio). Academic Press.

Kocherlakota, K. S., Wu, J., McDermott, J., & Abmayr, S. M. (2008). Analysis of the Cell Adhesion Molecule Sticks-and-Stones Reveals Multiple Redundant Functional Domains, Protein-Interaction Motifs and Phosphorylated Tyrosines That Direct Myoblast Fusion in Drosophila melanogaster. *Genetics*, *178*(3). Retrieved from http://www.genetics.org/content/178/3/1371?ijkey=20926b5b2ee0ee01e6e520673d31fbea5ff3b2d5&keytype2=tf_ipsecsha

Kurts, C., Panzer, U., Anders, H.-J., & Rees, A. J. (2013). The immune system and kidney disease: basic concepts and clinical implications. *Nature Reviews Immunology*, *13*(10), 738–753. https://doi.org/10.1038/nri3523

Kusakabe, M., & Nishida, E. (2004). The polarity-inducing kinase Par-1 controls Xenopus gastrulation in cooperation with 14-3-3 and aPKC. *The EMBO Journal*, *23*(21), 4190–201. https://doi.org/10.1038/sj.emboj.7600381

Lehtonen, S., Ryan, J. J., Kudlicka, K., Iino, N., Zhou, H., & Farquhar, M. G. (2005). Cell junction-associated proteins IQGAP1, MAGI-2, CASK, spectrins, and -actinin are components of the nephrin multiprotein complex. *Proceedings of the*

National Academy of Sciences, *102*(28), 9814–9819. https://doi.org/10.1073/pnas.0504166102

Lemmers, C., Michel, D., Lane-Guermonprez, L., Delgrossi, M.-H., Médina, E., Arsanto, J.-P., & Le Bivic, A. (2003). CRB3 Binds Directly to Par6 and Regulates the Morphogenesis of the Tight Junctions in Mammalian Epithelial Cells. *Molecular Biology of the Cell*, *15*(3), 1324–1333. https://doi.org/10.1091/mbc.E03-04-0235

Linneweber, G. A., Winking, M., & Fischbach, K.-F. (2015). The Cell Adhesion Molecules Roughest, Hibris, Kin of Irre and Sticks and Stones Are Required for Long Range Spacing of the Drosophila Wing Disc Sensory Sensilla. *PloS One*, *10*(6), e0128490. https://doi.org/10.1371/journal.pone.0128490

Liu, G., Kaw, B., Kurfis, J., Rahmanuddin, S., Kanwar, Y. S., & Chugh, S. S. (2003). Neph1 and nephrin interaction in the slit diaphragm is an important determinant of glomerular permeability. *The Journal of Clinical Investigation*, *112*(2), 209–21. https://doi.org/10.1172/JCI18242

Lizcano, J. M., Göransson, O., Toth, R., Deak, M., Morrice, N. A., Boudeau, J., … Alessi, D. R. (2004). LKB1 is a master kinase that activates 13 kinases of the AMPK subfamily, including MARK/PAR-1. *The EMBO Journal*, *23*(4), 833–43. https://doi.org/10.1038/sj.emboj.7600110

Macara, I. G. (2004a). Par proteins: Partners in polarization. *Current Biology*. https://doi.org/10.1016/S0960-9822(04)00078-8

Macara, I. G. (2004b). Par Proteins: Partners in Polarization. *Current Biology*, *14*(4), R160–R162. https://doi.org/10.1016/J.CUB.2004.01.048

Manfruelli, P., Arquier, N., Hanratty, W. P., & Sémériva, M. (1996). The tumor suppressor gene, lethal(2)giant larvae (1(2)g1), is required for cell shape change of epithelial cells during Drosophila development. *Development (Cambridge, England)*, *122*(7), 2283–94. Retrieved from http://www.ncbi.nlm.nih.gov/pubmed/8681808

Mathew, D., Gramates, L. S., Packard, M., Thomas, U., Bilder, D., Perrimon, N., … Budnik, V. (2002). Recruitment of Scribble to the synaptic scaffolding complex requires GUK-holder, a novel DLG binding protein. *Current Biology*, *12*(7), 531–539. https://doi.org/10.1016/S0960-9822(02)00758-3

Matsuzawa, K., Akita, H., Watanabe, T., Kakeno, M., Matsui, T., Wang, S., & Kaibuchi, K. (2016). PAR3-aPKC regulates Tiam1 by modulating suppressive internal interactions. *Molecular Biology of the Cell*, *27*(9), 1511–1523. https://doi.org/10.1091/mbc.e15-09-0670

Mechler, B. M., McGinnis, W., & Gehring, W. J. (1985). Molecular cloning of lethal(2)giant larvae, a recessive oncogene of Drosophila melanogaster. *The EMBO Journal*, *4*(6), 1551–7. Retrieved from http://www.ncbi.nlm.nih.gov/pubmed/3928370

Menon, M. C., Chuang, P. Y., & He, C. J. (2012). The glomerular filtration barrier: Components and crosstalk. *International Journal of Nephrology*. https://doi.org/10.1155/2012/749010

Moore, R., & Boyd, L. (2004). Analysis of RING Finger Genes Required for Embryogenesis in C. elegans. *Genesis*, *38*(1), 1–12. https://doi.org/10.1002/gene.10243

Morais-de-Sá, E., Mirouse, V., & St Johnston, D. (2010a). aPKC Phosphorylation of Bazooka Defines the Apical/Lateral Border in Drosophila Epithelial Cells. *Cell*, *141*(3), 509–523. https://doi.org/10.1016/j.cell.2010.02.040

Morais-de-Sá, E., Mirouse, V., & St Johnston, D. (2010b). aPKC Phosphorylation of Bazooka Defines the Apical/Lateral Border in Drosophila Epithelial Cells. *Cell*, *141*(3), 509–523. https://doi.org/10.1016/j.cell.2010.02.040

Morton, D. G., Shakes, D. C., Nugent, S., Dichoso, D., Wang, W., Golden, A., & Kemphues, K. J. (2002). The Caenorhabditis elegans par-5 Gene Encodes a 14-3-3 Protein Required for Cellular Asymmetry in the Early Embryo. *Developmental Biology*, *241*(1), 47–58. https://doi.org/10.1006/dbio.2001.0489

Motegi, F., & Seydoux, G. (2013). The PAR network: redundancy and robustness in a symmetry-breaking system. *Philosophical Transactions of the Royal Society of London. Series B, Biological Sciences*, *368*(1629), 20130010. https://doi.org/10.1098/rstb.2013.0010

Mullis, K. B., & Faloona, F. A. (1987). Specific Synthesis of DNA in Vitro via a Polymerase-Catalyzed Chain Reaction. *Methods in Enzymology*, *155*(C), 335–350. https://doi.org/10.1016/0076-6879(87)55023-6

Mundel, P., & Kriz, W. (1995). Structure and function of podocytes: an update. *Anatomy and Embryology*. https://doi.org/10.1007/BF00240371

Mundel, P., Reiser, J., Borja, A. Z. M., Pavenstädt, H., Davidson, G. R., Kriz, W., & Zeller, R. (1997). Rearrangements of the Cytoskeleton and Cell Contacts Induce Process Formation during Differentiation of Conditionally Immortalized Mouse Podocyte Cell Lines. *Experimental Cell Research*, *236*(1), 248–258. https://doi.org/10.1006/excr.1997.3739

Nakano, A., & Takashima, S. (2012). LKB1 and AMP-activated protein kinase: regulators of cell polarity. *Genes to Cells : Devoted to Molecular & Cellular Mechanisms*, *17*(9), 737–47. https://doi.org/10.1111/j.1365-2443.2012.01629.x

Nam, S.-C. (2003). Interaction of Par-6 and Crumbs complexes is essential for photoreceptor morphogenesis in Drosophila. *Development*, *130*(18), 4363–4372. https://doi.org/10.1242/dev.00648

New, L. A., Martin, C. E., & Jones, N. (2014). Advances in slit diaphragm signaling. *Curr Opin Nephrol Hypertens*, *23*(4), 420–430. https://doi.org/10.1097/01.mnh.0000447018.28852.b6

Pan, L., Chen, J., Yu, J., Yu, H., & Zhang, M. (2011). The structure of the PDZ3-SH3-GuK tandem of ZO-1 protein suggests a supramodular organization of the membrane-associated guanylate kinase (MAGUK) family scaffold protein core. *The Journal of Biological Chemistry*, *286*(46), 40069–74. https://doi.org/10.1074/jbc.C111.293084

Parsons, L. M., Portela, M., Grzeschik, N. A., & Richardson, H. E. (2014). Lgl regulates notch signaling via endocytosis, independently of the apical aPKC-Par6-Baz polarity complex. *Current Biology*, *24*(18), 2073–2084. https://doi.org/10.1016/j.cub.2014.07.075

Pavenstadt, H., Kriz, W., & Kretzler, M. (2003). Cell Biology of the Glomerular Podocyte. *Physiological Reviews*, *83*(1), 253–307. https://doi.org/10.1152/physrev.00020.2002

Plant, P. J., Fawcett, J. P., Lin, D. C. C., Holdorf, A. D., Binns, K., Kulkarni, S., & Pawson, T. (2003). A polarity complex of mPar-6 and atypical PKC binds, phosphorylates and regulates mammalian Lgl. *Nature Cell Biology*, *5*(4), 301–308. https://doi.org/10.1038/ncb948

Portela, M., Parsons, L. M., Grzeschik, N. A., & Richardson, H. E. (2015). Regulation of Notch signaling and endocytosis by the Lgl neoplastic tumor suppressor. *Cell Cycle (Georgetown, Tex.)*, *14*(10), 1496–506. https://doi.org/10.1080/15384101.2015.1026515

Prehoda, K. E. (2009). Polarization of Drosophila Neuroblasts During Asymmetric Division. *Cold Spring Harbor Perspectives in Biology*, *1*(2), a001388–a001388. https://doi.org/10.1101/cshperspect.a001388

Putaala, H., Soininen, R., Kilpeläinen, P., Wartiovaara, J., & Tryggvason, K. (2001). The murine nephrin gene is specifically expressed in kidney, brain and pancreas: inactivation of the gene leads to massive proteinuria and neonatal death. *Human Molecular Genetics*, *10*(1), 1–8. Retrieved from http://www.ncbi.nlm.nih.gov/pubmed/11136707

Qin, Y., Capaldo, C., Gumbiner, B. M., & Macara, I. G. (2005). The mammalian Scribble polarity protein regulates epithelial cell adhesion and migration through E-cadherin. *The Journal of Cell Biology*, *171*(6), 1061–1071. https://doi.org/10.1083/jcb.200506094

Reiser, J., & Altintas, M. M. (2016). Podocytes. *F1000Research*, *5*. https://doi.org/10.12688/f1000research.7255.1

Reiser, J., Kriz, W., Kretzler, M., & Mundel, P. (2000). The Glomerular Slit Diaphragm Is a Modified Adherens Junction. *Journal of the American Society of Nephrology*, *11*(1), 1–8. Retrieved from http://jasn.asnjournals.org/content/11/1/1.abstract

Roberts, S., Delury, C., & Marsh, E. (2012). The PDZ protein discs-large (DLG): The "Jekyll and Hyde" of the epithelial polarity proteins. *FEBS Journal*, *279*(19), 3549–3558. https://doi.org/10.1111/j.1742-4658.2012.08729.x

Roeth, J. F., Sawyer, J. K., Wilner, D. A., & Peifer, M. (2009). Rab11 helps maintain apical crumbs and adherens junctions in the Drosophila embryonic ectoderm. *PloS One*, *4*(10), e7634. https://doi.org/10.1371/journal.pone.0007634

Roselli, S., Heidet, L., Sich, M., Henger, A., Kretzler, M., Gubler, M.-C., & Antignac, C. (2004). Early glomerular filtration defect and severe renal disease in podocin-deficient mice. *Molecular and Cellular Biology*, *24*(2), 550–60. https://doi.org/10.1128/mcb.24.2.550-560.2004

Ruiz-Gómez, M., Coutts, N., Price, A., Taylor, M. V, & Bate, M. (2000). Drosophila dumbfounded: a myoblast attractant essential for fusion. *Cell*, *102*(2), 189–98. Retrieved from http://www.ncbi.nlm.nih.gov/pubmed/10943839

Satoh, D., Hirose, T., Harita, Y., Daimon, C., Harada, T., Kurihara, H., … Ohno, S. (2014). aPKCλ maintains the integrity of the glomerular slit diaphragm through trafficking of nephrin to the cell surface. *Journal of Biochemistry*, *156*(2), 115–28. https://doi.org/10.1093/jb/mvu022

Schena, F. P. (2005). Pathogenetic Mechanisms of Diabetic Nephropathy. *Journal of the American Society of Nephrology*, *16*(3_suppl_1), S30–S33. https://doi.org/10.1681/ASN.2004110970

Schnabel, E., Anderson, J. M., & Farquhar, M. G. (1990). The tight junction protein ZO-1 is concentrated along slit diaphragms of the glomerular epithelium. *Journal of Cell Biology*, *111*(3), 1255–1263. https://doi.org/10.1083/jcb.111.3.1255

Sellin, L., Huber, T. B., Gerke, P., Quack, I., Pavenstädt, H., & Walz, G. (2002). NEPH1 defines a novel family of podocin-interacting proteins. *FASEB*, (3). https://doi.org/10.1096/fj.02-0242fje

Shelton, C., Kocherlakota, K. S., Zhuang, S., & Abmayr, S. M. (2009). The immunoglobulin superfamily member Hbs functions redundantly with Sns in interactions between founder and fusion-competent myoblasts. *Development*, *136*(7), 1159–1168. https://doi.org/10.1242/dev.026302

Simons, M., Hartleben, B., & Huber, T. B. (2009). Podocyte polarity signalling. *Current Opinion in Nephrology and Hypertension*, *18*(4), 324–330. https://doi.org/10.1097/MNH.0b013e32832e316d

Simons, M., & Huber, T. B. (2008). It's not all about nephrin. *Kidney International*, *73*(6), 671–3. https://doi.org/10.1038/sj.ki.5002798

Smith, C. A., Lau, K. M., Rahmani, Z., Dho, S. E., Brothers, G., She, Y. M., … McGlade, C. J. (2007). aPKC-mediated phosphorylation regulates asymmetric membrane localization of the cell fate determinant Numb. *The EMBO Journal*, *26*(2), 468–480. https://doi.org/10.1038/sj.emboj.7601495

Somlo, S., & Mundel, P. (2000). Getting a foothold in nephrotic syndrome. *Nature Genetics*, *24*(4), 333–335. https://doi.org/10.1038/74139

Sotillos, S., Díaz-Meco, M. T., Caminero, E., Moscat, J., & Campuzano, S. (2004). DaPKC-dependent phosphorylation of Crumbs is required for epithelial cell polarity in *Drosophila*. *The Journal of Cell Biology*, *166*(4), 549–557. https://doi.org/10.1083/jcb.200311031

Sözen, M. A., Armstrong, J. D., Yang, M., Kaiser, K., & Dow, J. A. (1997). Functional domains are specified to single-cell resolution in a Drosophila epithelium. *Proceedings of the National Academy of Sciences of the United States of America*, *94*(10), 5207–12. Retrieved from http://www.ncbi.nlm.nih.gov/pubmed/9144216

Spicer, J., Rayter, S., Young, N., Elliott, R., Ashworth, A., & Smith, D. (2003). Regulation of the Wnt signalling component PAR1A by the Peutz–Jeghers syndrome kinase LKB1. *Oncogene*, *22*(30), 4752–4756. https://doi.org/10.1038/sj.onc.1206669

St Johnston, D. (2002). THE ART AND DESIGN OF GENETIC SCREENS: DROSOPHILA MELANOGASTER. *Nature Reviews Genetics*, *3*(3), 176–188. https://doi.org/10.1038/nrg751

Strand, D., Jakobs, R., Merdes, G., Neumann, B., Kalmes, A., Heid, H. W., … Mechler, B. M. (1994). The Drosophila lethal(2)giant larvae tumor suppressor protein forms homo-oligomers and is associated with nonmuscle myosin II heavy chain. *The Journal of Cell Biology*, *127*(5), 1361–73. Retrieved from http://www.ncbi.nlm.nih.gov/pubmed/7962095

Strünkelnberg, M., Bonengel, B., Moda, L. M., Hertenstein, A., de Couet, H. G., Ramos, R. G., & Fischbach, K. F. (2001). rst and its paralogue kirre act redundantly during embryonic muscle development in Drosophila. *Development (Cambridge, England)*, *128*(21), 4229–4239.

Su, W.-H., Mruk, D. D., Wong, E. W. P., Lui, W.-Y., & Cheng, C. Y. (2012). Polarity protein complex Scribble/Lgl/Dlg and epithelial cell barriers. *Advances in Experimental Medicine and Biology*, *763*, 149–70. Retrieved from http://www.ncbi.nlm.nih.gov/pubmed/23397623

Suzuki, A., Hirata, M., Kamimura, K., Maniwa, R., Yamanaka, T., Mizuno, K., … Ohno, S. (2004). aPKC Acts Upstream of PAR-1b in Both the Establishment and Maintenance of Mammalian Epithelial Polarity. *Current Biology*, *14*(16), 1425–1435. https://doi.org/10.1016/j.cub.2004.08.021

Suzuki, A., & Ohno, S. (2006). The PAR-aPKC system: lessons in polarity. *Journal of Cell Science*, *119*(6), 979 LP-987. Retrieved from http://jcs.biologists.org/content/119/6/979.abstract

Suzuki, A., Yamanaka, T., Hirose, T., Manabe, N., Mizuno, K., Shimizu, M., … Ohno, S. (2001). Atypical protein kinase C is involved in the evolutionarily conserved par protein complex and plays a critical role in establishing epithelia-specific junctional structures. *The Journal of Cell Biology*, *152*(6), 1183–96. Retrieved from http://www.ncbi.nlm.nih.gov/pubmed/11257119

Tepass, U. (2012). The Apical Polarity Protein Network in Drosophila Epithelial Cells: Regulation of Polarity, Junctions, Morphogenesis, Cell Growth, and Survival. *Annu. Rev. Cell Dev. Biol*, *28*, 655–85. https://doi.org/10.1146/annurev-cellbio-092910-154033

Tepass, U., Tanentzapf, and G., Ward, R., Fehon, and R., Tanentzapf, G., Ward, R., & Fehon, R. (2001). Epithelial Cell Polarity and Cell Junctions in Drosophila. *Annual Review of Genetics*, *35*(1), 747–84. https://doi.org/10.1146/annurev.genet.35.102401.091415

Tryggvason, K., Patrakka, J., & Wartiovaara, J. (2006). Hereditary Proteinuria Syndromes and Mechanisms of Proteinuria. *New England Journal of Medicine*, *354*(13), 1387–1401. https://doi.org/10.1056/NEJMra052131

Walther, R. F., & Pichaud, F. (2010). Crumbs/DaPKC-dependent apical exclusion of bazooka promotes photoreceptor polarity remodeling. *Current Biology*, *20*(12), 1065–1074. https://doi.org/10.1016/j.cub.2010.04.049

Wang, Q., Hurd, T. W., & Margolis, B. (2004). Tight Junction Protein Par6 Interacts with an Evolutionarily Conserved Region in the Amino Terminus of PALS1/Stardust. *Journal of Biological Chemistry*, *279*(29), 30715–30721. https://doi.org/10.1074/jbc.M401930200

Wang, Q., & Margolis, B. (2007). Apical junctional complexes and cell polarity. *Kidney International*, *72*, 1448–1458. https://doi.org/10.1038/sj.ki.5002579

Watts, J. L., Etemad-Moghadam, B., Guo, S., Boyd, L., Draper, B. W., Mello, C. C., … Kemphues, K. J. (1996). par-6, a gene involved in the establishment of asymmetry in early C. elegans embryos, mediates the asymmetric localization of PAR-3. *Development (Cambridge, England)*, *122*(10), 3133–3140.

Weavers, H., Prieto-Sánchez, S., Grawe, F., Garcia-López, A., Artero, R., Wilsch-Bräuninger, M., … Denholm, B. (2009). The insect nephrocyte is a podocyte-like cell with a filtration slit diaphragm. *Nature*, *457*(7227), 322–6. https://doi.org/10.1038/nature07526

Wei, S.-Y., Escudero, L. M., & Yu, F. (2005). Echinoid Is a Component of Adherens Junctions That Cooperates with DE-Cadherin to Mediate Cell Adhesion. *Developmental Cell*, *8*, 493–504. https://doi.org/10.1016/j.devcel.2005.03.015

Wirtz-Peitz, F., & Knoblich, J. A. (2006, May). Lethal giant larvae take on a life of their own. *Trends in Cell Biology*. https://doi.org/10.1016/j.tcb.2006.03.006

Wolf, G., & Ziyadeh, F. N. (2007). Cellular and molecular mechanisms of proteinuria in diabetic nephropathy. *Nephron - Physiology*, *106*(2), p26-31. https://doi.org/10.1159/000101797

Woods, D. F., & Bryant, P. J. (1991). The discs-large tumor suppressor gene of Drosophila encodes a guanylate kinase homolog localized at septate junctions. *Cell*, *66*(3), 451–464. https://doi.org/10.1016/0092-8674(81)90009-X

Woods, D. F., Hough, C., Peel, D., Callaini, G., & Bryant, P. J. (1996). Dlg protein is required for junction structure, cell polarity, and proliferation control in Drosophila epithelia. *The Journal of Cell Biology*, *134*(6), 1469 LP-1482. Retrieved from http://jcb.rupress.org/content/134/6/1469.abstract

Yamanaka, T., Horikoshi, Y., Izumi, N., Suzuki, A., Mizuno, K., & Ohno, S. (2006). Lgl mediates apical domain disassembly by suppressing the PAR-3-aPKC-PAR-6 complex to orient apical membrane polarity. *Journal of Cell Science*, *119*(10). Retrieved from http://jcs.biologists.org/content/119/10/2107?ijkey=6c7716be1307060550d7c83c34c564ce1157ade2&keytype2=tf_ipsecsha

Yamanaka, T., Horikoshi, Y., Sugiyama, Y., Ishiyama, C., Suzuki, A., Hirose, T., … Ohno, S. (2003). Mammalian Lgl forms a protein complex with PAR-6 and aPKC independently of PAR-3 to regulate epithelial cell polarity. *Current Biology : CB*, *13*(9), 734–43. Retrieved from http://www.ncbi.nlm.nih.gov/pubmed/12725730

Yamanaka, T., Horikoshi, Y., Suzuki, A., Sugiyama, Y., Kitamura, K., Maniwa, R., … Ohno, S. (2001). PAR-6 regulates aPKC activity in a novel way and mediates cell-cell contact-induces formation of the epithelial junctional complex. *Genes to Cells*, *6*(8), 721–731. https://doi.org/10.1046/j.1365-2443.2001.00453.x

Zhang, F., Zhao, Y., & Han, Z. (2013). An in vivo functional analysis system for renal gene discovery in Drosophila pericardial nephrocytes. *Journal of the American Society of Nephrology : JASN*, *24*(2), 191–7. https://doi.org/10.1681/ASN.2012080769

Zhang, Y., Guo, H., Kwan, H., Wang, J. W., Kosek, J., & Lu, B. (2007). PAR-1 Kinase Phosphorylates Dlg and Regulates Its Postsynaptic Targeting at the Drosophila Neuromuscular Junction. *Neuron*, *53*(2), 201–215. https://doi.org/10.1016/j.neuron.2006.12.016

Zhu, J., Shang, Y., Wan, Q., Xia, Y., Chen, J., Du, Q., & Zhang, M. (2014). Phosphorylation-dependent interaction between tumor suppressors Dlg and Lgl. *Cell Research*, *24*(4), 451–463. https://doi.org/10.1038/cr.2014.16

Zhuang, S., Shao, H., Guo, F., Trimble, R., Pearce, E., & Abmayr, S. M. (2009). Sns and Kirre, the Drosophila orthologs of Nephrin and Neph1, direct adhesion, fusion and formation of a slit diaphragm-like structure in insect nephrocytes. *Development (Cambridge, England)*, *136*(14), 2335–44. https://doi.org/10.1242/dev.031609

7 INDEX

7.1 Figure index

7.2 Table index

8 ABBREVIATIONS

Table 16 Abbreviations

(d)ATP	(Deoxy)adenosine triphosphate
(d)CTP	(Deoxy)cytotine triphosphate
(d)GTP	(Deoxy)guanosin triphosphate
(d)NTP	(Deoxy)nucleotid triphosphate
(d)TTP	(Deoxy)thymidine triphosphate
AJ	Adherens junction
ANF	Atrial natriuretic factor
ANP	Atrial natriuretic peptide
aPKC	atypical proteinkinase C
Arm	Armadillo
Baz	Bazooka
BM	Basement membrane
BSA	Bovine serum albumin
Crb	Crumbs
Ctcf	Corrected total cell fluorescence
DAPI	4’, 6-diamide-2’-phenylindole dihydrochloride
DE Cad	DE-Cadherin
Dlg	Discs-large

Table 16 continued

DNA	Deoxyribonucleic acid
DTT	Dithiothreitol
Duf	Dumfounded
E. coli	Escherichia coli
FP	Foot proccess(es)
GAL4	GAL4 transcription factor
GFP	Green fluorescent protein
GST	Gluthathione-S-transferase
Hbs	Hibris
IPTG	Isopropyl-β-D-thiogalactopyranosid
JAM	Junctional adhesion molecule
kb	kilobases
Kirre	Kin-of-Irre
LA	Lacuna area
Lgl	Lethal giant larvae
MAGI-1/2	membrane-associated guanylate kinase inverted 1/2
MAGUK	membrane-associated guanylate kinase (homologs)
MEX-5/6	Muscle excess-5/6
min	minutes

Table 16 continued

N	Nucleus
ND	Nephrocyte diaphragm
NHS	Normal horse serum
OD_{600}	optical density (of sample), measured at the wavelength of 600 nm
Par1	Partioning defective homologue-1
Par3	Partioning defective homologue-3
Par6	Partioning defective homologue-6
Scrib	Scribble
SDS	Sodium dodecyl sulfate
Sdt	Stardust
sec	seconds
SJ	Septate junction
Sns	Sticks-and-stones
TEMED	N,N,N',N'-tetramethylethylenediamine
Tiam1	T-cell lymphoma invasion and metastasis 1
TJ	Tight junction
Tris	Tris(hydroxymethyl)aminomethane
UAc	Uranylacetate

Table 16 continued

UAS	Upstream activated sequence
V	Volt
ZA	Zonula adherens
ZO-1	Zonula occludens-1, Tight-junction protein-1

9 DANKSAGUNG

Mein besonderer Dank gilt Prof. Dr. Dr. Michael Krahn für die Betreuung meiner Doktorarbeit, für die vielen Anregungen zur Durchführung der Experimente und seine Hinweise zur Anfertigung der Dissertation.

Ebenso möchte ich mich bei meinen Mentoren Prof. Dr. Stephan Schneuwly und Prof. Dr. Carsten Böger für ihre kritischen Anregungen während meiner Arbeit bedanken. Prof. Dr. Ralph Witzgall möchte ich für die Möglichkeit danken, an seinem Lehrstuhl diese Promotion durchführen zu können.

Ein großes Dankeschön an alle Mitarbeiter des Instituts für ihre Kollegialität und Beistand während meiner Laborzeit. Mein herzlicher Dank geht an Lucia Denk, Helga Schmidt-Othmen und Karin Schadendorf für ihre wundervolle technische und menschliche Unterstützung, Hilfestellung und Expertise zu allen möglichen und unmöglichen TEM-Experimenten.

Besonders möchte ich mich auch bei meinen Kollegen der AG Krahn bedanken, bei Sabine, Olga, Ina, Lars, Rui, Barbara und Daniela, bei Arnab, Zsanett, Christian und Thomas, für die gemeinsame Zeit und tolle Zusammenarbeit.

Ein Dank mit Prädikat geht an meine Kollegen und Freunde Florian Hochapfel, Giada Dogliotti und Markus Dietz, die mich durch alle Höhen und Tiefen gelotst haben.

Lucas, Danke für deine Kraft und deinen Glauben an mich.

Ich danke meinen Brüdern Bernhard und Roland und ganz besonders meinen Eltern Ingeborg und Armin Mendl, die mich immer unterstützt und auf meinem Lebensweg begleitet haben.